Aus der Klinik für Hals-, Nasen-, Ohrenheilkunde, Kopf- und Halschirurgie; Phoniatrie und Pädaudiologie
(Direktorin: Prof. Dr. Susanne Wiegand)
im Universitätsklinikum Schleswig-Holstein, Campus Kiel
an der Christian-Albrechts-Universität zu Kiel

Bildgebende und elektrophysiologische Diagnostik der Elektrodenlage von Cochlea-Implantaten

DISSERTATION
zur
Erlangung des akademischen Grades
Doctor rerum medicarum (Dr. rer. medic.)
der Medizinischen Fakultät
der Christian-Albrechts-Universität zu Kiel
vorgelegt von

Alexander Mewes
aus **Leipzig**

Kiel **2024**

Referent/in:	PD Dr. Matthias Hey
Korreferent/in:	Prof. Dr. Marcus Both
Datum der Disputation:	29. September 2025
Zum Druck genehmigt, Kiel, den	31. Juli 2025
	gez.: PD Dr. Matthias Hey (Vorsitzende/r der Prüfungskommission)

Für Ida, Mads und Tina.

Inhaltsverzeichnis

Abkürzungsverzeichnis

aDOI: Angular Depth of Insertion (anguläre Insertionstiefe)

CAE: Contour-Advance®-Elektrodenarray

CI: Cochlea-Implantat

CoI: Confidence Interval (Konfidenzintervall)

CUSUM: Analysis of Cumulative Sums (Analyse von kumulativen Summen)

DVT: Digitale Volumentomografie

E: Elektrode

ECAP: Electrically Compound Action Potential (Elektrisch evozierte Summenaktionspotentiale)

EMD: Elektroden-Modiolus-Abstand

HA: Hearing Aid (Hörgerät)

ICC: Intraclass Correlation Coefficient (Intraklass-Korrelationskoeffizient)

IGCIP: Image-Guided Cochlear Implant Programming (bildgebungsgestütze CI-Programmierung)

IPR: Interpercentile Range (Interperzentil-Bereich)

IQ: Image Quality (Bildqualität)

IR: Image Resolution (Bildauflösung)

LAPL: Loudest Acceptable Loudness Level (max. tolerierbare Lautheit)

LoA: Limits of Agreement (Toleranzgrenzen)

LSU: Linear Sequential Unmasking (linear sequentielle Demaskierung)

MOD: Achse des Modiolus

PTA4AC (4PTA0.5-4 kHz, 4PTA): Mittelwert der tonaudiometrischen Luftleitungshörschwelle über die Frequenzen 500, 1000, 2000 und 4000 Hz

RF, RW: Rundes Fenster (round window)

SME: Slim-Modiolar-Elektrodenarray

SPL: Sound Pressure Level (Schalldruckpegel)

ST: Scala tympani

SV: Scala vestibuli

T-ECAP: Schwellen von elektrischen evozierten Summenaktionspotentialen

TR: Translokation eines CI-Elektrodenarrays von Scala tympani in Scala vestibuli

Publikationsliste

A) Die Dissertation wurde in folgenden Zeitschriftenartikeln mit Peer-Review-Verfahren veröffentlicht:

Mewes, A., Burg, S., Brademann, G., Dambon, J.A. and Hey, M. (2022) Quality-assured training in the evaluation of cochlear implant electrode position: a prospective experimental study. BMC Med. Educ., 22(1), 386.

Mewes, A., Bennett, C., Dambon, J., Brademann, G. and Hey, M. (2023) Evaluation of CI electrode position from imaging: comparison of an automated technique with the established manual method. BMC Med. Imaging, 23(1), 143.

Liebscher*, T., **Mewes*, A.**, Hoppe, U., Hornung, J., Brademann, G. and Hey, M. (2021) Electrode translocations in perimodiolar cochlear implant electrodes: Audiological and electrophysiological outcome. Z. Med. Phys., 31(3), 265–275.

*geteilte Erstautorenschaft

Die Veröffentlichung erfolgt mit freundlicher Genehmigung des Verlags und der Mitautoren. Es wurden keine inhaltlichen Änderungen vorgenommen.

B) Weitere Veröffentlichungen mit Peer-Review-Verfahren

Mewes, A., Müller-Deile, J., Blau, M., Brademann, G., Hey, M. (2015) Breitbandige Energie-Absorbanz zur Mittelohrdiagnostik. Z. Audiol., 54(4), 138-147.

Hey, M., Wesarg, T., **Mewes, A.**, Helbig, A., Hornung, J., Lenarz, T., Briggs, R., Marx, M., Ramos, A., Stöver, T., Escudé, B., James, C. J., Aschendorff, A. (2018) Objective, audiological and quality of life measures with the CI532 slim modiolar electrode. Cochlear Implants Int., 20(2), 80-90.

Hey, M., Neben, N., Stöver, T., Baumann, U., **Mewes, A.**, Liebscher, T., Schüssler, M., Aschendorff, A., Wesarg, T., Büchner, A., Greenham, P., Hoppe, U. (2020) Outcomes for a clinically representative cohort of hearing-impaired adults using the Nucleus® CI532 cochlear implant. Eur. Arch. Otorhinolaryngol., 277(6), 1625-1635.

Mewes, A., Brademann, G., Hey, M. (2020) Comparison of Perimodiolar Electrodes: Imaging and Electrophysiological Outcomes. Otol. Neurotol., 41(7), e934-e944.

Hey, M., Böhnke, B., **Mewes, A.**, Munder, P., Mauger, S. J., Hocke, T. (2021) Speech comprehension across multiple CI processor generations: Scene dependent signal processing. Laryngoscope Investig. Otolaryngol., 6(4), 804-815.

Müller-Deile, J., Neben, N., Dillier, N., Büchner, A., **Mewes, A.**, Junge, F., Lai, W., Schüssler, M., Hey, M. (2021) Comparisons of electrophysiological and psychophysical fitting methods for cochlear implants. Int. J. Audiol., 2023, 62(2), 118-128.

Hey, M., Hersbach, A. A., Hocke, T., Mauger, S. J., Böhnke, B., **Mewes, A.** (2022) Ecological Momentary Assessment to Obtain Signal Processing Technology Preference in Cochlear Implant Users. J. Clin. Med., 11(10), 2941.

Hey, M., **Mewes, A.**, Hocke, T. (2022) Speech comprehension in noise-considerations for ecologically valid assessment of communication skills ability with cochlear implants. HNO, 70(12), 861-869.

Rieck, J. H., Beyer, A., **Mewes, A.**, Caliebe, A., Hey, M. (2023) Extended Preoperative Audiometry for Outcome Prediction and Risk Analysis in Patients Receiving Cochlear Implants. J. Clin. Med., 12(9):3262.

Dambon, J., **Mewes, A.**, Beyer, A., Dambon, J., Ambrosch, P., Hey. M. (2023) Facilitation properties in electrically evoked compound action potentials depending on spatial location and on threshold. Hear Res, 438, 108858.

Beyer, A., Rieck, J. H., **Mewes, A.**, Dambon, J. A., Hey, M. (2023) Erweiterte präoperative sprachaudiometrische Diagnostik im Rahmen der Cochleaimplantatversorgung. HNO, 71(12), 779-786.

C) Veröffentlichungen ohne Peer-Review-Verfahren

Mewes, A. (2018) Das ungenutzte Potenzial der Tympanometrie zur Mittelohrdiagnostik. HNO Nachrichten, 48(4), 30-34.

Mewes, A. (2019). Genauere Diagnostik durch Breitbandmessungen. HNO Nachrichten, 49(4), 18-22.

Mewes, A., Wiesner, T. (2020) Breitbandige Immittanz-Messungen Teil I: Messtechnische Grundlagen und Messergebnisse bei Erwachsenen. Z. Audiol., 59(2), 61-66.

Wiesner, T., **Mewes, A.** (2020) Breitbandige Immittanz-Messungen Teil II: Möglichkeiten und Besonderheiten bei Kindern. Z. Audiol., 59(3), 133-138.

Mewes, A. (2021) Tympanometrie zur Mittelohrdiagnostik. Sprache Stimme Gehör, 45, 5.

Mewes, A., Hey, M. (2022) Wie Audiologen bei chronischem Tinnitus und Hörverlust vorgehen. Schnecke, 115, 18-19.

D) Bachelorarbeit/Masterarbeit

Mewes, A. (2013) Breitbandige Messung und Analyse von akustisch evozierter auraler Reflektanz. Bachelorarbeit, Oldenburg.

Mewes, A. (2018) Verhältnis von elektrophysiologischen Kenndaten zur räumlichen intracochleären Elektrodenposition von Cochlea-Implantaten. Masterarbeit, Kaiserslautern.

Zusammenfassung

Hintergrund

Eine Einschränkung des Hörvermögens aufgrund eines hochgradigen bis an Taubheit grenzenden Hörverlusts kann zu Ausgrenzungen bei Gesprächen und im täglichen Umgang mit anderen Personen führen. In Fällen, bei denen ein Hörgerät die Symptome einer hochgradigen Hörstörung nicht bzw. nicht mehr ausreichend auszugleichen vermag, kann ein Cochlea-Implantat (CI) zum Einsatz kommen. Das Cochlea-Implantat ist eine elektronische Hörprothese zur Wieder- bzw. Ersterlangung akustischer Wahrnehmungen. Das CI besteht aus zu implantierenden und aus externen Komponenten (Abb. 1). Zu den am Körper getragenen externen Bestandteilen zählen der Sprachprozessor mit Mikrofonen, die Sendespule und die Energieversorgung. Die internen Komponenten umfassen den Neurostimulator mit Empfangsspule und das intracochleäre Elektrodenarray, die im Rahmen einer mikrochirurgischen Operation implantiert werden. Das Elektrodenarray umfasst je nach Hersteller zwischen 12 und 22 Elektroden, die in der Cochlea platziert werden, sowie herstellerabhängig eine extracochleäre Referenzelektrode.

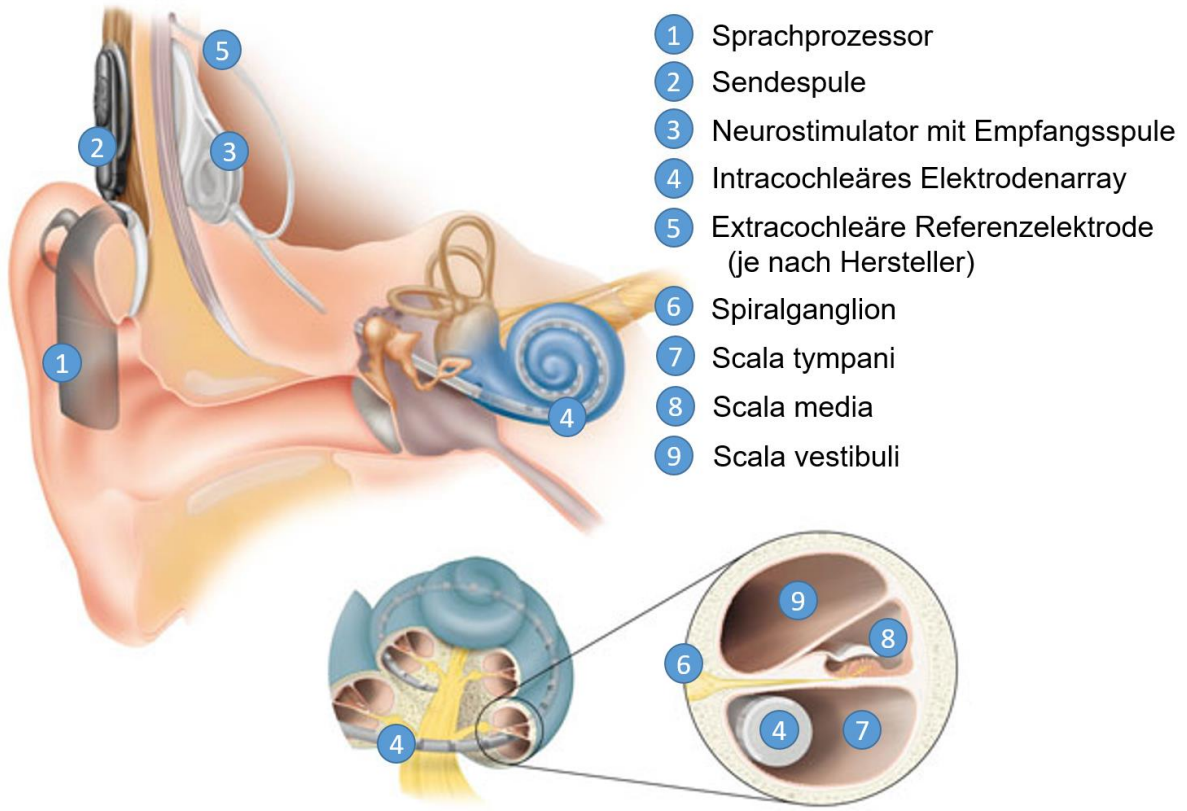

Abbildung 1: Bestandteile eines Cochlea-Implantats. Abbildung mit freundlicher Genehmigung von Cochlear. © Cochlear Limited 2024. Alle Rechte vorbehalten. Legende zur Abbildung wurde von Alexander Mewes mit Genehmigung von Cochlear modifiziert.

Das Grundprinzip eines Cochlea-Implantats besteht darin, dass Schall in elektrische Pulse umgewandelt wird, welche die Zellkörper der Spiralganglienzellen stimulieren und die dadurch ausgelöste Erregung von den auditorischen Zentren des Gehirns als Höreindruck gedeutet wird. Da nur Reizpulse mit genügender Intensität eine Erregung auslösen können, ist es aus funktionaler Sicht von Bedeutung, das Elektrodenarray in der Cochlea möglichst dicht am Modiolus zu platzieren, welcher die Innenwand der Cochlea formt und die Spiralganglienzellen enthält. Hierfür erfolgt die Positionierung des Elektrodenarrays idealtypisch vollständig und ohne Knickung in der Scala tympani der Cochlea (Abb. 1). Für den Nachweis dieser Positionierung kann eine einfache Röntgenaufnahme angefertigt werden, welche senkrecht zur Achse des Modiolus und komplanar zur basalen Windung der Cochlea ausgerichtet ist (Cohen *et al.*, 1996; Xu *et al.*, 2000). Allerdings variiert der Abstand der einzelnen Elektroden zu den Spiralganglienzellen untereinander und zwischen den Patienten, je nach Größe der Cochlea, Elektrodentyp und in Abhängigkeit von der Insertionstiefe der Elektroden in der Cochlea (Esquia Medina *et al.*, 2015; Mewes,

2018; Mewes *et al.*, 2020). Hier können röntgenologische Untersuchungen des Abstands einzelner Elektroden relativ zu den Spiralganglienzellen zur Anwendung kommen, welche über den einfachen Nachweis des intracochleär liegenden Elektrodenarrays hinausgehen. Diese Distanzmessungen können bei gemeinsamer Betrachtung der Insertionstiefe im Einzelfall klinisch von Interesse sein, wenn das postoperative Sprachverstehen der Patient*innen schlechter ist als erwartet und/oder wenn sich die funktionale Ankopplung der Elektroden an die Spiralganglienzellen widrig dem Regelfall darstellt. Erkenntnisse zur funktionalen Ankopplung ergeben sich aus elektrophysiologischen Messungen wie bspw. der Registrierung von elektrisch evozierten Summenaktionspotentialen (ECAPs), deren Messvorrichtung in modernen CI-Systemen bereits integriert ist. Diese Summenaktionspotentiale entstehen bei elektrischer Reizung ausreichender Intensität an einer beliebigen intracochleären Elektrode, und können von einer benachbarten Elektrode abgeleitet und anschließend durch Telemetrie über den Sprachprozessor zur Analyse bereitgestellt werden. Die Ergebnisse einer ECAP-Messung werden von verschiedenen Faktoren beeinflusst, u. a. von anatomischen Abnormitäten des Innenohres oder abnormem Gewebewachstum in der Cochlea (Müller *et al.*, 2015; Simoni *et al.*, 2020). Überdies sind ECAPs vom Abstand der Elektroden zu den Spiralganglienzellen abhängig (Van Wermeskerken *et al.*, 2009; Degen *et al.*, 2020; Mewes *et al.*, 2020), was im Einzelfall die Messung dieser Größe für die Differentialdiagnostik erforderlich macht. Ein Sonderfall hierbei stellen Elektrodentranslokationen zwischen den Skalen dar. Translokationen des Elektrodenarrays treten auf, wenn das Array nach primärer Insertion in die Scala tympani die Basilarmembran perforiert und schließlich, mit größerem Abstand zu den Spiralganglienzellen, in der Scala vestibuli zum Liegen kommt (Abb. 1 in Liebscher *et al.*, 2021). Eine Translokation beeinflusst die funktionale Elektroden-Hörnerv-Ankopplung im Vergleich zu einer vollständigen Scala-tympani-Insertion auf zwei Wegen. Einerseits durch die partiell vergrößerten Abstände der Elektroden zu den Spiralganglienzellen, und andererseits durch ein zusätzliches Trauma der cochleären Binnenstrukturen.

Die Beurteilung der Skalenlokalisation von Elektrodenarrays und der Elektrodenlage relativ zu den Spiralganglienzellen gelingt im klinischen Alltag mit tomografischen Aufnahmen wie CT (Lane *et al.*, 2007) und Digitaler Volumentomografie, DVT

(Husstedt *et al.*, 2002; Aschendorff *et al.*, 2004, 2005). Der Vorteil dieser Methoden im Vergleich zu einer einfachen Röntgenaufnahme besteht darin, dass Innenohrstrukturen wie bspw. das runde Fenster oder der Modiolus genauer und in beliebiger Raumorientierung abgebildet werden können. Unserer klinischen Erfahrung nach führt dieser Vorteil damit auch zu genaueren Messergebnissen bei der Insertionstiefe, welche häufig als Winkelmaß (aDOI, „angular depth of insertion“) relativ zum runden Fenster gemessen wird (Abb. 2).

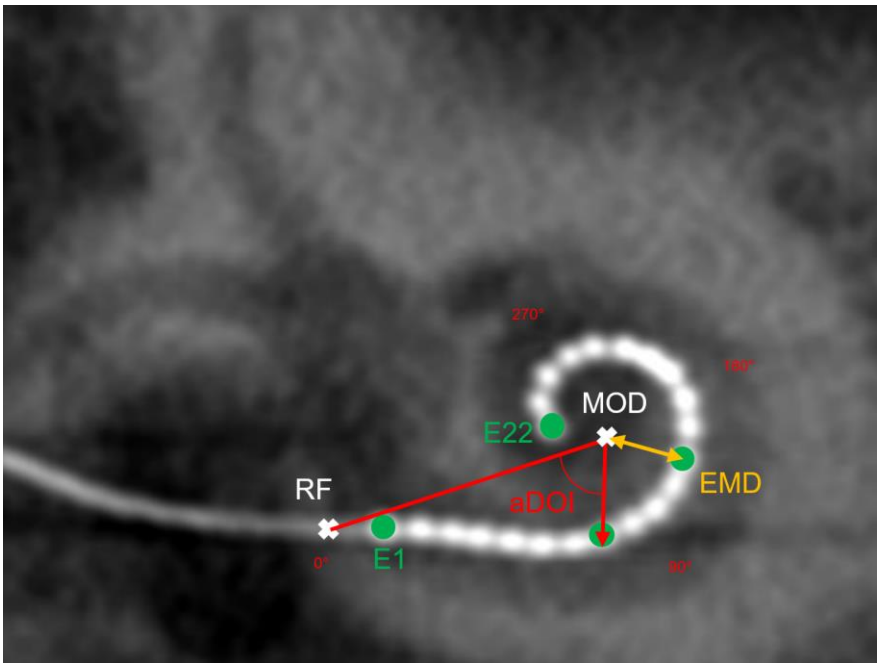

Abbildung 2: Schematische Darstellung von Lageparametern zur Beschreibung der CI-Elektrodenlage: Insertionstiefe als Winkelmaß „aDOI“ (angular depth of insertion), gemessen relativ zur Linie zwischen der modiolären Achse „MOD“ und dem Zentrum des runden Fensters „RF“ (0°); Elektroden-Modiolus-Abstand „EMD“, Distanz zwischen dem Zentrum einer Elektrode „E“ und der modiolären Achse MOD. Eigene Darstellung.

Mit den Verfahren CT und DVT ergeben sich, trotz der genannten Vorteile gegenüber einer Röntgenaufnahme, diagnostische Einschränkungen im Hinblick auf die Elektrodenlage, welche einerseits in der Untersuchungstechnik und andererseits in den Auswertemethoden begründet liegen. Es liegt in der Natur einer tomografischen Untersuchung, die auf der Abschwächung von Röntgenstrahlung basiert, dass die knöchernen Strukturen des Innenohres und die Elektroden gut abgebildet werden können, während die Spiralganglienzellen selbst nicht darstellbar sind. Aus diesem Grund erfolgt die röntgenologische Beurteilung der Elektrodenlage relativ zu den Spiralganglienzellen, indem der Abstand einer einzelnen Elektrode zur Achse des Modiolus gemessen wird (Abb. 2). Zudem ist in klinischen CT- und DVT-Aufnahmen

mit eingeschränkter Bildqualität die Skalenlokalisation durch die geringgradige Sichtbarkeit der intracochleären Membranen erschwert. Den Sonderfall der Elektrodentranslokation zwischen Scala tympani und Scala vestibuli betreffend, beschreiben CT und DVT zwar die lageabhängigen Veränderungen, jedoch nicht die Auswirkungen des zusätzlichen Traumas der intracochleären Strukturen auf die funktionale Ankopplung der Elektroden an die Spiralgan glienzellen. Hier können elektrophysiologische Daten wie Schwellen von ECAP-Messungen eine sinnvolle Ergänzung darstellen. Zum jetzigen Zeitpunkt fehlen jedoch Arbeiten zur Untersuchung der Beziehung von ECAP-Messungen und Elektrodenlage an einem großen, homogenen Kollektiv an Patient*innen.

Die genannten, auf die Untersuchungstechnik bezogenen Limitierungen treffen im klinischen Alltag auf weitere Einschränkungen, welche die Auswertemethode betreffen. Die Analyse von Daten zur Elektrodenlage, wie Elektroden-Modiolus-Distanz, Insertionstiefe und Skalenlokalisation, erfolgt in der klinischen Routine meistens durch händische Rekonstruktion der zur Auswertung erforderlichen Schnittbilder aus den CT- bzw. DVT-Aufnahmen. Aufgrund der Subjektivität der manuellen Auswertemethode kann es zu diagnostischen Fehlern kommen, wenn die oben genannten kritischen Landmarken von der untersuchenden Person nicht wahrgenommen oder fehlgedeutet werden (Graber *et al.*, 2005; McCreadie and Oliver, 2009; Lee *et al.*, 2013; Busby *et al.*, 2018). Hier setzen moderne, teil- oder quasi-vollautomatische Auswertemethoden wie OTOPLAN (otologische Planungssoftware von CAScination in Kooperation mit MED-EL), Nautilus (KardioME in Kooperation mit Oticon) (Margeta *et al.*, 2022) und IGCIP („Image-Guided Cochlear Implant Programming“, Vanderbilt University) (Noble *et al.*, 2013) an. Die Eliminierung menschlicher Fehler bei der Beurteilung der CI-Elektrodenlage durch Automatisierung hat das Potential, die Konsistenz und die Genauigkeit der Auswertung zu verbessern. Allerdings fehlen bislang unabhängige Untersuchungen zur Messgenauigkeit solcher Verfahren, damit diese uneingeschränkt in den klinischen Alltag implementiert werden können.

Das erste Ziel der vorliegenden Dissertation war es, die diagnostischen Fehler zu quantifizieren, welche bei der klinischen, manuellen Beurteilung von metrischen Lagemaßen wie Elektroden-Modiolus-Abstand und Insertionstiefe (Abb. 2) auftreten können (Mewes *et al.*, 2022). Die Betrachtung erfolgte unter dem Aspekt der

Erfahrenheit der Auswerter bei der Befundung der CI-Elektrodenlage. Mit den hierbei ermittelten Werten zur Reliabilität als Referenz, erfolgte als zweite Fragestellung ein Vergleich zwischen der manuellen Auswertung der Elektrodenlage und dem quasi-vollautomatischen Ansatz nach IGCIP (Mewes *et al.*, 2023). In einer dritten Fragestellung wurde an einem großen, homogenen Kollektiv an Patient*innen der Frage nachgegangen, ob und wie die Messung von ECAP-Schwellen zur Untersuchung von Elektrodentranslokationen zwischen der Scala tympani und Scala vestibuli genutzt werden können (Liebscher *et al.*, 2021).

Die Ergebnisse dieser drei Fragestellungen werden im Folgenden übergeordnet bewertet und diskutiert.

Zur Reliabilität von Elektroden-Modiolus-Abständen und Insertionstiefe durch manuelle Auswertung von erfahrenen Untersucher*innen

Diagnostische Fehler in der Radiologie resultieren meistens aus einer Kombination von systembezogenen Faktoren und kognitiv-perzeptuellen Verzerrungen bei der untersuchenden Person (Graber *et al.*, 2005; McCreadie and Oliver, 2009; Lee *et al.*, 2013; Busby *et al.*, 2018). Kognitiv-perzeptuelle Verzerrungen können sowohl bei unerfahrenen als auch bei erfahrenen Auswerter*innen auftreten, wobei es unerfahrenen Untersucher*innen insbesondere an adäquatem Wissen und Fähigkeiten mangelt und sie bei ihrer Entscheidungsfindung für vorzeitige und unpassende Schlüsse sowie Missinterpretationen anfällig sind (Braun *et al.*, 2017). Unerfahrenheit bringt jedoch den Vorteil mit sich, dass Untersucher*innen bei ihrer Entscheidungsfindung besonders analytisch vorgehen, während erfahrene Auswerter*innen bei höherer Arbeitsgeschwindigkeit eher zu vorzeitigen Schlüssen neigen und damit diagnostische Fehler produzieren können (Kahneman, 2011). Zum jetzigen Zeitpunkt existiert weder ein standardisiertes Vorgehen zur Qualitätssicherung bei der Beurteilung der CI-Elektrodenlage, noch eine Methode zum Training von unerfahrenen Auswerter*innen. Zudem mangelt es in der Literatur bei Arbeiten zu Elektroden-Modiolus-Abständen an Angaben der Intra- bzw. Interrater-Abweichung oder es ist einfach nur die statistische Stärke der Übereinstimmung zwischen mehreren Messreihen einer untersuchenden Person oder zwischen den Messreihen von mehreren untersuchenden Personen

angegeben. Um die Ergebnisse von Elektroden-Modiolus-Distanzen diagnostisch werten zu können ist es aber wichtig, Kenntnis über die Abweichungen von Test und Retest bei einer untersuchenden Person bzw. zwischen den verschiedenen Auswerter*innen zu besitzen. Im Rahmen der vorliegenden Dissertation wurden sowohl Test-Retest-Abweichungen bei einem erfahrenen Untersucher, als auch Abweichungen zwischen zwei Auswertern ermittelt. Durch die Publikation dieser Daten soll dazu beigetragen werden, eine fortlaufende klinische Qualitätskontrolle bei der Messung von Elektroden-Modiolus-Abständen (EMD) und der angulären Insertionstiefe (aDOI) (Abb. 2) zu etablieren, indem die Ergebnisse als Referenz genutzt werden. Die Ergebnisse deuten an, dass die Reliabilität von EMD- und aDOI-Messungen selbst bei einem erfahrenen Auswerter verbessert werden kann. Für einen solchen Auswerter zeigten sich bei der wiederholten Messung von Elektroden-Modiolus-Abständen zunächst Abweichungen (±0,5 mm), die größer als die technische Bildauflösung waren (hier: bis zu 0,25 mm) und damit bei der klinischen Diagnostik von Bedeutung sind (Mewes *et al.*, 2022). Durch strukturierte Vereinheitlichung der Auswertemethode und mehrfache Messwiederholung gelang es, die Abweichungen zwischen diesem und einem weiteren Untersucher soweit zu reduzieren, dass sie der Bildauflösung entsprachen und auf die Auswertung keinen begrenzenden Einfluss hatten (Mewes *et al.*, 2023).

Qualitätssicherung bei der manuellen Beurteilung der CI-Elektrodenlage durch unerfahrene Untersucher*innen

Im Rahmen der vorliegenden Dissertation wurde ein qualitätsgesicherter iterierter Trainingsansatz mit statistischer Kontrolle implementiert, mit dem unerfahrene Auswerter*innen bei der Beurteilung der CI-Elektrodenlage angelernt und in ihrer Leistungsfähigkeit zielgerichtet auf das Niveau von erfahrenen Untersucher*innen geführt werden können. Der Trainingsansatz beinhaltet einerseits Techniken des vorsätzlichen Lernens („deliberate practice“), um der unerfahrenen auswertenden Person die fehlenden Kenntnisse bei der Beurteilung der CI-Elektrodenlage zu vermitteln. Andererseits wurden Maßnahmen implementiert, um die bei unerfahrenen Auswerter*innen identifizierten kognitiven Verzerrungen zu reduzieren („linear sequential unmasking“). Zur statistischen Kontrolle des Lernerfolgs dienten

Shewhart-Charts, die als etabliertes Kontrollwerkzeug aus der Ökonomie bekannt sind. Das Ziel der Studie war es, zunächst die prinzipielle Wirksamkeit der Methode nachzuweisen. Die Untersuchungen erfolgten deshalb exemplarisch mit einem einzelnen Medizinstudenten, dessen Lernkurve bei der Messung von Elektroden-Modiolus-Abständen und der angulären Insertionstiefe (Abb. 2) von Elektrodenarrays mit den Intrarater-Abweichungen (Test-Retest) eines erfahrenen Untersuchers verglichen worden sind. Die Test-Retest Abweichungen (0.1 bis 99.9. Perzentil) des erfahrenen Auswerters wurden mit ±0,5 mm für den Elektroden-Modiolus-Abstand, sowie mit -5° bis 8° (Elektrode 1) und -14° bis 16° (Elektrode 22) für die anguläre Insertionstiefe ermittelt. Ziel des Trainings war es, dass die Abweichungen zwischen dem Studenten und dem erfahrenen Untersucher gleich oder kleiner den Intrarater-Abweichungen des erfahrenen Auswerters lagen. Unter Implementierung des oben genannten Trainingsansatzes konnte gezeigt werden, dass der Medizinstudent dies nach vier (EMD) bzw. drei (aDOI) Messreihen erreichte (Abb. 4 und 5 in Mewes *et al.*, 2022). Auf Basis dieser Ergebnisse kann geschlussfolgert werden, dass es möglich ist, unerfahrene Untersucher*innen durch strukturiertes Training bei der Beurteilung der CI-Elektrodenlage auf das Leistungsniveau einer erfahrenen auswertenden Person heranzuführen. Diese Trainingsmethode erfordert zeitliche, personelle und materielle Ressourcen, befindet sich aber in Übereinstimmung mit internationalen Anforderungen an klinische Qualitätssicherung (Quality management systems - Fundamentals and vocabulary (EN ISO 9000:2015), 2015; Quality management systems - Requirements (EN ISO 9001:2015), 2015).

Verifizierung eines automatisierten Verfahrens zur Beurteilung der CI-Elektrodenlage

Bei der quantitativen manuellen Beurteilung der CI-Elektrodenlage kann es aufgrund von kognitiv-perzeptuellen Verzerrungen zu Messfehlern kommen, die, wie anhand der Elektroden-Modiolus-Abstände gezeigt werden konnte, die technische Bildauflösung übersteigen können und damit im klinischen Alltag und bei klinischen Studien nicht ignoriert werden dürfen. Die Verwendung automatischer Auswertemethoden hat das Potential, menschliche Fehler bei der Beurteilung der CI-Elektrodenlage zu eliminieren und damit die Konsistenz und die Genauigkeit der

Auswertung zu verbessern. Die IGCIP-Methode („Image-Guided Cochlear Implant Programming“) der Vanderbilt University erlaubt eine quasi-vollautomatische Auswertung der Elektrodenlage (Noble *et al.*, 2013). Bei dieser Methode wird ein Modell aus Verteilungspunkten („Atlas“) auf die präoperative CT-Aufnahme einer Person mit CI angepasst, um darin die anatomischen Strukturen des Innenohres zu segmentieren (Skinner *et al.*, 2007; Noble *et al.*, 2011; Reda, McRackan, *et al.*, 2014; Reda, Noble, *et al.*, 2014; Zhang *et al.*, 2016). Durch die Zusammenführung dieser Ergebnisse mit der postoperativen CT-Aufnahme, in welcher die intracochleären CI-Elektroden automatisch lokalisiert werden (Zhao *et al.*, 2014, 2017, 2019; Noble and Dawant, 2015), wird eine Reihe von Lageparametern zur Beurteilung der Elektrodenlage automatisch ermittelt. Im Rahmen der vorliegenden Studie war es das Ziel, automatisch bestimmte Ergebnisse von metrisch (EMD, aDOI) und nominal (Skalenlokalisation) skalierten Lageparametern zu verifizieren, indem diese mit der klinisch etablierten manuellen Auswertemethode verglichen worden sind.

Es konnte gezeigt werden, dass die Elektrodenarrays mit dem automatischen Verfahren bei allen 50 Aufnahmen in der Scala tympani lokalisiert wurden, was den Ergebnissen der händischen Vorauswahl entsprach. Bei der Messung von Elektroden-Modiolus-Abständen und der angulären Insertionstiefe zeigten sich hingegen systematische Unterschiede zwischen der automatischen und manuellen Auswertemethode, welche primär auf eine unterschiedliche Lokalisation der modiolären Achse als anatomische Referenz zur Messung dieser beiden Lageparameter zurückzuführen waren (Abb. 2, 4 und 5 in Mewes *et al.*, 2023). Bei der automatischen Auswertemethode wurde der kleinstmögliche Abstand jeder einzelnen Elektrode zur Achse des Modiolus, dessen Außenfläche die Innenwand der Cochlea repräsentiert, gemessen, während die manuelle Messung bei allen Elektroden stets bis zum Helicotrema erfolgte. Das Helicotrema als Ursprung der modiolären Achse ist zwar robust zu detektieren, kann jedoch bei basalen Elektroden zu ungenauen EMD-Ergebnissen führen, wenn die modioläre Achse nicht senkrecht zur basalen Ebene der Cochlea verläuft. In diesem Fall stimmt die Position des Helicotrema nicht mit der Position der modiolären Achse im basalen Bereich der Cochlea überein, weshalb es zu diagnostischen Fehlern bei der Messung von EMD an basalen Elektroden kommen kann.

Im Gegensatz zur Messung von EMD muss bei den Ergebnissen der angulären Insertionstiefe von einer eingeschränkten diagnostischen Validität der automatischen Methode ausgegangen werden, da die Winkel gegen eine nicht standardisierte 0°-Referenzebene gemessen werden. Diese Ebene verläuft tangential durch das runde Fenster und das Zentrum der modiolären Achse im basalen Bereich der Cochlea. Da diese Methode nicht dem Konsens zu einem einheitlichen Koordinatensystem der Cochlea (Verbist *et al.*, 2010) entspricht, bei welchem die 0°-Referenzebene durch das runde Fenster und das Helicotrema verläuft, ist die Vergleichbarkeit der automatisch ermittelten aDOI-Werte mit dem Konsens entsprechend ermittelten Messwerten reduziert.

Aufgrund der eingeschränkten diagnostischen Validität bei der aDOI-Messung kann geschlussfolgert werden, dass das IGCIP-Verfahren bei den hier untersuchten Lageparametern zum jetzigen Zeitpunkt nur für die Messung von EMD und der Skalenlokalisation klinisch nutzbar ist. Allerdings kann diese Folgerung aufgrund der händischen Vorauswahl nur für tomografische Aufnahmen ohne Bewegungsartefakte getroffen werden, da nur solche Aufnahmen in dieser Studie analysiert worden sind. DVT-Aufnahmen mit Bewegungsartefakten führten stets zu einer Fehlermeldung bei der IGCIP-Software (nicht publizierte Voruntersuchung). Da die Häufigkeit von Bewegungsartefakten nicht gering war (ca. ¼ der Fälle), schränkt dies den klinischen Nutzen von IGCIP zum jetzigen Zeitpunkt weiter ein.

Analyse von ECAP-Schwellen zur Beurteilung der Skalenlokalisation von Elektrodenarrays

Die Skalenlokalisation von CI-Elektroden in tomografischen Aufnahmen stellt eine nominale Größe dar. Eine einzelne Elektrode kann entweder in der Scala tympani oder in der Scala vestibuli liegen. Von klinischer Bedeutung ist insbesondere die Detektion einer Translokation des Elektrodenarrays, unter welcher die partielle Lage der Arrays innerhalb der Scala vestibuli nach primärer Insertion in die Scala tympani verstanden wird (Abb. 1 in Liebscher *et al.*, 2021). Aufgrund der nominalen Wertigkeit der Skalenlokalisation kann für diesen Lageparameter keine zahlenmäßige Reliabilität angegeben werden. Die manuelle Bestimmung der Skalenlokalisation unterliegt aber einer gewissen Messunsicherheit, da mit der eingeschränkten

Bildauflösung in klinischen DVT- und CT-Aufnahmen die intracochleären Membranen und damit die Kanäle der Hörschnecke unserer klinischen Erfahrung nach kaum bis gar nicht detektierbar sind. Zudem kann es auch bei der händischen Beurteilung der Skalenlage zu kognitiv-perzeptuellen Verzerrungen durch die untersuchende Person kommen. Als ergänzende Untersuchungstechnik zu CT und DVT kann die Messung von ECAPs zur Anwendung kommen, da Schwellen von ECAPs mit dem Elektroden-Modiolus-Abstand korrelieren (Van Wermeskerken *et al.*, 2009; Mewes *et al.*, 2020; Schvartz-Leyzac *et al.*, 2020).

In der vorliegenden bizentrischen Studie konnte an einem großen (N=255), homogenen Kollektiv an Patient*innen gezeigt werden, dass eine Translokation des Elektrodenarrays zu höheren ECAP-Schwellen an apikalen und medialen Elektroden führt als eine vollständige Insertion in die Scala tympani, und damit zu einer beeinträchtigten funktionalen Ankopplung der Elektroden an die Spiralganglienzellen. Dies kann damit erklärt werden, dass die partielle Lage der Elektroden in der Scala vestibuli mit größeren Elektroden-Modiolus-Abständen (Roland *et al.*, 2000) und damit höheren elektrophysiologischen Schwellen verbunden ist (Mittmann *et al.*, 2015, 2016). Für beide untersuchten perimodiolaren Elektrodenarray-Typen fanden sich Elektrodenbereiche, bei denen die Streubereiche (25.-75. Perzentil) der ECAP-Schwellen beider Gruppen nicht überlappten. Überdies hat die Messung von ECAP-Schwellen das Potential, bei einer Translokation nicht nur die unerwünschten lagebezogenen Abweichungen zu berücksichtigen, sondern gleichzeitig auch die Wirkung des zusätzlichen Traumas in Folge der Perforation der Basilarmembran zu erfassen (Liebscher *et al.*, 2023) . Die Messung von ECAP-Schwellen stellt damit, in Ergänzung zur Bildgebung, ein wichtiges diagnostisches Werkzeug bei der Detektion und Analyse von Elektrodentranslokationen dar.

Schlussfolgerungen

Die vorliegende Dissertation adressiert diagnostische Einschränkungen bei der Beurteilung der CI-Elektrodenlage, welche sich aus den röntgenologischen Untersuchungsmethoden und den Methoden zu deren Auswertung ergeben. Die Auswertung von DVT- und CT-Aufnahmen erfolgt im klinischen Alltag meistens

manuell. Dabei kann es zu diagnostischen Fehlern kommen, wenn kritische Landmarken von der untersuchenden Person nicht oder nicht korrekt wahrgenommen oder fehlgedeutet werden. In den vorliegenden Arbeiten fanden sich bei manueller Auswertung von Elektroden-Modiolus-Abständen (EMD) und der angulären Insertionstiefe (aDOI) intra- und interindividuelle Abweichungen in einer Größenordnung, welche die technische Bildauflösung übertrafen. Diese Abweichungen sind deshalb klinisch relevant und sollten sowohl in der klinischen Routine als auch bei zukünftigen Studien stets angegeben werden. Allerdings konnte gezeigt werden, dass intra- und interindividuelle Abweichungen durch gezielte Verringerung von kognitiv-perzeptuellen Verzerrungen reduziert werden können. Für unerfahrene Untersucher*innen wurde hierfür ein strukturierter Trainingsansatz entwickelt, mit dem die Leistungsfähigkeit bei der Messung von EMD und aDOI auf das Niveau von erfahrenen Untersucher*innen angehoben werden kann.

Durch Automatisierung der Bildauswertung mittels IGCIP kann die Validität von EMD-Messungen erhöht werden, da der kleinstmögliche Abstand zur modiolären Achse gemessen wird, was klinisch von größerem Interesse ist als der manuell gemessene Abstand zum Helicotrema. Das untersuchte IGCIP-Verfahren liefert jedoch nur für Artefakt-freie Aufnahmen zuverlässige Ergebnisse und verwendet bei der Messung der angulären Insertionstiefe ein Koordinatensystem, welches nicht dem Konsens entspricht.

Den Sonderfall der Elektrodentranslokation betreffend, beschreiben CT und DVT zwar die lageabhängigen Veränderungen im Vergleich zu einer vollständigen Insertion in die Scala tympani, jedoch nicht die Auswirkungen des zusätzlichen Traumas der intracochleären Strukturen auf die funktionale Ankopplung der Elektroden an die Spiralganglienzellen. Es konnte gezeigt werden, dass Messungen von ECAP-Schwellen das Potenzial besitzen, Elektrodentranslokationen zwischen der Scala tympani und Scala vestibuli zu detektieren, und die Ankopplung dabei funktional unter Berücksichtigung aller Einflussfaktoren zu beschreiben. Zum jetzigen Zeitpunkt kann damit geschlussfolgert werden, dass eine vollständige Beurteilung der Elektrodenlage neben der anatomischen, bildgebenden Diagnostik auch auf das elektrophysiologische Methodeninventar zurückgreifen sollte, welches in den heutigen CI-Systemen bereits integriert ist.

Literaturverzeichnis

Aschendorff, A., Kubalek, R., Hochmuth, A., Bink, A., Kurtz, C., Lohnstein, P., Klenzner, T. and Laszig, R. (2004) Imaging procedures in cochlear implant patients – evaluation of different radiological techniques. Acta Otolaryngol., (sup552), 46–49.

Aschendorff, A., Kubalek, R., Turowski, B., Zanella, F., Hochmuth, A., Schumacher, M., Klenzner, T. and Laszig, R. (2005) Quality control after cochlear implant surgery by means of rotational tomography. Otol. Neurotol., 26(1), 34–37.

Braun, L.T., Zwaan, L., Kiesewetter, J., Fischer, M.R. and Schmidmaier, R. (2017) Diagnostic errors by medical students: Results of a prospective qualitative study. BMC Med. Educ., 17(1), 1–7.

Busby, L.P., Courtier, J.L. and Glastonbury, C.M. (2018) Bias in radiology: The how and why of misses and misinterpretations. Radiographics, 38(1), 236–247.

Cohen, L.T., Xu, J., Xu, S.A. and Clark, G.M. (1996) Improved and simplified methods for specifying positions of the electrode bands of a cochlear implant array. Am. J. Otol., 17(6), 859–865.

Degen, C.V., Büchner, A., Kludt, E. and Lenarz, T. (2020) Effect of electrode to modiolus distance on electrophysiological and psychophysical parameters in CI patients with perimodiolar and lateral electrode arrays. Otol. Neurotol., 41(9), e1091–e1097.

Esquia Medina, G.N., Borel, S., Nguyen, Y., Ambert-Dahan, E., Ferrary, E., Sterkers, O. and Grayeli, A.B. (2015) Is electrode-modiolus distance a prognostic factor for hearing performances after cochlear implant surgery? Audiol. Neurotol., 18(6), 406–413.

Graber, M.L., Franklin, N. and Gordon, R. (2005) Diagnostic error in internal medicine. Arch. Intern. Med., 165(13), 1493–1499.

Husstedt, H.W., Aschendorff, A., Richter, B., Laszig, R. and Schumacher, M. (2002) Nondestructive three-dimensional analysis of electrode to modiolus proximity. Otol. Neurotol., 23(1), 49–52.

Kahneman, D. (2011) Thinking, fast and slow. New York: Farrar, Straus & Giroux.

Lane, J.I., Witte, R.J., Driscoll, C.L.W., Shallop, J.K., Beatty, C.W. and Primak, A.N. (2007) Scalar localization of the electrode array after cochlear implantation: Clinical experience using 64-slice multidetector computed tomography. Otol. Neurotol., 28(5), 658–662.

Lee, C.S., Nagy, P.G., Weaver, S.J. and Newman-Toker, D.E. (2013) Cognitive and system factors contributing to diagnostic errors in radiology. Am. J. Roentgenol., 201(3), 611–617.

Liebscher, T., Mewes, A., Hoppe, U., Hornung, J., Brademann, G. and Hey, M. (2021) Electrode translocations in perimodiolar cochlear implant electrodes: Audiological and electrophysiological outcome. Z. Med. Phys., 31(3), 265–275.

Liebscher, T., Hornung, J. and Hoppe, U. (2023) Electrically evoked compound action potentials in cochlear implant users with preoperative residual hearing. Front. Hum. Neurosci., 17.

Margeta, J., Hussain, R., López Diez, P., Morgenstern, A., Demarcy, T., Wang, Z., Gnansia, D., Martinez Manzanera, O., Vandersteen, C., Delingette, H., Buechner, A., Lenarz, T., Patou, F. and Guevara, N. (2022) A Web-Based Automated Image Processing Research Platform for Cochlear Implantation-Related Studies. J. Clin. Med., 11(22), 6640.

McCreadie, G. and Oliver, T.B. (2009) Eight CT lessons that we learned the hard way: an analysis of current patterns of radiological error and discrepancy with particular emphasis on CT. Clin. Radiol., 64(5), 491–499.

Mewes, A. (2018) Verhältnis von elektrophysiologischen Kenndaten zur räumlichen intracochleären Elektrodenposition von Cochlea-Implantaten. Masterarbeit, Kaiserslautern.

Mewes, A., Burg, S., Brademann, G., Dambon, J.A. and Hey, M. (2022) Quality-assured training in the evaluation of cochlear implant electrode position: a prospective experimental study. BMC Med. Educ., 22(1), 386.

Mewes, A., Bennett, C., Dambon, J., Brademann, G. and Hey, M. (2023) Evaluation of CI electrode position from imaging: comparison of an automated technique with the established manual method. BMC Med. Imaging, 23(1), 143.

Mewes, A., Brademann, G. and Hey, M. (2020) Comparison of perimodiolar electrodes: Imaging and electrophysiological outcomes. Otol. Neurotol., 41(7), e934–e944.

Mittmann, P., Todt, I., Ernst, A., Rademacher, G., Mutze, S., Göricke, S., Schlamann, M., Ramalingam, R., Lang, S., Christov, F. and Arweiler-Harbeck, D. (2016) Electrophysiological Detection of Scalar Changing Perimodiolar Cochlear Electrode Arrays: A Long Term Follow-up Study. Eur. Arch. Oto-Rhino-Laryngology, 273(12), 4251–4256.

Mittmann, P., Ernst, A. and Todt, I. (2015) Intraoperative electrophysiologic variations caused by the scalar position of cochlear implant electrodes. Otol. Neurotol., 36(6), 1010–1014.

Müller, A., Hocke, T. and Mir-Salim, P. (2015) Intraoperative findings on ECAP-measurement: Normal or special case? Int. J. Audiol., 54(4), 257–264.

Noble, J.H., Labadie, R.F., Majdani, O. and Dawant, B.M. (2011) Automatic segmentation of intracochlear anatomy in conventional CT. IEEE Trans. Biomed. Eng., 58(9), 2625–2632.

Noble, J.H., Labadie, R.F., Gifford, R.H. and Dawant, B.M. (2013) Image-Guidance enables new methods for customizing cochlear implant stimulation strategies. IEEE Trans. Neural Syst. Rehabil. Eng., 21(5), 820–829.

Noble, J.H. and Dawant, B.M. (2015) Automatic graph-based localization of cochlear implant electrodes in CT. Med. image Comput. Comput. Interv., 9350, 152–159.

Quality management systems - Fundamentals and vocabulary (EN ISO 9000:2015) (2015). Available at: https://www.iso.org/obp/ui/#iso:std:iso:9000:ed-4:v1:en.

Quality management systems - Requirements (EN ISO 9001:2015) (2015). Available at: https://www.iso.org/standard/62085.html.

Reda, F.A., Noble, J.H., Labadie, R.F. and Dawant, B.M. (2014) An artifact-robust, shape library-based algorithm for automatic segmentation of inner ear anatomy in post-cochlear-implantation CT. Proc. SPIE--the Int. Soc. Opt. Eng., 9034, 90342V.

Reda, F.A., McRackan, T.R., Labadie, R.F., Dawant, B.M. and Noble, J.H. (2014) Automatic segmentation of intra-cochlear anatomy in post-implantation CT of

unilateral cochlear implant recipients. Med. Image Anal., 18(3), 605–615.

Roland, J.T., Fishman, A.J., Alexiades, G. and Cohen, N.L. (2000) Electrode to Modiolus Proximity: A Fluoroscopic and Histologic Analysis. Am. J. Otol., 21(2), 218–25.

Schvartz-Leyzac, K.C., Holden, T.A., Zwolan, T.A., Arts, H.A., Firszt, J.B., Buswinka, C.J. and Pfingst, B.E. (2020) Effects of Electrode Location on Estimates of Neural Health in Humans with Cochlear Implants. JARO - J. Assoc. Res. Otolaryngol., 21(3), 259–275.

Simoni, E., Gentilin, E., Candito, M., Borile, G., Romanato, F., Chicca, M., Nordio, S., Aspidistria, M., Martini, A., Cazzador, D. and Astolfi, L. (2020) Immune Response After Cochlear Implantation. Front. Neurol., 11, 341.

Skinner, M.W., Holden, T.A., Whiting, B.R., Voie, A.H., Brunsden, B., Neely, J.G., Saxon, E.A., Hullar, T.E. and Finley, C.C. (2007) In vivo estimates of the position of Advanced Bionics electrode arrays in the human cochlea. Ann. Otol. Rhinol. Laryngol., 116(4), 2–24.

Verbist, B.M., Skinner, M.W., Cohen, L.T., Leake, P.A., James, C., Boëx, C., Holden, T.A., Finley, C.C., Roland, P.S., Roland, J.T., Haller, M., Patrick, J.F., Jolly, C.N., Faltys, M.A., Briaire, J.J. and Frijns, J.H.M. (2010) Consensus panel on a cochlear coordinate system applicable in histologic, physiologic, and radiologic studies of the human cochlea. Otol. Neurotol., 31(5), 722–730.

Van Wermeskerken, G.K.A., Van Olphen, A.F. and Graamans, K. (2009) Imaging of electrode position in relation to electrode functioning after cochlear implantation. Eur. Arch. Oto-Rhino-Laryngology, 266(10), 1527–1531.

Xu, J., Xu, S.A., Cohen, L.T. and Clark, G.M. (2000) Cochlear view: Postoperative radiography for cochlear implantation. Am. J. Otol., 21(1), 49–56.

Zhang, D., Liu, Y., Noble, J.H. and Dawant, B.M. (2016) Automatic localization of landmark sets in head CT images with regression forests for image registration initialization. Proc. SPIE--the Int. Soc. Opt. Eng., 9784, 97841M.

Zhao, Y., Dawant, B.M., Labadie, R.F. and Noble, J.H. (2014) Automatic localization of cochlear implant electrodes in CT. Med. image Comput. Comput. Interv., 17(Pt 1),

331–338.

Zhao, Y., Chakravorti, S., Labadie, R.F., Dawant, B.M. and Noble, J.H. (2019) Automatic graph-based method for localization of cochlear implant electrode arrays in clinical CT with sub-voxel accuracy. Med. Image Anal., 52(615), 1–12.

Zhao, Y., Dawant, B.M. and Noble, J.H. (2017) Automatic localization of cochlear implant electrodes in CTs with a limited intensity range. Proc. SPIE--the Int. Soc. Opt. Eng., 10133, 101330T 11 pp.

Artikel 1: Quality-assured training in the evaluation of cochlear implant electrode position: a prospective experimental study

Mewes et al. BMC Medical Education (2022) 22:386
https://doi.org/10.1186/s12909-022-03464-x

BMC Medical Education

RESEARCH Open Access

Quality-assured training in the evaluation of cochlear implant electrode position: a prospective experimental study

Alexander Mewes[1*], Sebastian Burg[2], Goetz Brademann[1], Jan Andreas Dambon[1] and Matthias Hey[1]

Abstract

Background: The objective of this study was to demonstrate the utility of an approach in training predoctoral medical students, to enable them to measure electrode-to-modiolus distances (EMDs) and insertion-depth angles (aDOIs) in cochlear implant (CI) imaging at the performance level of a single senior rater.

Methods: This prospective experimental study was conducted on a clinical training dataset comprising patients undergoing cochlear implantation with a Nucleus® CI532 Slim Modiolar electrode ($N = 20$) or a CI512 Contour Advance electrode ($N = 10$). To assess the learning curves of a single medical student in measuring EMD and aDOI, interrater differences (senior–student) were compared with the intrarater differences of a single senior rater (test–retest). The interrater and intrarater range were both calculated as the distance between the 0.1th and 99.9th percentiles. A "deliberate practice" training approach was used to teach knowledge and skills, while correctives were applied to minimize faulty data-gathering and data synthesis.

Results: Intrarater differences of the senior rater ranged from −0.5 to 0.5 mm for EMD and −14° to 16° for aDOI (respective medians: 0 mm and 0°). Use of the training approach led to interrater differences that matched this after the 4th (EMD) and 3rd (aDOI) feedback/measurement series had been provided to the student.

Conclusions: The training approach enabled the student to evaluate the CI electrode position at the performance level of a senior rater. This finding may offer a basis for ongoing clinical quality assurance for the assessment of CI electrode position.

Keywords: Cochlear implant, Quality assurance, Electrode position, Electrode-to-modiolus distance, Angular depth of insertion

Background

Intracochlear positioning of the cochlear implant (CI) electrode is essential for successful placement of the CI adjacent to the modiolus with minimum intracochlear trauma. The electrode's position is determined postoperatively, routinely by radiographic imaging techniques such as computer tomography (CT) or digital volume tomography (DVT). Therefore, measurements of electrode-to-modiolus distance (EMD) and angular depth of insertion (aDOI) are of clinical interest.

Within the framework of university education, these parameters are also measured by predoctoral medical students, and their inexperience may lead to diagnostic errors (missing findings or misinterpretation of findings) [1, 2]. Diagnostic errors are due primarily to cognitive bias, sources of which are, in radiology, usually associated with problems of visual perception

*Correspondence: alexander.mewes@uksh.de
[1] Universitätsklinikum Schleswig-Holstein (UKSH), Campus Kiel, Department of Otorhinolaryngology, Head and Neck Surgery, Kiel, Germany
Full list of author information is available at the end of the article

(scanning, recognition or interpretation) [1, 3]. According to Graber et al. (2018) [3], sources of cognitive bias include inadequate knowledge or skill on the part of the rater, faulty data-gathering (i.e., gathering and measuring information on relevant variables) and faulty information synthesis (i.e., processing and verification) [1, 3]. In medicine, the most common sources of bias are linked to poor information synthesis, and this can be subdivided into further factors [3, 4].

The weight of these cognitive factors depends on the expertise of the rater. While experienced raters are especially vulnerable to drawing premature conclusions (fast or type 1 thinking) [5], the major problems in decision-making by medical students are inadequate knowledge and skills, faulty context generation, faulty triggering, misidentification and premature conclusions [4]. However, an inexperienced rater will have a more analytical approach to decision-making, even though this (type 2) thinking needs more time. Type 2 thinking by medical students can thus provide a basis for careful CI image evaluation. For this, the student must be given the specific knowledge and skills on the one hand, while correctives are applied to minimize faulty data collection and information synthesis on the other.

Therefore, the aim of this work was (1) to use "deliberate training" (in the sense of Ericsson et al. [6, 7]), to prepare a single student for this task while also reducing cognitive bias; (2) to analyze the student's learning curves in measuring EMD and aDOI.

Our results lead us to hypothesize that it is possible to train a student such that he/she can measure EMD and aDOI at the level of an experienced senior rater.

Methods

Training approach

Deliberate practice to improve knowledge and skills

We assumed that the student had sufficient basic knowledge about the anatomy of the ear while still lacking specific skills, i.e., techniques for evaluating the intracochlear electrode position, software handling and knowledge about the influence of image-processing on the measurement results (especially effects of contrast enhancement and filtering). To teach these skills and bring the student up to the target performance level of an experienced senior rater, "deliberate practice" as defined by Ericsson et al. [6, 7] was conducted, including adequate access to training resources, a well-qualified trainer, learning goals to be achieved by the student, immediate feedback from the trainer and repeated fresh attempts by the student to achieve the goals gradually [6, 7].

Correctives to reduce faulty data-gathering and faulty information synthesis

As mentioned above, faulty context generation is a principal factor in diagnostic errors by medical students. However, decision-making by students may be affected by other cognitive biases, as noted in the background section. Therefore, our training approach addresses the following most common factors in information synthesis performed by medical students [4]. To reduce such bias, the following correctives, based on the taxonomy of Graber et al. (2018) [3], were implemented.

Faulty data-gathering

- Structured gathering of valid position parameters to describe the intracochlear electrode position (EMD, aDOI);
- Use of a consensual universal co-ordinate system of the cochlea to allow comparisons between raters.

Faulty information synthesis

- Considering several image reformations of the inner ear to detect the critical cochlear co-ordinates (e.g., round window, modiolar axis);
- Rater's freedom from expectations regarding the electrode position;
- Performance benchmark (target performance level) with continuous feedback of the rater's results; feedback when rater exceeds control limits;
- Awareness of current evidence in cochlear-implant-imaging evaluation (recurring feedback, constructive criticism, suggestions and support);
- Masking of relevant case information that allows conclusions about the electrode position, e.g. surgical report.

Following the idea of linear sequential unmasking (LSU) in nuclear physics [8] and forensics [9, 10], our clinical workflow in assessing the CI electrode position (EMD and aDOI measurements) was sequenced linearly as follows:

(1). Fitting a section plane to the basal cochlear turn within the sagittal plane;
(2). On the basis of this plane, reconstruction of the "cochlear view" (a two-dimensional cross-sectional image perpendicular to the modiolus and coplanar with the basal turn of the cochlea [11–15]);

(3). Optimizing the visualization of the electrode contacts by image-filtering and adjusting the image contrast;
(4). Applying a universal co-ordinate system with the helicotrema as center of the modiolus [12];
(5). Detecting required landmarks (helicotrema, round window; Fig. 1);
(6). Measuring the EMD from the center of the modiolus (helicotrema) to the center of each of the electrode contacts E1, E6, E11, E16 and E22 [16];
(7). Defining a line from the round window through the modiolus to the lateral wall of the cochlear as reference for measuring the aDOI;
(8). Measuring the aDOI at electrode contacts E1 and E22. The round window was set as zero degree angle [12].

Each of these steps was presented (unmasked) as a learning goal to the student in a sequential manner; irrelevant case information was masked as far as possible.

Design and setting of the study

The performance of the student during training (repeated feedback/measurement series) was compared with the target performance level achieved by a single senior rater. A prospective experimental study design was chosen. The study was located at a tertiary referral medical center with a cochlear-implant program.

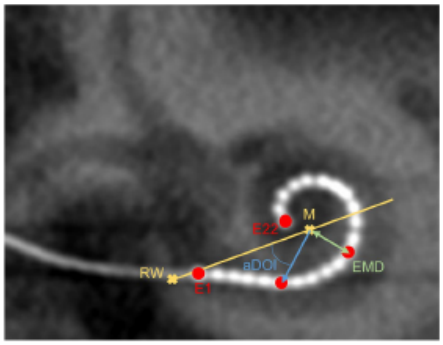

Fig. 1 Schematic illustration of the electrode-to-modiolus distance (EMD) and angular depth of insertion (aDOI) to be measured. Applying the cochlear view, EMD was measured from the center of the modiolus "M" (helicotrema) to the center of an electrode contact "E". A line from the round window "RW" through the modiolus to the lateral wall of the cochlear was the reference for measuring aDOI

Subjects

Imaging analysis was done within a clinical training dataset ($N = 30$) consisting two (repeated) EMD and aDOI measurement series of the senior rater. Subjects within this training dataset underwent cochlear implantation with a Nucleus® CI532 Slim Modiolar electrode ($N = 20$) or CI512 Contour Advance electrode ($N = 10$). Median age at implantation was 48 years (interquartile range, IQR: 30 years) and median preoperative PTA4AC was 96 dB (IQR 18 dB). $PTA4_{AC}$ indicated air-conduction pure-tone average threshold (0.5, 1, 2, 4 kHz) measured monaurally with circumaural headphones. Further demographic and CI-related characteristics of the subjects are given in Table 1. All subjects met the following inclusion criteria: round-window approach for intracochlear electrode insertion; absence of tip-foldovers and buckles of the electrode; absence of repeated insertions of the electrode; no anatomical abnormalities of the cochlear and auditory nerve. Furthermore, only tomography results with adequate image quality were analyzed, reducing system-related errors in distance and aDOI measurements. Adequate image quality was defined as the absence of artifacts due to motion and/or beam hardening.

Imaging analysis

Imaging was performed during the first week after cochlear implantation as part of our clinical routine. Within the training data set, computer tomography (CT) was used for all CI512 implants and digital volume tomography (DVT) was used for all CI532 implants. Imaging parameters were consistent with respect to an imaging voltage of 70–120 kV, a tube current of 1.1–5 mA/frame with pulsed X-ray emission and an exposure time of 7 s. Resolution and isotropic voxel size are given in Table 1. EMD and aDOI values were extracted from the "cochlear view" (Fig. 1) as previously described. In order to avoid confounding bias, the influence of the type of imaging and the resolution (matrix and voxel size) on the EMD/aDOI interrater differences under investigation was analyzed. For this, statistical tests mentioned in the following section were used to compare the central tendencies of two or more samples.

The software "KaVo eXam Vision" (KaVo Dental GmbH) was available for reconstructing the cochlear view and measuring the distances directly. Each cochlear-view image was further converted to JPEG format for measurement of aDOI using the software "ImageJ" (National Institutes of Health, Bethesda, MD). The lines drawn in this sectional view (EMD) served as the basis for the angle measurements.

Table 1 Demographic, CI-related and imaging characteristics of the subjects

Subject number	Sex	Ear implanted	Etiology of unilateral hearing loss	Implant type	Imaging type	Image matrix	Image voxel size (mm^3)
1	F	R	Unknown	CI512	CT	1280 × 1280	0.125 × 0.125 × 0.125
2	M	R	Otosclerosis	CI512	CT	800 × 600	0.2 × 0.2 × 0.2
3	M	R	Meniere's disease	CI512	CT	640 × 640	
4	F	R	Sudden hearing loss	CI512	CT	1280 × 1280	0.125 × 0.125 × 0.125
5	F	L	Unknown	CI512	CT	800 × 600	0.2 × 0.2 × 0.2
6	F	L	Familial	CI512	CT	1280 × 1280	0.125 × 0.125 × 0.125
7	M	R	Meniere's disease	CI512	CT	1280 × 1280	0.125 × 0.125 × 0.125
8	M	R	Unknown	CI512	CT	1280 × 1280	0.125 × 0.125 × 0.125
9	M	L	Unknown	CI512	CT	1280 × 1280	0.125 × 0.125 × 0.125
10	F	R	Infection	CI512	CT	1280 × 1280	0.125 × 0.125 × 0.125
11	M	R	Unknown	CI512	CT	1280 × 1280	0.125 × 0.125 × 0.125
12	F	R	Unknown	CI512	CT	1280 × 1280	0.125 × 0.125 × 0.125
13	M	L	Familial	CI532	DVT	800 × 600	0.2 × 0.2 × 0.2
14	M	R	Infection	CI532	DVT	800 × 600	0.2 × 0.2 × 0.2
15	F	L	Infection	CI532	DVT	640 × 640	0.25 × 0.25 × 0.25
16	F	R	Infection	CI532	DVT	640 × 640	0.25 × 0.25 × 0.25
17	F	L	Sudden hearing loss	CI532	DVT	800 × 600	0.2 × 0.2 × 0.2
18	M	R	Infection	CI532	DVT	640 × 640	0.25 × 0.25 × 0.25
19	M	L	Sudden hearing loss	CI532	DVT	640 × 640	0.25 × 0.25 × 0.25
20	F	L	Familial	CI532	DVT	640 × 640	0.25 × 0.25 × 0.25
21	F	L	Syndromal	CI532	DVT	640 × 640	0.25 × 0.25 × 0.25
22	M	L	Sudden hearing loss	CI532	DVT	640 × 640	0.25 × 0.25 × 0.25
23	F	R	Unknown	CI532	DVT	800 × 600	0.2 × 0.2 × 0.2
24	F	L	Unknown	CI532	DVT	640 × 640	0.25 × 0.25 × 0.25
25	M	L	Familial	CI532	DVT	640 × 640	0.25 × 0.25 × 0.25
26	M	R	Sudden hearing loss	CI532	DVT	640 × 640	0.25 × 0.25 × 0.25
27	M	L	Unknown	CI532	DVT	640 × 640	0.25 × 0.25 × 0.25
28	M	R	Unknown	CI532	DVT	640 × 640	0.25 × 0.25 × 0.25
29	F	R	Ototoxic	CI532	DVT	640 × 640	0.25 × 0.25 × 0.25
30	F	L	Sudden hearing loss	CI532	DVT	800 × 600	0.2 × 0.2 × 0.2

Data analysis

All statistical analyses were performed using the MATLAB™ software (The MathWorks, Inc., Natick, Massachusetts). The measurable variables are EMD and aDOI interrater differences (single senior rater – single student rater) in comparison of the senior's intrarater differences (test–retest of each image by the single rater). Shewhart charts were used to check whether interrater differences appeared to be within the target range (interpercentile range of the senior rater's intrarater differences). The interpercentile range (IPR) was defined as the distance between the 0.1th and 99.9th percentiles (P0.1 and P99.9). Since the data were not normally distributed, these percentiles were used here as control limits equivalent to ±3 standard deviation as originally defined by Shewhart [17]. Thus, results by the student are "out of control" if interrater differences exceed the IPR of the senior rater's intrarater differences.

The Shapiro–Wilk test was applied for testing whether the data were normally distributed. Since normal distribution did not apply to all variables, the Wilcoxon test was used to compare the central tendencies of two samples, and Friedman's test was used for comparing the central tendencies of several samples. Multiple-comparison post-hoc corrections using Dunn's test were applied to determine which samples differed from each other. The Brown–Forsythe test was applied to compare the variance of two samples. Statistical significance was defined as $p < 0.05$.

Intrarater reliability was analyzed by intraclass correlation and Bland–Altman analysis. Intraclass correlation coefficient (ICC) was also used to calculate the strength of agreement between the two raters. Following

the convention for intraclass correlation by McGraw and Wong [18], a 2-way mixed-effects model, multiple raters/measurements type with absolute agreement definition was chosen.

Results

Analysis of target performance

Intrarater reliability was calculated as the difference from two EMD and aDOI measurement series (test–retest) made by a single senior rater served as target performance level for the student. To present results clearly, EMD was summarized across all five electrode contacts measured (EMD_5). Neither central tendencies ($p = 0.77$) nor variances ($p = 0.24$) of the senior's intrarater EMD_5 differences differed statistically among these five electrode contacts. However, statistically significant differences were found in the variances of aDOI measurement series differences between contacts E1 and E22 ($p < 0.001$); therefore, these results were further analyzed, separately, for each of those contacts.

Sufficient intrarater reliability of the senior rater was ensured by means of intraclass correlation and Bland–Altman analysis. For EMD_5, the intraclass correlation coefficient ranged from 0.98 to 0.99, corresponding to an excellent intrarater reliability [19]. Intrarater reliability ranged from good to excellent for aDOI at electrode contacts E1 and E22, with ICC ranging from 0.82 to 0.96 and from 0.91 to 0.98, respectively.

As the intraclass correlation coefficient is expected to be high in repeated measurements by a single rater, intraclass correlation was supplemented by a Bland–Altman analysis. For EMD_5, the median difference (median bias) was 0 mm for the senior rater (Fig. 2; percentiles P0.1/P99.9 = ± 0.5 mm). Analyzing the aDOI at electrode contacts E1 and E22 revealed a median difference of − 1° and 0°, respectively (Fig. 3). The percentiles P0.1 and P99.9 were found to be − 5° and 8° for E1 and − 14° and 16° for E22. Median bias and spread did not vary with the average of the two measurement series, for all three variables (EMD_5, aDOI at E1, aDOI at E22).

Learning curves of the student rater

The Shewhart control chart for EMD_5 is shown in Fig. 4. In each measurement series by the student, interrater EMD_5 differences (average of two series by the senior rater relative to the student) were plotted. Error bars cover the IPR of these interrater differences, according to the control limits given by the (intrarater) IPR of the senior rater. Interrater differences did not differ from senior intrarater differences in any of the four measurement series when central tendencies were compared ($p = 0.46$). However, a learning effect was observed with respect to the scatter of the interrater differences. This scatter became smaller with successive measurement series; the target performance level was achieved in the 4th series. The intraclass correlation coefficient for the interrater

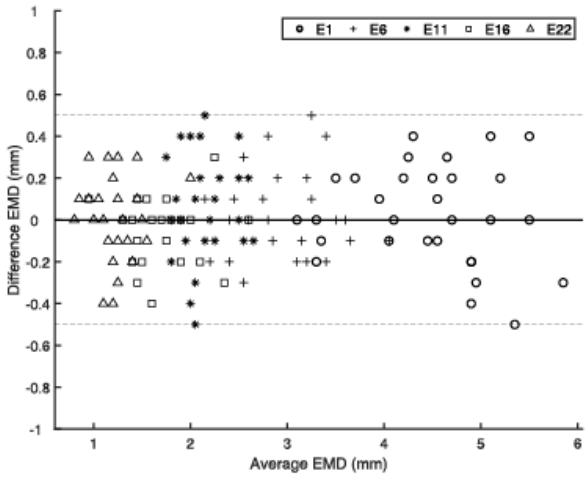

Fig. 2 Differences versus averages of two EMD measurement series made by a senior rater ($N = 30$). Applying the cochlear view, EMD was measured from the center of the modiolus (helicotrema) to the center of each of the electrode contacts E1, E6, E11, E16 and E22. A bold solid line indicates the median value (bias) of the senior rater's intrarater differences; both dotted lines cover the 0.1th to 99.9th interpercentile range

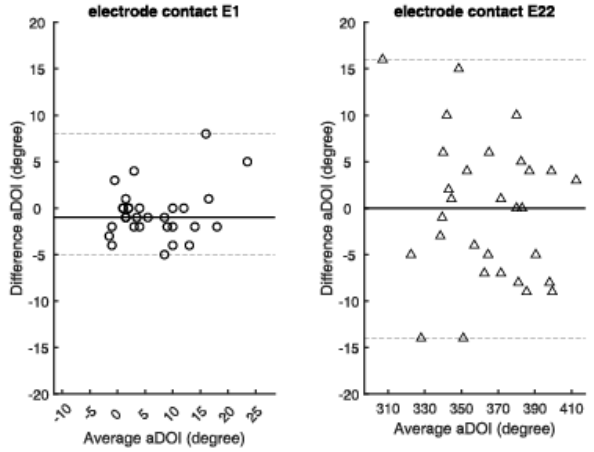

Fig. 3 Differences versus averages of two aDOI measurement series made by a senior rater ($N = 30$). Applying the cochlear view, a line from the round window through the modiolus to the lateral wall of the cochlear was the reference for measuring the aDOI at electrode contacts E1 (left panel) and E22 (right panel). A bold solid line indicates the median value (bias) of the senior rater's intrarater differences; both dotted lines cover the 0.1th to 99.9th interpercentile range

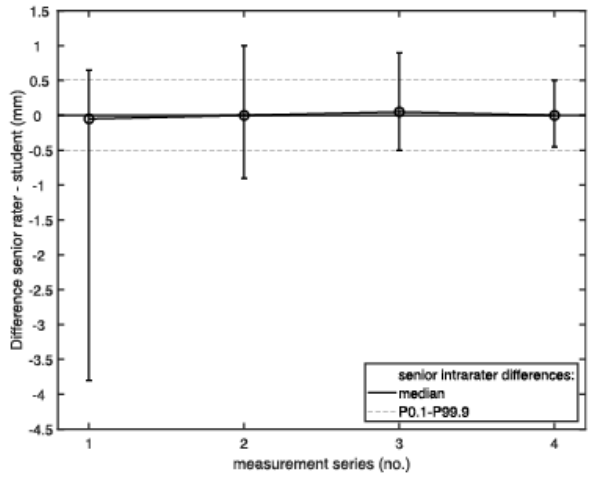

Fig. 4 Shewhart chart of a student measuring EMD ($N = 30$). In each measurement series, interrater EMD differences (average of two series by a senior rater – student) are plotted. Error bars cover the 0.1th to 99.9th interpercentile range (IPR) of these interrater differences, according to the control limits given by the senior rater's intrarater IPR (dotted lines). A bold solid line indicates the median value of the senior rater's intrarater differences. Median interrater differences are linked across the four measurement series by a thin solid line

IPR of this final series and the intrarater IPR of the senior rater ranged from 0.98 to 0.99.

Analysis of interrater aDOI differences at electrode contacts E1 and E22 also showed a reduction in their scatter along the measurement series (Fig. 5). Compared with the EMD_5 results, however, an interrater IPR less than or equal to the senior rater's intrarater IPR was already achieved with the third measurement series. Intraclass correlation coefficient for the interrater IPR of this final series and the intrarater IPR of the senior rater ranged from 0.71 to 0.93 (E1) and from 0.88 to 0.97 (E22).

In both electrode types (CI512, CI532) and electrode contacts (E1, E22) tested, Friedman's test indicated significant differences between the four data samples (interrater differences in measurement series 1 to 3; senior intrarater differences; $p < 0.05$). Post-hoc analysis revealed statistically significant differences between the student's first series and all others (for E1) and between this first series and the senior's intrarater differences (E22; Dunn's test, $p < 0.05$). Thus, in contrast to the EMD_5 findings, the aDOI results in the first measurement series differed from the target range not only in scatter, but also in central trend.

Confounding analysis

We identified the type of implant and imaging technique, and also image resolution and voxel size, as potential confounding variables in measuring the EMD and aDOI. Since CT was used for all CI512 implants and DVT was used for all CI532 implants, confounder analysis for type was done only once (CI512/CT versus CI532/DVT). Similarly for the image resolution, where the matrix and voxel size were linked: resolution low (640 × 640 and 0.25 mm), medium (800 × 600 and 0.2 mm) and high (1280 × 1280 and 0.125 mm). For both confounding variables, we investigated whether there were statistically significant differences in interrater differences between the characteristics.

Considering the EMD_5, no significant differences were found for type ($p = 0.99$) or resolution ($p = 0.86$).

In contrast, aDOI measurements at electrode contact E22 revealed a significant difference for type ($p < 0.01$). Interrater differences for C512/CT measurements were lower than for CI532/DVT (median −9° versus 1°, IPR 28° versus 17°) – i.e., the student reported greater aDOI values in CI512/CT than the senior rater. However, at electrode contact E1, interrater aDOI differences did not differ significantly between the two types ($p = 0.06$).

Considering the image resolution for interrater aDOI differences at electrode contacts E1 and E22, Friedman's test indicated significant differences between the resolution categories (low/medium/high; $p < 0.05$). Post-hoc analyses revealed significantly different mean ranks for the low- and high-resolution samples (Dunn's test, $p < 0.05$). The median of the aDOI differences was shifted to more negative values for the low resolution (E1: −4° with IPR 7 degree; E22: −8°, IPR 17°) than for the high resolution (E1: 0°, IPR 10°; E22: 3°, IPR 28°). This resulted

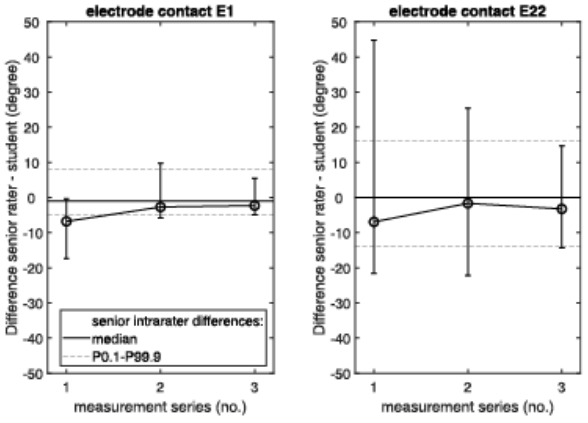

Fig. 5 Shewhart chart of the student measuring the aDOI at electrode contact E1 (left panel) and E22 (right panel). In each of the student's measurement series, interrater EMD differences (average of two series by a senior rater – student; $N = 30$) are plotted. Error bars show the 0.1th to 99.9th interpercentile range (IPR) of these interrater differences, according to the control limits given by the intrarater IPR of the senior rater (dotted lines). A bold solid line indicates the median value of the senior rater's intrarater differences. Median interrater differences are linked across the three measurement series by a thin solid line

from larger measured aDOI values of the student in images with low resolution compared with those of high resolution.

Nevertheless, confounding effects of implant/imaging type and resolution on aDOI were within the intrarater IPR of the senior rater, so no further allowance was made for them.

Discussion

Even with the introduction of automated tools for analyzing post-operative CI images [20–24], the manual evaluation of CI electrode position is still of general interest in clinical practice. However, findings can be missing or misinterpreted. For such diagnostic errors, sources of cognitive bias are of great importance, and can influence both experienced and inexperienced raters [4, 5]. Therefore, clinical quality assurance should both address the training of inexperienced raters and monitor continuously the performance of experienced raters.

To the best of our knowledge, no quality–assurance methods exist to train inexperienced raters in clinical evaluation of the CI electrode position. In this study, we introduce an approach that enabled a medical student to measure electrode-to-modiolus distances and angular insertion depth, both at the performance level of an experienced rater. This training approach requires time, staff and material resources, but is in line with international demands on clinical quality assurance [25, 26].

Moreover, the performance data within this training approach can be used as a benchmark to establish an ongoing clinical quality control. Benchmarking diagnostic performance is a key corrective strategy for reducing cognitive bias and has already been described as useful for quality control in radiology [1, 27, 28]. This seems reasonable, as raters are apparently vulnerable to heuristic failures, even when their learning process is complete [5].

Owing to the simplicity of this process, especially with regard to the small number of measurement series made by the student, we decided to use a Shewhart chart (an established statistical control tool in economics) to monitor training success [17]. However, Shewhart analysis is inefficient in detecting small changes (up to ±2 standard deviations) of the variable being monitored [29]. Thus, further clinical benchmarking could combine a Shewhart control chart with an analysis of cumulative sums (CUSUM) [30, 31]. A CUSUM chart is more efficient in detecting small changes in the process mean, as the control limits are more complex in design than with Shewhart (mostly V-mask design versus constant terms). Although the design of a CUSUM control chart may be complex, it has already been shown useful in evaluating competence in clinical procedures [32–35].

Use of even reference (target) data obtained by a single senior rater may limit their representativeness compared with a benchmark with data from several experienced raters. However, this work was to test only the general procedure, as a proof of concept. The measurable variables (EMD and aDOI differences between student and senior rater) were therefore compared with the latter's intrarater differences for independence of the EMD and aDOI magnitude: the senior rater's intrarater reliability in measuring EMD and aDOI was conformed by both correlations and by a Bland–Altman analysis. Nevertheless, our results simply demonstrate successful learning curves in measuring EMD and aDOI for a single student compared with a single senior rater.

For the last measurement series of both EMD and aDOI, the median was close to zero for intrarater differences of the senior rater as well as for interrater differences. However, we also analyzed the scatter. Following common practice in Shewhart analysis, this scatter covered 99.8% of data (± 3 standard deviations as defined by Shewhart [17]). Intrarater EMD differences (± 0.5 mm), on the one hand, were greater than the resolution used here (≤ 0.25 mm) and are thus clinically relevant. Nonetheless, the literature lacks comparative data for intrarater and interrater EMD differences. In several studies electrode-to-modiolus distances in cochlear implants was measured [16, 36–44]. However, information on intrarater or interrater differences is omitted, or simply the agreement between two raters is calculated; this was found to be similar to our results (ICC for EMD between 0.77 and 1 [40]).

In contrast to EMD, Fernandes et al. (2018) [45] measured aDOI and found a mean difference of −0.9° with a standard deviation of 43°. Since interrater differences were calculated for several raters, a greater scatter seems reasonable compared with the intrarater dispersion (up to 16°) for the single rater in the present study. Svrakic et al. (2015) [46] observed average intrarater aDOI differences within 10°, but provide no data on dispersion. Furthermore, without reporting intrarater or interrater differences, Escudé et al. (2006) [47] stated that aDOI measurements were performed by highly experienced radiologists. As cognitive bias can lead to diagnostic errors even for experienced raters, we suggest always quantifying the error made by the rater(s) when interpreting measurements in CI imaging. The central tendency and the scatter of intrarater/interrater differences should be indicated.

Conclusions

Evaluating CI electrode position by subjective image-processing may be affected by cognitive bias. The training of inexperienced raters marks the first step toward

quality-assured evaluation of CI images. By the training approach presented here, a single medical student became able to measure electrode-to-modiolus distances and insertion-depth angles at the performance level of a single senior rater. This approach should allow systematic teaching of knowledge and skills while applying corrective strategies to reduce faulty data-gathering and synthesis. Shewhart control charts can be used to monitor individual learning curves. Benchmarking the performance as a key corrective strategy can provide a basis for ongoing clinical quality assurance in evaluating the CI electrode position. This should also include quantifying the error made by rater(s) in interpreting measurements in CI imaging.

Abbreviations
EMD: Electrode-to-Modiolus Distance; aDOI: Angular Depth Of Insertion; CI: Cochlear Implant; CT: Computer Tomography; DVT: Digital Volume Tomography; LSU: Linear Sequential Unmasking; IQR: Interquartile Range; PTA4AC: Air-Conduction Pure-Tone Average threshold (0.5, 1, 2, 4 kHz); IPR: Interpercentile Range; ICC: Intraclass Correlation Coefficient; CUSUM: Analysis of Cumulative Sums.

Supplementary Information

The online version contains supplementary material available at https://doi.org/10.1186/s12909-022-03464-x.

Additional file 1. The raw aDOI and EMD data collected from imaging for analysis. M1 indicates measurement series no. 1, M2 series no. 2, etc.

Acknowledgements
Not applicable.

Authors' contributions
The study was designed by AM and MH. AM and SB collected the data. AM analyzed and interpreted the data. The manuscript was written by AM. All authors read and approved the final manuscript.

Funding
Open Access funding enabled and organized by Projekt DEAL.

Availability of data and materials
All data obtained and analyzed during this study are included in this published article and its supplementary information files.

Declarations

Ethics approval and consent to participate
The Ethics Committee at the Faculty of Medicine of Kiel University (CAU) approved all experimental protocols (reference: D457/20). Informed consent was obtained from all subjects as part of a general declaration of consent in clinical research. We confirm that all methods were carried out in accordance with relevant guidelines and regulations.

Consent for publication
Not applicable.

Competing interests
AM, GB, JAD and MH declare general financial support by Cochlear Ltd. (research grant to institution). Cochlear Ltd. was not involved in the study design, data collection and analysis, decision to publish, or preparation of this manuscript. JAD receives financial support within the framework of the clinician-scientist program of Kiel University's faculty of medicine. SB received no financial support for the research, authorship or publication of this article.

Author details
[1]Universitätsklinikum Schleswig-Holstein (UKSH), Campus Kiel, Department of Otorhinolaryngology, Head and Neck Surgery, Kiel, Germany. [2]Christian-Albrechts-Universität (CAU) zu Kiel, Faculty of Medicine, Kiel, Germany.

Received: 3 February 2022 **Accepted:** 13 May 2022
Published online: 20 May 2022

References

1. Lee CS, Nagy PG, Weaver SJ, Newman-Toker DE. Cognitive and system factors contributing to diagnostic errors in radiology. Am J Roentgenol. 2013;201(3):611–7.
2. Busby LP, Courtier JL, Glastonbury CM. Bias in radiology: the how and why of misses and misinterpretations. Radiographics. 2018;38(1):236–47.
3. Graber ML, Franklin N, Gordon R. Diagnostic error in internal medicine. Arch Intern Med. 2005;165(13):1493–9.
4. Braun LT, Zwaan L, Kiesewetter J, Fischer MR, Schmidmaier R. Diagnostic errors by medical students: results of a prospective qualitative study. BMC Med Educ. 2017;17(1):1–7.
5. Kahneman D. Thinking, fast and slow. New York: Farrar, Straus & Giroux; 2011. p. 19–89.
6. Ericsson KA, Krampe RT, Tesch-Römer C. The role of deliberate practice in the acquisition of expert performance. Psychol Rev. 1993;100(3):363–406.
7. Ericsson KA, Harwell KW. Deliberate practice and proposed limits on the effects of practice on the acquisition of expert performance: why the original definition matters and recommendations for future research. Front Psychol. 2019;10:2396.
8. Klein JR, Roodman A. Blind analysis in nuclear and particle physics. Annu Rev Nucl Part Sci. 2005;55:141–63.
9. Dror IE, Thompson WC, Meissner CA, Kornfield I, Krane D, Saks M, et al. Letter to the editor- context management toolbox: a linear sequential unmasking (LSU) approach for minimizing cognitive bias in forensic decision making. J Forensic Sci. 2015;60(4):1111–2.
10. Krane DE, Ford S, Gilder JR, Inman K, Jamieson A, Koppl R, et al. Sequential unmasking: a means of minimizing observer effects in forensic DNA interpretation. J Forensic Sci. 2008;53(4):1006–7.
11. Cohen LT, Xu J, Xu SA, Clark GM. Improved and simplified methods for specifying positions of the electrode bands of a cochlear implant array. Am J Otol. 1996;17(6):859–65.
12. Verbist BM, Skinner MW, Cohen LT, Leake PA, James C, Boëx C, et al. Consensus panel on a cochlear coordinate system applicable in histologic, physiologic, and radiologic studies of the human cochlea. Otol Neurotol. 2010;31(5):722–30.
13. Xu J, Xu SA, Cohen LT, Clark GM. Cochlear view: postoperative radiography for cochlear implantation. Am J Otol. 2000;21(1):49–56.
14. Eisenhut F, Lang S, Taha L, Doerfler A, Iro H, Hornung J. Merged volume rendered flat-panel computed tomography for postoperative cochlear implant assessment. Clin Neuroradiol. 2020;30(4):721–8.
15. Struffert T, Hertel V, Kyriakou Y, Krause J, Engelhorn T, Schick B, et al. Imaging of cochlear implant electrode array with flat-detector CT and conventional multislice CT: comparison of image quality and radiation dose. Acta Otolaryngol. 2010;130(4):443–52.
16. Mewes A, Brademann G, Hey M. Comparison of perimodiolar electrodes: imaging and electrophysiological outcomes. Otol Neurotol. 2020;41(7):e934–44.
17. Shewhart WA. Economic control of quality of manufactured product. New York: Van Nostrand; 1931.
18. McGraw KO, Wong SP. Forming inferences about some Intraclass correlation coefficients. Psychol Methods. 1996;1(1):30–46.
19. Koo TK, Li MY. A guideline of selecting and reporting intraclass correlation coefficients for reliability research. J Chiropr Med. 2016;15(2):155–63.
20. Noble JH, Schuman TA, Wright CG, Labadie RF, Dawant BM. Automatic identification of cochlear implant electrode arrays for post-operative assessment. In: Med Imaging 2011 Image Process, vol. 7962; 2011. p. 796217.

21. Zhao Y, Dawant BM, Labadie RF, Noble JH. Automatic localization of cochlear implant electrodes in CT. Med Image Comput Comput Assist Interv. 2014;17(Pt 1):331–8.
22. Noble JH, Dawant BM. Automatic graph-based localization of cochlear implant electrodes in CT. Med Image Comput Comput Assist Interv. 2015;9350:152–9.
23. Bennink E, Peters JPM, Wendrich AW, Jan Vonken E, Van Zanten GA, Viergever MA. Automatic localization of cochlear implant electrode contacts in CT. Ear Hear. 2017;38(6):e376–84.
24. Zhao Y, Labadie RF, Dawant BM, Noble JH. Validation of automatic cochlear implant electrode localization techniques using µCTs. J Med Imaging. 2018;5(03):1.
25. EN ISO 9000:2015, Quality management systems - Fundamentals and vocabulary.
26. EN ISO 9001:2015: Quality management systems - Requirements.
27. Soffa DJ, Lewis RS, Sunshine JH, Bhargavan M. Disagreement in interpretation: a method for the development of benchmarks for quality assurance in imaging. J Am Coll Radiol. 2004;1(3):212–7.
28. Ruutiainen AT, Scanlon MH, Itri JN. Identifying benchmarks for discrepancy rates in preliminary interpretations provided by radiology trainees at an academic institution. J Am Coll Radiol. 2011;8(9):644–8.
29. Montgomery DC. Introduction to statistical quality control. New York: Wiley; 1996.
30. Wald A. Sequential Analysis. New York: Wiley; 1947.
31. Page ES. Continous inspection schemes. Biometrika. 1984;41(1–2):100–15.
32. Van Rij AM, McDonald JR, Pettigrew RA, Putterill MJ, Reddy CK, Wright JJ. Cusum as an aid to early assessment of the surgical trainee. Br J Surg. 1995;82(11):1500–3.
33. Hammond EJ, McIndoe AK. Cusum: a statistical method to evaluate competence in practical procedures. Br J Anaesth. 1996;77(4):562.
34. Novick RJ, Stitt LW. The learning curve of an academic cardiac surgeon: use of the CUSUM method. J Card Surg. 1999;14(5):312–20.
35. Bolsin S, Colson M. The use of the cusum technique in the assessment of trainee competence in new procedures. Int J Qual Heal Care. 2000;12(5):433–8.
36. Balkany TJ, Eshraghi AA, Yang N. Modiolar proximity of three perimodiolar cochlear implant electrodes. Acta Otolaryngol. 2002;122(4):363–9.
37. Husstedt HW, Aschendorff A, Richter B, Laszig R, Schumacher M. Nondestructive three-dimensional analysis of electrode to modiolus proximity. Otol Neurotol. 2002;23(1):49–52.
38. Saunders E, Cohen L, Aschendorff A, Shapiro W, Knight M, Stecker M, et al. Threshold, comfortable level and impedance changes as a function of electrode-modiolar distance. Ear Hear. 2002;23(Suppl 1):28–40.
39. Van Wermeskerken GKA, Van Olphen AF, Graamans K. Imaging of electrode position in relation to electrode functioning after cochlear implantation. Eur Arch Oto-Rhino-Laryngology. 2009;266(10):1527–31.
40. Verbist BM, Joemai RMS, Briaire JJ, Teeuwisse WM, Veldkamp WJH, Frijns JHM. Cochlear coordinates in regard to cochlear implantation: a clinically individually applicable 3 dimensional CT-based method. Otol Neurotol. 2010;31(5):738–44.
41. Esquia Medina GN, Borel S, Nguyen Y, Ambert-Dahan E, Ferrary E, Sterkers O, et al. Is electrode-modiolus distance a prognostic factor for hearing performances after cochlear implant surgery? Audiol Neurotol. 2015;18(6):406–13.
42. Long CJ, Holden TA, McClelland GH, Parkinson WS, Shelton C, Kelsall DC, et al. Examining the electro-neural interface of cochlear implant users using psychophysics, CT scans, and speech understanding. J Assoc Res Otolaryngol. 2014;15(2):293–304.
43. Davis TJ, Zhang D, Gifford RH, Dawant BM, Labadie RF, Noble JH. Relationship between electrode-to-modiolus distance and current levels for adults with cochlear implants. Otol Neurotol. 2016;37(1):31–7.
44. Van Der Beek FB, Briaire JJ, Van Der Marel KS, Verbist BM, Frijns JHM. Intracochlear position of cochlear implants determined using CT scanning versus fitting levels: higher threshold levels at basal turn. Audiol Neurotol. 2016;21(1):54–67.
45. Fernandes V, Wang Y, Yeung R, Symons S, Lin V. Effectiveness of skull X-RAY to determine cochlear implant insertion depth. J Otolaryngol Head Neck Surg. 2018;47(1):1–7.
46. Svrakic M, Friedmann DR, Berman PM, Davis AJ, Roland JT, Svirsky MA. Measurement of cochlear implant electrode position from intraoperative post-insertion skull radiographs. Otol Neurotol. 2015;36(9):1486–91.
47. Escudé B, James C, Deguine O, Cochard N, Eter E, Fraysse B. The size of the cochlea and predictions of insertion depth angles for cochlear implant electrodes. Audiol Neurotol. 2006;11(Suppl 1):27–33.

Publisher's Note

Artikel 2: Evaluation of CI electrode position from imaging: comparison of an automated technique with the established manual method

Mewes et al. BMC Medical Imaging (2023) 23:143
https://doi.org/10.1186/s12880-023-01102-6

BMC Medical Imaging

RESEARCH Open Access

Evaluation of CI electrode position from imaging: comparison of an automated technique with the established manual method

Alexander Mewes[1*], Christopher Bennett[2], Jan Dambon[1], Goetz Brademann[1] and Matthias Hey[1]

Abstract

Background A manual evaluation of the CI electrode position from CT and DVT scans may be affected by diagnostic errors due to cognitive biases. The aim of this study was to compare the CI electrode localization using an automated method (image-guided cochlear implant programming, IGCIP) with the clinically established manual method.

Methods This prospective experimental study was conducted on a dataset comprising *N*=50 subjects undergoing cochlear implantation with a Nucleus® CI532 or CI632 Slim Modiolar electrode. Scalar localization, electrode-to-modiolar axis distances (EMD) and angular insertion depth (aDOI) were compared between the automated IGCIP tool and the manual method. Two raters made the manual measurements, and the interrater reliability (±1.96·SD) was determined as the reference for the method comparison. The method comparison was performed using a correlation analysis and a Bland-Altman analysis.

Results Concerning the scalar localization, all electrodes were localized both manually and automatically in the scala tympani. The interrater differences ranged between ±0.2 mm (EMD) and ±10° (aDOI). There was a bias between the automatic and manual method in measuring both localization parameters, which on the one hand was smaller than the interrater variations. On the other hand, this bias depended on the magnitude of the EMD respectively aDOI. A post-hoc analysis revealed that the deviations between the methods were likely due to a different selection of mid-modiolar axis.

Conclusions The IGCIP is a promising tool for automated processing of CT and DVT scans and has useful functionality such as being able to segment the cochlear using post-operative scans. When measuring EMD, the IGCIP tool is superior to the manual method because the smallest possible distance to the axis is determined depending on the cochlear turn, whereas the manual method selects the helicotrema as the reference point rigidly. Functionality to deal with motion artifacts and measurements of aDOI according to the consensus approach are necessary, otherwise the IGCIP is not unrestrictedly ready for clinical use.

Keywords Cochlear implant, IGCIP, Electrode localization, Electrode-to-modiolus-distance, EMD, Angular depth of insertion, aDOI; imaging

*Correspondence:
Alexander Mewes
alexander.mewes@uksh.de
[1] Department of Otorhinolaryngology, Head and Neck Surgery, Universitätsklinikum Schleswig-Holstein (UKSH), Campus Kiel, Arnold-Heller-Straße 3, 24105 Kiel, Germany
[2] Cochlear Ltd., Sydney, Australia

Background

Obtaining information about the intracochlear location of the electrode is of importance for the treatment of severe to profound hearing loss with a cochlear implant (CI). During the surgical phase, the surgeon must know whether the electrode has been placed

inside of the cochlea as intended. Prior to initial stimulation, the audiologist must be aware of the number of electrodes inserted into the cochlea and whether there is the presence of a tip fold-over. A tip fold-over is efficiently visualized with an X-ray image, however, other placement characteristics of clinical benefit are not able to be derived from X-ray imaging. To detect an incomplete insertion, it is helpful to measure the angular depth of insertion (aDOI) at the most basal electrode relative to the round window. Measurements of aDOI can be useful to balance, or at least to better evaluate, pitch perception in bilateral CI fittings between the ears. In additional to the insertion depth, information about the scalar localization and the proximity of the electrodes to the spiral ganglion cells are also of clinical interest for speech processor fitting. In clinical practice, these two spatial parameters can be examined in circumstances where the patients' postoperative speech understanding is worse than expected [1–6], or if ECAP thresholds or C and T levels are pathologically high [7–17]. When considering the development of new CI electrode arrays, measurements of the electrode-to-modiolar axis distance EMD with other physiological characteristics of cochlea are of importance to verify whether the arrays are behaving as intended.

High-resolution imaging techniques such as Computer Tomography (CT) or Digital Volume Tomography (DVT) are required instead of an X-ray to evaluate electrode array placement as landmarks or structural features of cochlea are not visible in X-ray images. Spatial parameters such as EMD, aDOI and scalar localization are extracted from two-dimensional planes that are reformatted by multiplanar reconstruction of the 3D volume data set. In clinical practice this procedure is conducted by manual image-processing and may be affected by diagnostic errors (missing findings or misinterpretation of findings). Diagnostic errors in radiology commonly result from a combination of system-related factors and cognitive-perceptual biases that can be present in both experienced and inexperienced raters [18–23]. The use of accurate, automatic electrode localization techniques could be helpful in reducing such diagnostic errors. Braithwaite et al. (2016) [24] and Bennink et al. (2017) [25] proposed semi-automated approaches for locating electrode arrays, that require manual initialization. A fully automated approach for determining the electrode position was developed at Vanderbilt University (which is currently not yet approved for general clinical use). This tool was designed to localize the electrode array as accurately as possible to identify and deactivate electrode contacts that may cause undesired channel interaction (image-guided cochlear implant programming, IGCIP) [26]. The primary spatial parameter that IGCIP uses for programming modifications is the shortest distance between the center of each electrode and the modiolar surface along the length of the modiolus [26] which is different to electrode-to-modiolar axis distances (EMD). That is, the modiolar surface represents the interface between the spiral ganglion cells and the intracochlear cavities (ST, SV). In addition, other established spatial parameters such aDOI, EMD and the scalar localization are also determined automatically with the IGCIP tool. Although the automatic electrode localization within IGCIP was ensured by experts [27], there is no external verification of the validity of these spatial parameters.

The aim of this work was therefore to compare the spatial parameters EMD, aDOI and scalar localization between the automatic approach and the clinically established manual method. The research question is whether one can measure these spatial parameters and attain comparable results with either the automatic or manual method.

Methods

Aim, design and setting of the study

This comparison study determines if two methods (automatic and manual) measure spatial parameters for locating the CI electrode array in an equivalent manner. A prospective experimental study design was chosen. The study was conducted at a tertiary referral medical center with a cochlear-implant program.

Subjects

Fifty adult subjects were to be included in the study who underwent cochlear implantation with a Nucleus® CI532 or CI632 Slim Modiolar electrode in the period of June 2019 to September 2021. The subjects also met the following inclusion criteria: void of adverse placements (buckles, tip fold-over); void of cochlear malformation; void of reinsertion of the array; available post-operative CT or DVT scan with isotropic voxel size $\lesssim 0.25$ mm and no less than ¼ head scan. A total of 123 patients were available that met the criteria, from which, 29 post-operative DVT scans (24%) had to be discarded due to motion artifacts which would have prevented a clear determination of electrode position. Motion artifacts were detected by manual screening of all scans for double contours. From the remaining patients, fifty subjects for this study were randomly selected. A post-operative DVT was analyzed for each of the fifty subjects. The DVT unit of this study was the 3D eXam by KaVo (Biberbach, Germany). Patients were seated during the scanning. All scans were performed with an image voltage of 120 kV, a tube current of 5 mA with pulsed X-ray emission, and an exposition time of 7 seconds. Data on image resolution, as

well as demographic and CI-related characteristics of the study population, are provided in Table 1.

Manual image analysis

Conventional DICOM viewers ("RadiAnt DICOM viewer", Medixant; "KaVO eXam Vision", KaVo Dental GmbH) were used for the manual measurements and the verification of the scalar localization of the electrode array as well as for checking the image quality (visual assessment). Two experts with experience in evaluating the electrode placement measured each of the 50 image sets [7, 16, 23]. The manual CI localization was performed in accordance with a consensus panel on a cochlear coordinate system [28], in which the mid-modiolar axis is perpendicular to a plane through the basal turn of the cochlea, with the helicotrema as the origin of this axis ('cochlear view') [16, 28, 29].

Spatial parameters were measured and extracted from this two-dimensional cross-sectional plane, and the center of the helicotrema has been used as the mid-modiolar axis (Fig. 1). To detect the helicotrema, the 2D plane of the cochlear view was moved along the mid-modiolar axis in the direction of the apex until the helicotrema was visible. Spatial parameters included:

- $aDOI_{manual}$, angle of insertion depth, relative to the chord produced between the mid-modiolar axis and the center of the round window (0°); the round window was directly detected visually in the cochlear view (Fig. 1).
- EMD_{manual}, distance from the center of an electrode to the mid-modiolar axis.
- Scalar localization of each electrode (scala tympani or scala vestibuli).

The parameters aDOI and EMD were measured at each even-numbered electrode and at electrode E1 of the total of 22 electrodes. From our experience, EMD and aDOI measurements at every second electrode provides a good compromise between accuracy, time requirements and the clinical interest.

The interrater reliability of measuring the aDOI and EMD manually was determined for the complete study population to be able to interpret the findings of the method comparison against *a priori* criteria. That is, the two raters have measured each spatial parameter once.

The scalar localization for each electrode was determined by further processing the cochlear view: A cross-section of the intracochlear lumen (transmodiolar reformation) and a curved reconstruction of the electrode path within the cochlea ("unrolling" the cochlea) [1, 7, 30–33].

Automatic image analysis

Automated data were calculated from DICOM measurements using the IGCIP tool. The first step in this method was to identify and to segment the anatomical structures of the inner ear (e.g., scala tympani, ST; scala vestibuli, SV; mid-modiolar axis) using post-operative DVT images [6, 34–37]. That is, a point distribution model ("atlas") of the cochlea is nonrigidly warped to register to a new patient DVT.

Each point of the model can be allocated to an anatomical landmark (e.g., center of the round window, RW; outer wall of the ST at 180° insertion depth). Pre-operative CT or DVT images were not available for all subjects. Post-operative DVT images were exclusively used for consistent segmentation of the cochlear anatomy [36, 37]. In a second step, the post-operative image was subsequently analyzed to locate the intracochlear electrodes [38–41] and merged with the post-operative image that included the segmented cochlear anatomy. Both the anatomy and electrode localization were visually verified to ensure that the automatic process was accurate (i.e. that all relevant anatomical structures and the electrodes had been located correctly).

By combining the two images created in steps one and two, a range of implant-to-anatomy measurements was automatically calculated and exported [42–44]. These included the following spatial parameters to be analyzed in this study:

- $aDOI_{auto}$, angle of insertion depth of each electrode, relative to the chord produced between the mid-modiolar axis and the center of the round window (0°), see Fig. 5 in [45] as an example.
- EMD_{auto}, minimal distance of the center of each electrode to the mid-modiolar axis. This is consistent with a cylindrical coordinate system where the mid-modiolar axis is the z-axis and the radius is the distance from the electrode to the axis. Fig. 1 in [41] visualizes the relationship between an CI electrode array and the modiolus exemplarily.
- Scalar localization of each electrode (scala tympani or scala vestibuli), see Fig. 5 in [45] as an example.

The EMD, aDOI and the scalar localization data were automatically calculated and exported by the IGCIP tool.

Confounding analysis

As a check for any confounding bias, the influence of image quality (IQ) and image resolution (matrix and voxel size) on the spatial parameters under investigation was analyzed. IQ was assessed subjectively in terms of image noise, contrast, sharpness and artifacts. For each of the

Table 1 Demographic, CI-related and imaging characteristics of the subjects

Subject number	Ear implanted	Etiology of unilateral hearing loss	Implant type	Image matrix	Size of isotropic image voxel (mm^3)	Image quality sum score (0 to 12)
1	L	Infection	CI632	640 x 640	0.25	4
2	R	Otosclerosis	CI632	800 x 800	0.2	5
3	R	Infection	CI632	800 x 800	0.2	7
4	L	Unknown	CI632	800 x 800	0.2	6
5	L	Syndromal	CI632	800 x 800	0.2	6
6	R	Unknown	CI632	800 x 800	0.2	5
7	R	Sudden hearing loss	CI632	800 x 800	0.2	7
8	R	Otosclerosis	CI632	640 x 640	0.25	7
9	L	Infection	CI632	800 x 800	0.2	5
10	L	Familial	CI632	800 x 800	0.2	5
11	R	Unknown	CI632	800 x 800	0.2	6
12	L	Unknown	CI632	800 x 800	0.2	7
13	L	Sudden hearing loss	CI632	800 x 800	0.2	8
14	R	Unknown	CI632	800 x 800	0.2	6
15	R	Meniere's disease	CI532	800 x 800	0.2	5
16	L	Granulomatosis	CI532	640 x 640	0.25	6
17	R	Congenital	CI632	800 x 800	0.2	7
18	L	Sudden hearing loss	CI632	800 x 800	0.2	5
19	R	Sudden hearing loss	CI632	800 x 800	0.2	6
20	R	Unknown	CI632	800 x 800	0.2	7
21	R	Sudden hearing loss	CI632	640 x 640	0.25	7
22	L	Sudden hearing loss	CI632	800 x 800	0.2	5
23	R	Trauma	CI632	800 x 800	0.2	4
24	L	Sudden hearing loss	CI632	800 x 800	0.2	6
25	R	Meniere's disease	CI632	800 x 800	0.2	5
26	R	Sudden hearing loss	CI632	640 x 640	0.25	6
27	R	Trauma	CI632	800 x 800	0.2	4
28	L	Ototoxic	CI632	800 x 800	0.2	7
29	L	Sudden hearing loss	CI632	800 x 800	0.2	6
30	L	Sudden hearing loss	CI632	800 x 800	0.2	8
31	L	Congenital	CI632	800 x 800	0.2	5
32	R	Otosclerosis	CI632	800 x 800	0.2	4
33	L	Otosclerosis	CI632	800 x 800	0.2	6
34	R	Unknown	CI632	800 x 800	0.2	5
35	R	Unknown	CI632	800 x 800	0.2	8
36	R	Congenital	CI632	800 x 800	0.2	7
37	L	Congenital	CI632	800 x 800	0.2	5
38	L	Unknown	CI632	800 x 800	0.2	7
39	R	Sudden hearing loss	CI632	640 x 640	0.25	8
40	R	Otosclerosis	CI632	800 x 800	0.2	7
41	R	Infection	CI532	640 x 640	0.25	5
42	R	Unknown	CI632	800 x 800	0.2	5
43	R	Meniere's disease	CI632	800 x 800	0.2	4
44	R	Otosclerosis	CI632	800 x 800	0.2	6
45	R	Infection	CI632	800 x 800	0.2	6
46	L	Sudden hearing loss	CI632	800 x 800	0.2	8
47	R	Sudden hearing loss	CI632	800 x 800	0.2	8
48	R	Unknown	CI632	800 x 800	0.2	5

Table 1 (continued)

Subject number	Ear implanted	Etiology of unilateral hearing loss	Implant type	Image matrix	Size of isotropic image voxel (mm^3)	Image quality sum score (0 to 12)
49	R	Sudden hearing loss	CI632	800 x 800	0.2	7
50	R	Unknown	CI632	800 x 800	0.2	6

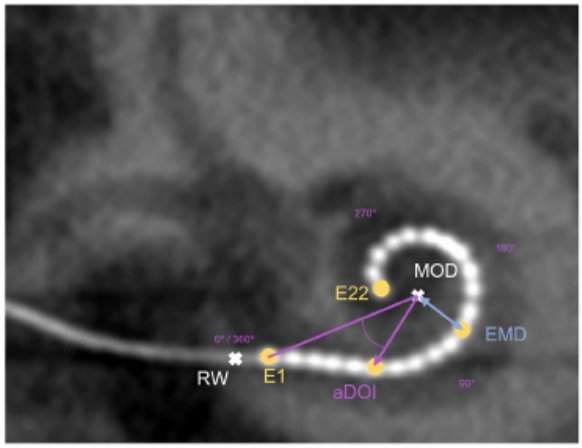

Fig. 1 Schematic illustration of spatial parameters to be measured: aDOI, angle of insertion depth, relative to the chord produced between the mid-modiolar axis "MOD" (helicotrema) and the center of the round window "RW" (0°); EMD, distance from the center of an electrode "E" to MOD

landmarks round window, mid-modiolar axis, electrodes and outer wall of the cochlear, the image quality was rated on a 4-point scale: 0, nondiagnostic; 1, sufficient for diagnostic use; 2, more than basic diagnostic; 3, diagnostic without restrictions [46]. A total IQ score was calculated from the sum of the points for all four structures, ranged from 0 to 12. IQ sum score, resolution and isotropic voxel size for each DVT scan are given in Table 1. For both confounding variables (image quality, image resolution), we investigated whether there were statistically significant differences in the bias between the methods. For this, the Wilcoxon test was used to compare the central tendencies of two samples, and an ANOVA was used for comparing the central tendencies of several samples.

Data analysis

All statistical analyses were performed using the MATLAB™ software (The MathWorks, Inc, Natick, Massachusetts). The variables analyzed were EMD, aDOI and scalar localization of each electrode, each of which measured manually and with the automatic tool. As aDOI and EMD were only measured manually at each even-numbered electrodes and E1, only these electrodes were used for the method comparison.

The Kolmogorov-Smirnov test was applied for testing whether the data were normally distributed. The analysis of data followed a procedure in a method-comparison study as suggested by Hanneman (2008) [47]. This procedure includes examining the relationship of the corresponding paired values as well as bias and precision statistics.

Visual inspection of scatter diagrams was conducted to examine potential relationships between the various parameters. The Pearson Product-moment correlation r and the confidence interval (*CoI*) were calculated for the purpose of interpretation.

Bias and precision statistics were generated with Bland-Altman plots to determine agreement between both methods [48–50]. To obtain the bias and the precision ("limits of agreement"), the mean values and ±1.96

standard deviations were calculated to all differences between the methods. As bias and precision statistics are calculated across all data points, proportional errors do not appear in the calculation. Therefore, the percentage error was calculated to consider the proportion between the magnitude of measurements and the bias/limits of agreement quantitatively. This error was obtained by dividing the limits of agreement (upper limit minus lower limit) by the mean value of the measurements obtained with the established (manual) method [51].

The interrater reliability (±1.96 standard deviation) of both raters served as the *a priori* criterion against which the method's bias and precision statistics were interpreted. The rater's interrater reliability in measuring the spatial parameters was confirmed by both an intraclass correlation (2-way mixed-effects model, multiple raters/measurements type with absolute agreement) and a Bland–Altman analysis.

Results

A priori calculation

Interrater differences of each spatial parameter were calculated as the difference from two manual measurement series made by two raters. For EMD, the bias (mean value of the differences) was 0 mm and the precision (±1.96 standard deviation) was ±0.2 mm. Analyzing the aDOI revealed a bias of 0° and the precision was found to be ±10°. The interrater precision of each parameter served a priori as the maximum value that would indicate acceptable agreement between the methods and precision of the difference. The interrater reliability was conformed by an excellent [52] intraclass correlation (ICC: 0.99 and 1), and, as mentioned above, by evidence of no bias in the interrater differences.

Method comparison of electrode location characteristics

Concerning the scalar localization, all 600 analyzed electrodes (12 electrodes × 50 arrays) were localized both manually and automatically in the scala tympani. No scalar crossing into the scala vestibuli was observed.

Scatter diagrams and Bland-Altman plots for EMD and aDOI are shown in Figs. 2 and 3. Each Bland-Altman plot (right) represents the automatic method minus the manual method depending on the corresponding average of automatic and manual measurement, with the bias (mean of differences) and the limits of agreement (±1.96 standard deviation). As illustrated in Figs. 2 and 3 (left panels), the data points for both the EMD and aDOI fall near on a line of equality, suggesting there is some degree of agreement between the methods. The correlation coefficient was r =0.95 (95% CoI = [0.94, 0.95]) for EMD and r = 0.99 (95% CoI = [0.99, 1]) for aDOI, respectively, with a significance level of p<0.001. Regarding the Bland-Altman plots (Figs. 2 and 3, right panels),

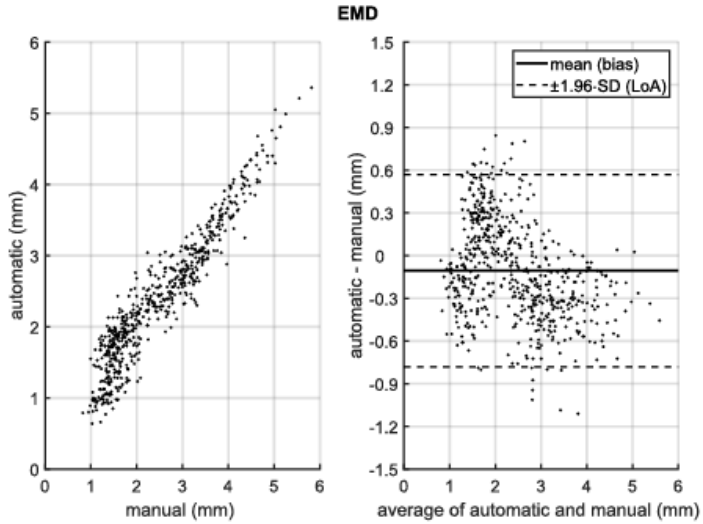

Fig. 2 (left) Scatter diagram of electrode-to-modiolar axis distances (EMD) measured manually and with the automatic tool; (right) Bland-Altman plot of EMD with mean (bias) and ±1.96 standard deviation (limits of agreement, LoA) differences between the automatic and manual method. EMD was analyzed from N=50 electrode arrays at each even-numbered electrode contact from E2 to E22, as well as at E1

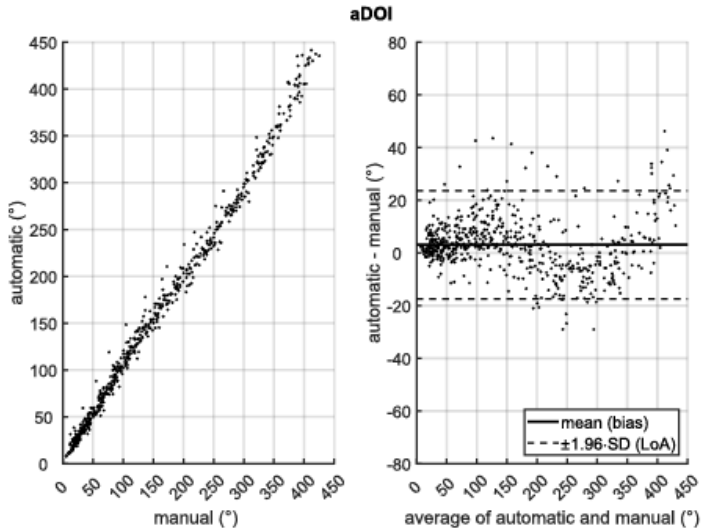

Fig. 3 (left) Scatter diagram of insertion depth angles (aDOI) measured manually and with the automatic tool; (right) Bland-Altman plot of aDOI with mean (bias) and ±1.96 standard deviation (limits of agreement, LoA) differences between the automatic and manual method. aDOI was analyzed from *N*=50 electrode arrays at each even-numbered electrode contact from E2 to E22, as well as at E1

there was no clinically relevant systematic bias between the methods as the bias fall within ±1.96 standard deviation of the manual interrater differences (EMD: -0.1 mm bias compared to ±0.2 mm ±1.96·SD; aDOI: 2° bias compared to ±10° ±1.96·SD). Nonetheless, the percentage error was calculated with 55% for EMD and 26% for aDOI, indicating a clinical importance of a proportional error to the magnitude of the measurements. The difference patterns of both Bland-Altman plots, by visual observation, are partially periodic and heteroskedastic. A polar plot was created to visualize the differences in the electrode localization between both methods in an electrode-specific manner (Fig. 4). With the automatic and manual method measured, the polar plot illustrates the mean value of aDOI and EMD for each of the 12 electrodes analyzed. Visual inspection of the polar plot gives rise to a suspicion that there is a systematic bias in the electrode localization due to the selection of the mid-modiolar axis.

Figure 5 presents a hypothetical scenario of an insertion of an electrode array inside of the cochlear and markups are generated using two different likely locations of the mid-modiolar axis. In this scenario the two sets of EMD are generated, one for each location of the mid-modiolar axis. Starting with electrode E8 the differences between the EMD are small. As the electrode number increases to E11, the difference between both sets of EMD increases. Thereafter, due to the way in which the electrode array conforms to the spiral shape of the cochlear duct, the differences decrease to E16 and then begin to increase. Thus, the difference in this hypothetical scenario confirm to a partial periodic pattern. In the hypothetical example displayed in Fig. 5 it was observed the variance pattern of differences between sets of EMD measurements are function of systematic differences in measurements. The systematic differences in measurements are caused by the initial section of the mid-modiolar axis of the cochlear view of the DVT scan. These systematic differences may be addressed by the adoption of uniform methods of achieving the cochlear and selecting the location of the mid-modiolar axis. Alternatively, as described in the next section, the systematic difference may be addressed by post-hoc algorithmic adjustment of electrode positions.

Algorithm to achieve post-hoc collocation of the mid-modiolar axis

The coordinates of the electrodes were measured relative to the selected mid-modiolar axis. For repeated sets of measures where each set was measured by a different rater, the distance between the selected modioli of the different raters is unknown. Unless the selections of the mid-modiolar axis

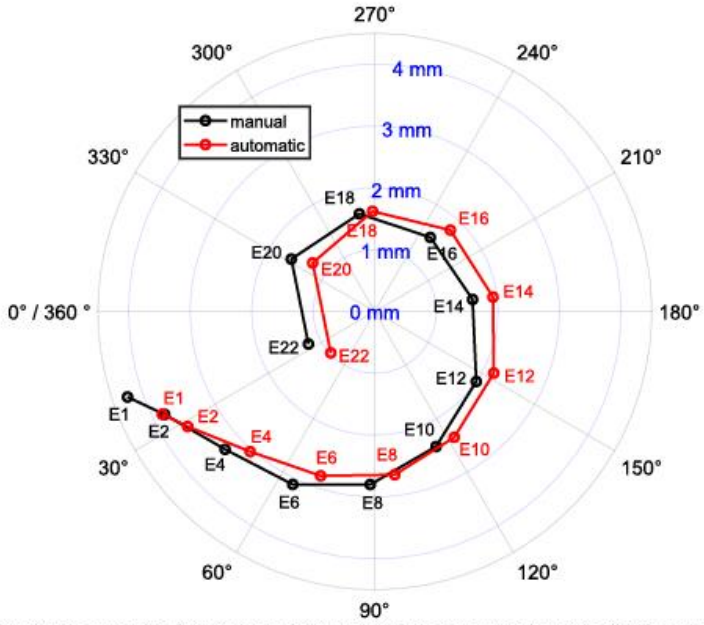

Fig. 4 Polar plot, illustrating the mean value of EMD (radius) and aDOI (angle) with the automatic and manual method for each of the electrodes analyzed (E1, E2, E4, E6, E8, E10, E12, E14, E16, E18, E20, E22). The center of the polar plot represents the mid-modiolar axis (helicotrema) of the cochlea

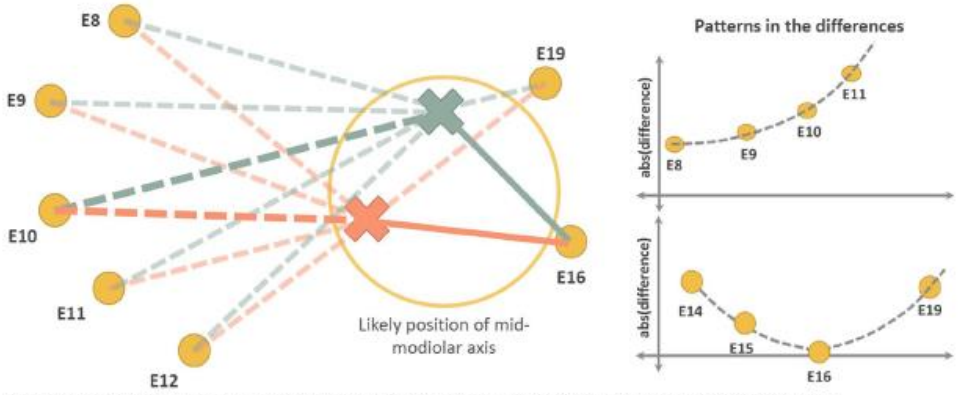

Fig. 5 Difference pattern effect from selecting different position of the mid-modiolar axis in a hypothetical CI electrode insertion

are relative to another coordinate system such as the medical image, it is not possible to directly adjust the measurements to having matching modioli. If the modioli were to be collocated, the resultant differences between the EMD of the different sets would be due to differences in the identification of the center of the round window as well as of the

locations of the electrodes in the DVT scan. As described by Fig. 5, the partial periodic difference pattern is likely due to a difference in the selection of the mid-modiolar axis. The closer the modioli are collocated, the less pronounced is the partial periodic difference pattern. It can be inferred, to post-hoc achieve a better match of the modioli of set of measurements, the coordinates of a set of electrodes can be uniformly altered in such a way to minimise the magnitude of the partial period difference pattern, where the magnitude of the partial period difference pattern can be measured by Pearson's correlation (ρ) between the sets of measurements. A correlation value closer to 0 conveys a greater difference in the selection of the mid-modiolar axis (more pronounced difference pattern), a correlation value closer (+)1 conveys a smaller difference (less pronounced difference pattern). This process can be automated by calculating the uniform alteration in coordinates by minimising a cost function via an optimisation algorithm.

$$EMD = [EMD_1, EMD_2, \ldots, EMD_{22}] \tag{1}$$

$$aDOI = [aDOI_1, aDOI_2, \ldots, aDOI_3] \tag{2}$$

where EMD is an array of EMD where each element is an individual measurement corresponds to an electrode, and $aDOI$ is an array of aDOI where each element is an individual measurement corresponds to an electrode.

$$E_x = EMD \times \cos(aDOI) \tag{3}$$

$$E_y = EMD \times sin(aDOI) \tag{4}$$

where E_x is an array of x-coordinates with 22 elements where each element corresponds to an electrode, and E_y is an array y-coordinates with 22 elements where each element corresponds to an electrode.

$$E_{x,t} = E_x + shift_x \tag{5}$$

$$E_{y,t} = E_y + shift_y \tag{6}$$

where $E_{x,t}$ is the altered x-coordinates, $shift_x$ is the value of the alteration on the x-axis, $E_{y,t}$ the altered y-coordinates, and $shift_y$ is the value of the alteration on the y-axis.

$$EMD_t = \sqrt{E_{x,t}^2 + E_{y,t}^2} \tag{7}$$

$$aDOI_t = artan2(E_{y,t}^2, E_{x,t}^2) \tag{8}$$

$$aDOI_{t,i} = \begin{cases} aDOI_{t,i} + 2\pi, if\ aDOI_{t,i} < 0 \\ aDOI_{t,i} \end{cases}, for\ 1 \le i \le 22 \tag{9}$$

$$aDOI_{t,i} = \begin{cases} aDOI_{t,i} + 2\pi, if (\sum_{j=1}^{i-1} (aDOI_{t,j} \ge \frac{3\pi}{2} \cap aDOI_{t,j} \le 2\pi \cap aDOI_{t,j+1} \ge 0 \cap aDOI_{t,j+1} \le \frac{\pi}{2})) > 0 \\ aDOI_{t,i} \end{cases}, for\ 2 \le i \le 22 \tag{10}$$

where the EMD_t is the altered EMD, and $aDOI_t$ is the altered $aDOI$.

$$cost\left(shift_x, shift_y\right) = \left(1 - \rho(EMD_t^{set_1}, EMD^{set_2})\right) + \left(1 - \rho(aDOI_t^{set_1}, aDOI^{set_2})\right) \tag{11}$$

where $cost\left(shift_x, shift_y\right)$ calculates the cost of the uniformly altered coordinates of the set 1 (set_1) of the measurements.

Figure 6 display the Bland-Altman plot for EMD and aDOI from Figs. 2 and 3 after the optimization algorithm has been applied. For both variables, EMD and aDOI, smaller limits of agreement were obtained after optimization, i.e., a more precise agreement between both methods. The ±1.96-fold standard deviation was reduced after optimization by 71% for the EMD (0.7 mm to 0.2 mm) and by 33% for the aDOI (21° to 14°). The remaining standard deviation was thus within the range of ±1.96-fold SD for the interrater deviation of the manual method. It is then not of clinical relevance that a slight periodic pattern of aDOI differences remained even with the post-hoc algorithmic adjustment (Fig. 6, right panel).

Confounding analysis

It was analyzed whether the confounding variables image quality score (IQ) and image resolution (IR) had an impact on the bias between both methods for each of the two spatial parameters (EMD, aDOI). The Wilcoxon test was used to compare the central bias tendencies of both IR samples (0.2 mm versus 0.25 mm voxel size) and a one-way ANOVA was used for comparing the central tendencies of the five IQ samples (IQ scores 4, 5, 6, 7 and 8). Only these

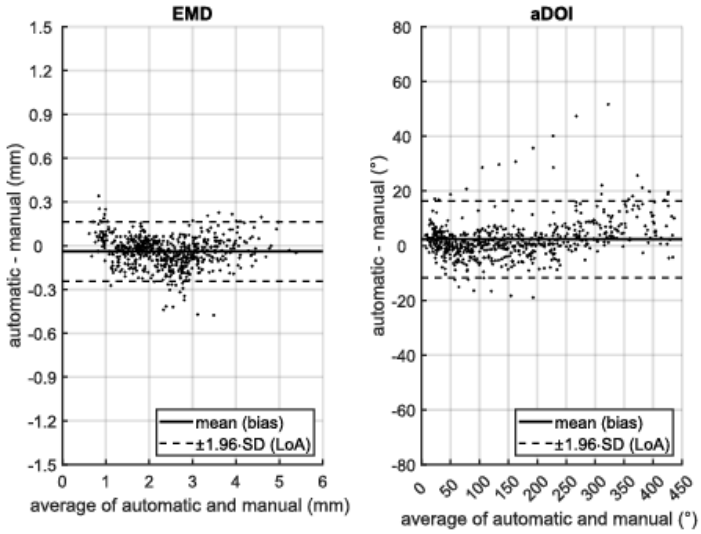

Fig. 6 Differences between the automatic and manual method after eliminating the systematic differences may be addressed by selecting a different location of the mid-modiolar axis. Bland-Altman plots of EMD (left) and aDOI (right) with mean (bias) and ±1.96 standard deviation (limits of agreement, LoA) differences between the automatic and manual method. EMD and aDOI were analyzed from *N*=50 electrode arrays at each even-numbered electrode contact from E2 to E22, as well as at E1

five IQ scores were analyzed as the measured scores covered this range of values (frequency relative to *N*=50 subjects: IQ4 10%, IQ5 28%, IQ6 26%, IQ7 24%, IQ8 12%).

When considering the image resolution IR, there were statistically significant differences in the bias between 0.2 mm and 0.25 mm ($p<0.001$ and $p<0.05$) for both EMD and aDOI, but these differences were within the range of ±1.96-fold SD for the interrater deviation of the manual method.

In the analysis of IQ, no significant differences were found between the five IQ samples for both EMD ($p=0.22$) and aDOI ($p=0.59$) using ANOVA. Thus, neither IR nor IQ had a relevant influence on the method comparison in this study and were therefore not addressed in the further analysis.

Discussion

CT and DVT imaging provide CI electrode array positioning and cochlear anatomical information beyond what is possible by X-ray. Current standard practice to derive this information involves manual measurements. Vanderbilt University's IGCIP tool is a quasi-fully automated approach to provide information about the intracochlear electrode location to the audiologist, who is generally inexperienced in imaging and its analysis. This automated approach reduces financial and human resources by allowing audiologists to perform the evaluation with the tool themselves, rather than having it performed by a radiologist. Furthermore, automation has the potential to improve the quality of CI electrode localization by eliminating human error and improving consistency and accuracy. For general clinical use automated techniques in processing CT or DVT images are required to be as accurate and precise as manual measurements of experience experts. As far as the authors of this paper is aware the IGCIP tool is yet to be approved for use in clinical practice.

It was therefore the aim of this study to contribute to assessment of the validity of IGCIP. For this objective, spatial parameters of clinical and research interest (EMD, aDOI, scalar localization) were compared between the IGCIP approach and the clinically established approach of manual measurements.

Methodical limitations

This study cannot assess the "accuracy" of the automated approach, because the manual approach is not a gold standard that is calibrated to be highly accurate and consistent. This work was rather a method-comparison study, comparing a less-established method with a clinically established method, and thus calculating the "bias" between the two approaches. Regardless of this limitation, the claim of the present study was to compare the

automatic approach with a manual method that was as accurate as possible. For this reason, two raters with experience in evaluating CI electrode location made the manual measurements. The interrater reliability was confirmed by an excellent intraclass correlation and the ±1.96-fold SD of the EMD interrater differences was in the range of the image resolution (0.2 to 0.25 mm). It must be noted that this interrater reliability was achieved after repeated series of manual measurements, since at the study's beginning there were some methodological differences between the raters in the detection of relevant landmarks (round window, mid-modiolar axis). To calibrate the manual method as accurate as possible, both raters had to follow the consensus panel on a cochlear coordinate system [28] exactly. It can be assumed that there are probably larger variations between different raters in the manual evaluation of the CI electrode localization in everyday clinical practice than the results here demonstrate.

Additional limiting factors address the extent to which the data can be compared. The bias reported are on parameters that were derived from Cartesian coordinates. Computation of a rigid transformation between automatic and manual electrode labels could specify and quantify the bias in more detail. However, this was not feasible as the data required was not available from the automatic tool. Another limitation is that solely 2D projections were used for the manual evaluation, while the automatic method processed 3D data. For a direct comparison, both methods should the spatial parameters from a 3D dataset. In this work the evaluation of 2D projections was chosen as a reference as it is the clinically established method.

Effect of image quality

With the automatic IGCIP tool, it was possible to successfully analyze the electrode position in all 50 images. The image resolution parameters used here (voxel sizes 0.2 mm and 0.25 mm) and the image quality score had no influence on the results of the automatic evaluation compared to the manual evaluation. When evaluating the clinical usability of the IGCIP tool, it should be noted that only images absent of motion artifacts were analyzed in this study. In a preliminary examination of the tool, the presence of such artifacts resulted in an error message, and the frequency of DVT scans with motion artifacts was not low at 24% of the 123 subjects that were initially available. This would mean that in up to a quarter of the cases available for the evaluation of the electrode position would have to be conducted done manually. The presence of these motion artifacts would reduce the accuracy of the manual measurements in comparison to nominal scans.

In this study, post-operative DVT scans were used instead of pre-operative scans to segment the intracochlear structures due an absence of pre-operative scans for a sizeable number of subjects. At our clinic, pre-operative scans are performed off-site at different radiology centers. These datasets were not completely been available at the time of the study, and available scans were performed with different acquisition parameters, which would have led to an additional bias in this study. The ability to segment the intracochlear structures with post-operative DVT scans demonstrated the versatility and usefulness of the IGCIP tool. Accuracy of the segmentation of the cochlear structures, including critical landmarks such as the mid-modiolar axis and the round window, may have been obscured by the metallic electrode artifacts in post-operative scans [27, 37]. From the use and analysis of the tool we believe that the IGCIP tool was found to be accurate in determining the CI electrode position even when the cochlear structures were segmented with post-operative scans [37].

Selection of the mid-modiolar axis

It was demonstrated that the differences between the automatic and manual method in localization the electrode position were primarily due to a different selection of the mid-modiolar axis. The influence of the localization of this axis on both electrode modiolus distance and angular insertion depth is obvious, as it is a significant landmark for the measurement of these two parameters (see sections "Manual image analysis" and "Automatic image analysis"). Manual image evaluation in this work was performed in accordance with a consensus panel on a cochlear coordinate system [28], in which the mid-modiolar axis is perpendicular to a plane through the basal turn of the cochlea, with the helicotrema as the origin of this axis. If the mid-modiolar axis is not perpendicular to the basal plane, it is imprecise to choose the helicotrema as a reference point for determining EMD in the *basal* region of the cochlea. It is therefore more reasonable to define the EMD as the smallest distance of an electrode to the mid-modiolar axis, which is the z-axis of the modiolus shaped as a cylinder, as is done in the IGCIP tool. Thus, EMD measurements with the automated method appear to be more accurate than with the clinical manual method used here. Unfortunately, it was not possible to verify the selection of the mid-modiolar axis with the IGCIP software, because the tool did not plot the axis to the user.

When determining the angular insertion depth aDOI, selecting the z-axis of the cylindrically shaped modiolus is less useful than for the EMD measurements. This is because in the case of an oblique mid-modiolar axis, the reference plane for measuring the aDOI would change

depending on the cochlear turn. With the IGCIP tool, the angular depth of insertion is measured in the 0° plane that is the plane that contains both the mid-modiolar axis line and the center of the round window (correspondence with Jack Noble, Vanderbilt University). This reference plane contains the center of the mid-modiolar axis in the *basal* turn of the cochlear, in the case of an oblique mid-modiolar axis, this may explain the deviating aDOI data compared to the manual method, in which the *helicotrema* has been selected as the center of the axis [28].

To reduce the variability between different electrode localization techniques, methods such as the algorithm proposed Wimmer et al. [53] couldbe widely implemented to robustly detect critical landmarks as the mid-modiolar axis. There are also opportunities for future research to address the development of electrode location parameters that are independent of critical landmarks such as the mid-modiolar axis. For this purpose, an update of the consensus panel reflecting advances in automation capabilities would be appreciated.

Conclusions

In all cases of DVT scans with a spatial resolution of 0.2 to 0.25 mm and absent motion artifacts, it was feasible to evaluate the electrode position with the IGCIP tool. Motion artifacts are not rare in our clinical practice (a quarter of cases), thus requiring a manual electrode localization when the post-operative DVT scan is used for segmentation of cochlear structures. There are systematic differences in the measurement of EMD and aDOI between the automatic and manual method, which is likely due to a different selection of the mid-modiolar axis. When controlling for the selection of the mid-modiolar axis the manual measurements and outputs of the tool are comparable. When measuring EMD, the IGCIP tool is superior to the manual method because the smallest possible distance to the axis is determined depending on the cochlear turn, whereas the manual method selects the helicotrema as the reference point rigidly. With respect to the measurement of aDOI, the IGCIP tool uses the center of the mid-modiolar axis in the *basal* plane of the cochlea (0° plane), which is not in accordance with the consensus panel on a cochlear coordinate system [28].

In conclusion, the IGCIP is a promising tool for the automated processing of CT and DVT images. The tool is able to detect key landmarks of the intracochlear structure and identify the location of the electrodes relative to these structures. Demonstrated by the methodology of this study, the functionality of being able to segment the cochlear with post-operative scans provides an additional benefit in circumstances where pre-operative scans are not available or are not of sufficient quality. The tool is equally as impacted as human rates in response to clinical anomalies such as motion artifacts in the images and systematic differences between measurements cause by the selection of the mid-modiolar axis. For general clinical use we recommend the addition of functionality to mitigate or deal with motion artifacts and a more streamlined approach for manual intervention of the selection of the mid-modiolar axis. Without usability with motion artifacts and measurements of aDOI according to the consensus approach, the IGCIP tool is not unrestricted ready for clinical use. For research purposes a translation of the outputs of the tool to the consensus paper on the cochlear coordinate system would be beneficial.

Abbreviations

CI	Cochlear Implant
CT	Computer Tomography
IGCIP	Image-guided Cochlear Implant Programming
EMD	Electrode-to-Modiolar axis Distance
aDOI	Angular Depth of Insertion
SD	Standard Deviation
DVT	Digital Volume Tomography
ST	Scala Tympani
SV	Scala Vestibuli
MOD	Mid-modiolar axis
DICOM	Digital Imaging and Communications in Medicine
E	Electrode
RW	Round Window
IQ	Image Quality
ICC	Intraclass Correlation Coefficient
CoI	Confidence Interval
LoA	Limits of Agreement
IR	Image Resolution

Acknowledgements
Not applicable.

Authors' contributions
The study was designed by AM and MH. AM and CB collected the data. AM and CB analyzed the data and AM interpreted the data. The manuscript was written by AM and CB. All authors read and approved the final manuscript.

Funding
Open Access funding enabled and organized by Projekt DEAL. This work was supported by Cochlear Ltd. (Sydney, Australia). Open Access funding made possible and organized by project DEAL.

Availability of data and materials
The datasets generated and/or analyzed during the current study are not publicly available due to a confidential agreement with the sponsor of the study (Cochlear Ltd., Australia) but are available from the corresponding author on reasonable request.

Declarations

Ethics approval and consent to participate
The Ethics Committee at the Faculty of Medicine of Kiel University (CAU) approved all experimental protocols (reference: D 522/21). Informed consent was obtained from all subjects. We confirm that all methods were carried out in accordance with relevant guidelines and regulations.

Consent for publication
Not applicable.

Competing interests
AM, JD, GB and MH declare general financial support by Cochlear Ltd. (research grant to institution). CB is an employee of Cochlear Ltd. (Sydney, Australia). CB contributed to the data collection, analysis, and preparation of this manuscript. Cochlear Ltd. was not involved in the study design and decision to publish. The authors alone are responsible for the content and writing of this paper. JD receives financial support within the framework of the clinician-scientist program of Kiel University's faculty of medicine.

Received: 13 February 2023 **Accepted:** 13 September 2023
Published online: 29 September 2023

References

1. Aschendorff A, Kromeier J, Klenzner T, Laszig R. Quality control after insertion of the Nucleus Contour and Contour Advance electrode in adults. Ear Hear. 2007. https://doi.org/10.1097/AUD.0b013e318031542e.
2. Wanna GB, Noble JH, Carlson ML, Gifford RH, Dietrich MS, Haynes DS, et al. Impact of electrode design and surgical approach on scalar location and cochlear implant outcomes. Laryngoscope. 2014. https://doi.org/10.1002/lary.24728.
3. Holden LK, Finley CC, Firszt JB, Holden TA, Brenner C, Potts LG, et al. Factors affecting open-set word recognition in adults with cochlear implants. Ear Hear. 2013. https://doi.org/10.1097/AUD.0b013e3182741aa7.
4. O'Connell BP, Cakir A, Hunter JB, Francis DO, Noble JH, Labadie RF, et al. Electrode location and angular insertion depth are predictors of audiologic outcomes in cochlear implantation. Otol Neurotol. 2016. https://doi.org/10.1097/MAO.0000000000001125.
5. Chakravorti S, Noble JH, Gifford RH, Dawant BM, O'Connell BP, Wang J, et al. Further evidence of the relationship between cochlear implant electrode positioning and hearing outcomes. Otol Neurotol. 2019. https://doi.org/10.1097/MAO.0000000000002204.
6. Skinner MW, Holden TA, Whiting BR, Voie AH, Brunsden B, Neely JG, et al. In vivo estimates of the position of Advanced Bionics electrode arrays in the human cochlea. Ann Otol Rhinol Laryngol. 2007. https://doi.org/10.1177/000348940711600401.
7. Liebscher T, Mewes A, Hoppe U, Hornung J, Brademann G, Hey M. Electrode translocations in perimodiolar cochlear implant electrodes: Audiological and electrophysiological outcome. Z Med Phys. 2020. https://doi.org/10.1016/j.zemedi.2020.05.004.
8. Müller A, Hocke T, Mir-Salim P. Intraoperative findings on ECAP-measurement: normal or special case? Int J Audiol. 2015. https://doi.org/10.3109/14992027.2014.969410.
9. Long CJ, Holden TA, McClelland GH, Parkinson WS, Shelton C, Kelsall DC, et al. Examining the electro-neural interface of cochlear implant users using psychophysics, CT scans, and speech understanding. JARO - J Assoc Res Otolaryngol. 2014. https://doi.org/10.1007/s10162-013-0437-5.
10. Perenyi A, Toth F, Dimak B, Nagy R, Schoerg P, Jori J, et al. Electrophysiological measurements with electrode types of different perimodiolar properties and the same cochlear implant electronics - A retrospective comparison study. J Otolaryngol - Head Neck Surg. 2019. https://doi.org/10.1186/s40463-019-0361-8.
11. Mittmann P, Ernst A, Todt I. Intraoperative electrophysiologic variations caused by the scalar position of cochlear implant electrodes. Otol Neurotol. 2015. https://doi.org/10.1097/MAO.0000000000000736.
12. Mittmann P, Todt I, Ernst A, Rademacher G, Mutze S, Göricke S, et al. Electrophysiological detection of scalar changing perimodiolar cochlear electrode arrays: A long term follow-up study. Eur Arch Oto-Rhino-Laryngology. 2016. https://doi.org/10.1007/s00405-016-4175-2.
13. van Wermeskerken GKA, van Olphen AF, Graamans K. Imaging of electrode position in relation to electrode functioning after cochlear implantation. Eur Arch Otorhinolaryngol. 2009. https://doi.org/10.1007/s00405-009-0939-2.
14. Poley M, Overmyer E, Craun P, Holcomb M, Reilly B, White D, et al. Does pediatric cochlear implant insertion technique affect intraoperative neural response telemetry thresholds? Int J Pediatr Otorhinolaryngol. 2015. https://doi.org/10.1016/j.ijporl.2015.05.038.
15. Degen CV, Büchner A, Kludt E, Lenarz T. Effect of electrode to modiolus distance on electrophysiological and psychophysical parameters in CI patients with perimodiolar and lateral electrode arrays. Otol Neurotol. 2020. https://doi.org/10.1097/MAO.0000000000002751.
16. Mewes A, Brademann G, Hey M. Comparison of perimodiolar electrodes: Imaging and electrophysiological outcomes. Otol Neurotol. 2020. https://doi.org/10.1097/MAO.0000000000002790.
17. Shepherd RK, Hatsushika S, Clark GM. Electrical stimulation of the auditory nerve: The effect of electrode position on neural excitation. Hear Res. 1993. https://doi.org/10.1016/0378-5955(93)90265-3.
18. Lee CS, Nagy PG, Weaver SJ, Newman-Toker DE. Cognitive and system factors contributing to diagnostic errors in radiology. Am J Roentgenol. 2013. https://doi.org/10.2214/AJR.12.10375.
19. Busby LP, Courtier JL, Glastonbury CM. Bias in radiology: The how and why of misses and misinterpretations. Radiographics. 2018. https://doi.org/10.1148/rg.2018170107.
20. Braun LT, Zwaan L, Kiesewetter J, Fischer MR, Schmidmaier R. Diagnostic errors by medical students: Results of a prospective qualitative study. BMC Med Educ. 2017. https://doi.org/10.1186/s12909-017-1044-7.
21. Kahneman D. Thinking, fast and slow. New York: Farrar, Straus & Giroux; 2011.
22. McCreadie G, Oliver TB. Eight CT lessons that we learned the hard way: an analysis of current patterns of radiological error and discrepancy with particular emphasis on CT. Clin Radiol. 2009. https://doi.org/10.1016/j.crad.2008.12.010.
23. Mewes A, Burg S, Brademann G, Dambon JA, Hey M. Quality-assured training in the evaluation of cochlear implant electrode position: a prospective experimental study. BMC Med Educ. 2022. https://doi.org/10.1186/s12909-022-03464-x.
24. Braithwaite B, Kjer HM, Fagertun J, Ballester MAG, Dhanasingh A, Mistrik P, et al. Cochlear implant electrode localization in post-operative CT using a spherical measure. In: Proceedings of the 13th IEEE - International Symposium on Biomedical Imaging. Prague, Czech Republic: IEEE; 2016. https://doi.org/10.1109/ISBI.2016.7493512. [Cited 2022 Dec 9].
25. Bennink E, Peters JPM, Wendrich AW, Vonken E jan, Van Zanten GA, Viergever MA. Automatic localization of cochlear implant electrode contacts in CT. Ear Hear. 2017. https://doi.org/10.1097/AUD.0000000000000438.
26. Noble JH, Labadie RF, Gifford RH, Dawant BM. Image-Guidance enables new methods for customizing cochlear implant stimulation strategies. IEEE Trans Neural Syst Rehabil Eng. 2013. https://doi.org/10.1109/TNSRE.2013.2253333.
27. Zhao Y, Labadie RF, Dawant BM, Noble JH. Validation of automatic cochlear implant electrode localization techniques using µCTs. J Med Imaging. 2018. https://doi.org/10.1117/1.jmi.5.3.035001.
28. Verbist BM, Skinner MW, Cohen LT, Leake PA, James C, Boëx C, et al. Consensus panel on a cochlear coordinate system applicable in histologic, physiologic, and radiologic studies of the human cochlea. Otol Neurotol. 2010. https://doi.org/10.1097/MAO.0b013e3181d279e0.
29. Xu J, Xu SA, Cohen LT, Clark GM. Cochlear view: Postoperative radiography for cochlear implantation. Am J Otol. 2000. https://doi.org/10.1016/s0196-0709(00)80112-x.
30. Aschendorff A, Kubalek R, Turowski B, Zanella F, Hochmuth A, Schumacher M, et al. Quality control after cochlear implant surgery by means of rotational tomography. Otol Neurotol. 2005. https://doi.org/10.1097/00129492-200501000-00007.
31. Güldner C, Weiß R, Eivazi B, Bien S, Werner JA, Diogo I. Intracochlear electrode position: evaluation after deep insertion using cone beam computed tomography. HNO. 2012. https://doi.org/10.1007/s00106-012-2527-9.
32. Husstedt HW, Aschendorff A, Richter B, Laszig R, Schumacher M. Nondestructive three-dimensional analysis of electrode to modiolus proximity. Otol Neurotol. 2002. https://doi.org/10.1097/00129492-200201000-00012.
33. Lecerf P, Bakhos D, Cottier JP, Lescanne E, Trijolet JP, Robier A. Midmodiolar reconstruction as a valuable tool to determine the exact position of the cochlear implant electrode array. Otol Neurotol. 2011. https://doi.org/10.1097/MAO.0b013e318229d4dd.

34. Noble JH, Labadie RF, Majdani O, Dawant BM. Automatic segmentation of intracochlear anatomy in conventional CT. IEEE Trans Biomed Eng. 2011. https://doi.org/10.1109/TBME.2011.2160262.
35. Reda FA, McRackan TR, Labadie RF, Dawant BM, Noble JH. Automatic segmentation of intra-cochlear anatomy in post-implantation CT of unilateral cochlear implant recipients. Med Image Anal. 2014. https://doi.org/10.1016/j.media.2014.02.001.
36. Zhang D, Liu Y, Noble JH, Dawant BM. Automatic localization of landmark sets in head CT images with regression forests for image registration initialization. Proc SPIE Int Soc Opt Eng. 2016. https://doi.org/10.1117/12.2216925.
37. Reda FA, Noble JH, Labadie RF, Dawant BM. An artifact-robust, shape library-based algorithm for automatic segmentation of inner ear anatomy in post-cochlear-implantation CT. Proc SPIE Int Soc Opt Eng. 2014. https://doi.org/10.1117/12.2043260.
38. Zhao Y, Dawant BM, Labadie RF, Noble JH. Automatic localization of cochlear implant electrodes in CT. Med Image Comput Comput Assist Interv. 2014. https://doi.org/10.1007/978-3-319-10404-1_42.
39. Noble JH, Dawant BM. Automatic graph-based localization of cochlear implant electrodes in CT. Med Image Comput Comput Assist Interv. 2015. https://doi.org/10.1007/978-3-319-24571-3_19.
40. Zhao Y, Dawant BM, Noble JH. Automatic localization of cochlear implant electrodes in CTs with a limited intensity range. Med Imaging 2017 Image Process. 2017. https://doi.org/10.1117/12.2254569.
41. Zhao Y, Chakravorti S, Labadie RF, Dawant BM, Noble JH. Automatic graph-based method for localization of cochlear implant electrode arrays in clinical CT with sub-voxel accuracy. Med Image Anal. 2019. https://doi.org/10.1016/j.media.2018.11.005.
42. Zhao Y, Dawant BM, Noble JH. Automatic selection of the active electrode set for image-guided cochlear implant programming. J Med Imaging. 2016. https://doi.org/10.1117/1.jmi.3.3.035001.
43. Zhao Y, Dawant BM, Noble JH. Automatic electrode configuration selection for image-guided cochlear implant programming. Med Imaging 2015 Image-Guided Proced Robot Interv Model. 2015. https://doi.org/10.1117/12.2081473.
44. Zhang D. Selecting electrode configurations for image-guided cochlear implant programming using template matching. J Med Imaging. 2017. https://doi.org/10.1117/1.jmi.5.2.021202.
45. Zhao Y, Wang J, Li R, Labadie R, Dawant B, Noble J. Validation of image-guided cochlear implant programming techniques. arXiv:190910137. 2019.
46. Deák Z, Maertz F, Meurer F, Notohamiprodjo S, Mueck F, Geyer LL, et al. Submillisievert computed tomography of the chest using model-based iterative algorithm: Optimization of tube voltage with regard to patient size. J Comput Assist Tomogr. 2017. https://doi.org/10.1097/RCT.0000000000000505.
47. Hanneman SK. Design, analysis, and interpretation of method-comparison studies. AACN Adv Crit Care. 2008. https://doi.org/10.1097/01.AACN.0000318125.41512.a3.
48. Altman DG, Bland JM. Measurement in medicine: the analysis of method comparison studies. Stat. 1983. https://doi.org/10.2307/2987937.
49. Bland JM, Altman DG. Statistical methods for assessing agreement between two methods of clinical measurement. Lancet. 1986. https://doi.org/10.1016/S0140-6736(86)90837-8.
50. Bland M. An introduction to medical statistics by Martin Bland. 3rd ed. Oxford: Oxford University Press; 2000.
51. Molnar Z, Umgelter A, Toth I, Livingstone D, Weyland A, Sakka SG, et al. Continuous monitoring of ScvO2 by a new fibre-optic technology compared with blood gas oximetry in critically ill patients: a multicentre study. Intensive Care Med. 2007. https://doi.org/10.1007/s00134-007-0743-7.
52. Portney LG, Waltkins MP. Foundations of clinical research: applications to practice. 2nd ed. New Jersey: Prentice Hall; 2000.
53. Wimmer W, Vandersteen C, Guevara N, Caversaccio M, Delingette H. Robust cochlear modiolar axis detection in CT. Med Image Comput Comput Assist Interv. 2019. https://doi.org/10.1007/978-3-030-32254-0_1.

Publisher's Note

Artikel 3: Electrode translocations in perimodiolar cochlear implant electrodes: Audiological and electrophysiological outcome

ORIGINAL PAPER

Electrode translocations in perimodiolar cochlear implant electrodes: Audiological and electrophysiological outcome☆

Tim Liebscher[a,*,1], **Alexander Mewes**[b,1], **Ulrich Hoppe**[a], **Joachim Hornung**[a], **Goetz Brademann**[b], **Matthias Hey**[b]

[a] Friedrich-Alexander-Universität Erlangen-Nürnberg (FAU), ENT-Clinic, Department of Audiology, Waldstraße 1, 91054 Erlangen, Germany
[b] Universitätsklinikum Schleswig-Holstein (UKSH), Campus Kiel, Department of Otorhinolaryngology, Head and Neck Surgery, Arnold-Heller-Straße 3, 24105 Kiel, Germany

Received 6 February 2020; accepted 5 May 2020

Abstract

Introduction: *Despite using the soft-surgery technique, cochlear implantation may increase the damage of the intracochlear structures due to a scalar translocation of the electrode. The aim of this work was to investigate the incidence as well as the audiological and electrophysiological outcome for electrode translocations and complete scala tympani insertions of perimodiolar electrodes within a large group of patients.*

Material and methods: *The investigations were performed retrospectively on 255 adult subjects with a Nucleus Contour Advance or Slim Modiolar electrode (Cochlear Ltd.). The scalar position was assessed by postoperative rotational tomography. Intraoperative and one year after CI activation measured ECAP thresholds were examined as well as the postoperative speech recognition in quiet using the Freiburg monosyllable word test.*

Results: *The incidence of a translocation was significantly lower with the Slim Modiolar than with the Contour Advance electrode (5.1% versus 32.3%; $p < 0.05$). With a scala tympani placement the median speech recognition score was 75% (range: 20- 100%) with the Contour Advance and 72.5% (range: 27.5-95%) with the Slim Modiolar electrode. In cases with an electrode translocation, speech recognition scores show a median of 75% (range: 45-100%) and 73.8% (range: 40-80%), respectively. No significant differences in speech recognition were found between translocations and scala tympani insertions with both electrodes. Compared to scala tympani insertions, electrode translocations yielded higher ECAP thresholds at apical and medial electrode contacts ($p < 0.05$).*

Conclusion: *The incidence of an electrode translocation is determined for both perimodiolar electrode types analyzed in this work. ECAP measurements provide additional information for detecting translocations compared to radiological imaging. However, the postoperative speech recognition in quiet was not affected by the scalar position in the electrodes examined here.*

Keywords: Cochlear implant, Speech recognition, Electrically evoked compound action potential, Electrode location, Scalar translocation, Computed tomography, Electrode design

☆ Preprint submitted to Journal of Information Processing and Management.

* Corresponding author: Friedrich-Alexander-Universität Erlangen-Nürnberg (FAU) ENT-Clinic, Department of Audiology. Waldstraße 1 91054 Erlangen, Germany. Tel.: +49 9131 85-32980.
E-mail: tim.liebscher@uk-erlangen.de (T. Liebscher).

[1] These authors contributed equally to this work (joint first authorship).

Z Med Phys **31** (2021) 265–275
https://doi.org/10.1016/j.zemedi.2020.05.004
www.elsevier.com/locate/zemedi

1 Introduction

The outcome of a cochlear implant (CI) rehabilitation is determined by multiple factors; e.g. duration of auditory deprivation, grade of hearing loss, residual speech recognition, patient's age at implantation, CI experience and fitting of the patient-related speech processor adjustments [1–6]. However, the correct positioning of the electrode into the cochlea marks the first step of a successful implantation with regard to a complete scala tympani (ST) insertion of the electrode with the least amount of additional trauma as possible. A scala tympani insertion of the electrode leads to a closer placement to the spiral ganglion cells and a better postoperative speech recognition compared to a scala vestibuli insertion [7].

During the insertion of the electrode there is a risk of a translocation, in which the electrode passes from ST through the basilar membrane into the scala vestibuli (SV). This results in larger distances to the ganglion cells and a severe physical trauma [8] which decreases the likelihood of preserving residual hearing [7,9]. Several studies have also demonstrated that a partial or complete SV insertion can impair postoperative speech recognition compared to a complete scala tympani insertion [7,9–11].

The incidence of an electrode translocation is influenced by the electrode design and the surgical approach [9,11–13] as well as the surgeon's expertise [14]. Pre-curved electrodes were designed to be perimodiolar positioned as close as possible to the spiral ganglion cells. However, these electrodes show a higher risk of a translocation than straight electrodes that are placed along the lateral wall of the ST [8], since they are stiffer and hence more traumatic during insertion. The translocation rate with the perimodiolar Nucleus Contour

Advance electrode (CAE; Cochlear Ltd., Sydney, NSW, Australia) can be significantly reduced by optimizing the mechanical electrode characteristics and the surgical technique [7].

The recently introduced Slim Modiolar electrode CI532 (SME; Cochlear Ltd., Sydney, NSW, Australia) is much thinner and more flexible than the CAE (e.g., CI24RE(CA) or CI512). First results show no incidence of electrode translocation and therefore less trauma [15], so that this electrode can also be considered for hearing preservation in subjects with residual hearing [16,17]. In terms of audiological outcome, a recent study presented equal or better outcomes in speech recognition scores with the SME compared to the straight electrodes CI422 and CI522 (Cochlear Ltd., Sydney, NSW, Australia) [18]. In addition, compared to the CAE no significant differences were found in speech performance outcomes [19]. In case of an electrode translocation, the additional intracochlear trauma and larger electrode-to-modiolus distances may alter the nerve–electrode interaction. Therefore, both electrophysiological thresholds and behavioral stimulation levels can differ. Responses of the auditory nerve can be recorded via electrically evoked compound action potentials (ECAPs). ECAPs provide feedback about the physiological status of the peripheral auditory system and are also used to estimate relationship of the electrode-to-modiolus distance [20–24]. Studies already presented that profiles of ECAP thresholds (T-ECAP) differ for various electrode designs because of their different positioning in the cochlear. Since the electrode contacts of a perimodiolar electrode are located closer to the modiolus than those of straight electrodes, T-ECAPs tend to be lower [21,25]. In the case of an electrode translocation, patients tend to have higher T-ECAPs in the more apical regions of the electrode compared to patients with a complete ST position [26,27].

The aim of this study was to evaluate, (I) if the incidence of an electrode translocation is influenced by the electrode design in perimodiolar electrodes (Nucleus CAE and SME); (II) if an electrode translocation impacts the postoperative speech recognition and (III) if a translocation effects the threshold levels of electrophysiological (ECAP) measures. Based on our clinical experience, we hypothesize that a translocation is less common with the SME and does not affect the speech recognition. We also expect higher ECAP thresholds in the more apical cochlear regions in cases with translocation, since the electrode there has a larger distance to the spiral ganglion cells.

2 Material and methods

2.1 Study design

This work was a retrospective, cross-sectional study of 255 adult subjects recruited from two German clinics (Erlangen, Kiel). All subjects undergoing cochlear implantation in the period of November 2009 to December 2018 with a CI532 SME (n = 156) or CI512 CAE (n = 99) and available postoperative tomography were included in this study, meeting the inclusion criteria as described in section 2.2.

ECAP and speech recognition data were collected one year after CI activation (± two months). Additionally, intraoperative ECAP thresholds were analyzed. Imaging was performed in the first week after the surgery. Subjects agreed to participate in this study as part of a general declaration of consent in clinical research. Positive votes from the local ethics committees were obtained (references: AZ 466/17 Kiel, 162_17 Bc Erlangen).

2.2 Subjects

Participants were native German speakers and at least 18 years of age at the time of implantation. Onset of severe to profound hearing loss had to be postlingual. The tomography image was performed within one week after surgery and had to have adequate quality for a clear determination of the electrode position.

The following exclusion criteria were applied: only partially inserted/not completely inserted electrodes; tip-foldover of the electrode; reimplantation(s) or reinsertion(s) of the

Table 1
Demographic and CI-related characteristics of the subjects. 4PTA0.5-4 kHz indicates air-conduction pure-tone average threshold (0.5, 1, 2, 4 kHz) measured monaurally with circumaural headphones; HA, hearing aid. Electrode position in scala tympani (ST), scala vestibuli (SV) or electrode translocation (TR) from ST to SV with regard to the insertion approach. The p-value resulted from statistical testing on significant differences between both electrodes (Mann-Whitney U-test, Chi-squared test with Yate's correction).

	Contour Advance Electrode (n = 99)				Slim Modiolar Electrode (n = 156)				*p-value*
$4PTA_{0.5\text{-}4\ kHz}$ preoperative (dB HL)	Median: 99 (range: 59-120)				Median: 98 (range: 59-120)				0.658
Age at Implant (Yr)	Median: 61 (range: 18-88)				Median: 65 (range: 21-87)				0.055
Monosyllabic @ 65 dB SPL with HA preoperative (%)	Median: 0 (range: 0-45)				Median: 0 (range: 0-55)				0.420
Gender (Female/Male)	47/52				82/74				0.443
Etiologies									
Cholesteatoma	n = 1				n = 1				
COM					n = 1				
Familial	n = 8				n = 2				
Infection	n = 2				n = 9				
Medicinal	n = 1				n = 2				
Meniere's disease	n = 11				n = 9				
Noise					n = 3				
Meningitis	n = 9								
Otosclerosis	n = 3				n = 3				
Sudden hearing loss	n = 9				n = 23				
Syndromal	n = 1				n = 4				
Trauma	n = 4				n = 3				
Unknown	n = 50				n = 96				
Scalar localization	ST	TR	SV	Σ	ST	TR	SV	Σ	
Surgical approach									< 0.001
Cochleostomy	7	2	1	10	1	1	0	2	
Round window	25	16	0	41	127	6	0	133	
Round window with cochleostomy	33	14	1	48	20	1	0	21	

electrode; ossifications or other abnormalities of the cochlear or abnormalities of the auditory nerve; cognitive disorders. Demographic subject and CI-related characteristics of the subjects are given in Table 1.

2.3 Surgery

This study was performed on subjects treated with a CAE or SME. Perimodiolar placement of the CAE was achieved by pull-back the inner stylet while inserting the electrode into the cochlea (advance off-stylet technique, AOS) [28–30]. With the SME, the inner stylet was replaced by an external sheath. After the electrode has been pulled into the sheath, both are introduced into the cochlear until the sheath has been completely inserted. The final perimodiolar electrode placement was reached by further insertion of the electrode while retracting the sheath (advance through the sheath technique) [31,32]. Both electrode types were inserted using a soft surgery technique. Electrode-related information on the surgical approach are given in Table 1. In each clinic, the surgical procedure was performed by one experienced surgeon.

2.4 Imaging analysis

Depending on the executing clinic various scanners for computer tomography (CT) and digital volume tomography (DVT) were used, applying the following measurement parameters: imaging voltage of 70-120 kV, a tube current of 1.1-5 mA/frame with pulsed X-ray emission and an exposition time of 7 s. Rear projection was used to create 3-D volume data sets (DICOM) according to a 360° rotation of the X-ray detector system around the studied area. Voxel sizes were less than 0.3 mm.

2.5 Scalar electrode position

Two cross-sectional reconstructions of the 3-D volume data set were used to determine the scalar position of the electrode within the cochlea: “unrolling” the cochlea by a curved reformation of the electrode path within the cochlea, and a transmodiolar reconstruction (cross section of the intracochlear lumen) [7,33–36]. Both two-dimensional images were obtained by further processing the “cochlear view”, that is a cross-sectional image perpendicular to the modiolus axis and coplanar to the basal turn of the cochlea [37–41]. The electrode could be either located in the scala tympani or in the scala vestibuli. In addition, a scalar translocation of the electrode from scala tympani to scala vestibuli could occur. An example of each category is shown in Figure 1. The position of a translocation was reported as electrode contact number (E1-E22). High contact numbers correspond to the apical portion of the electrode; low numbers correspond to the basal portion. If the translocation could not be clearly determined between two adjacent electrode contacts, the half of these contact numbers was stated. The scalar position was independently verified by two clinical experts.

2.6 Speech recognition

Speech recognition with the CI was measured monaurally in free field condition in quiet using the Freiburg monosyllable word test at 65 dB SPL [42–44]. If recognition was not directly measured at 65 dB SPL, the average score of 60 and 70 dB SPL testing was used. Results were averaged in the case of repeated measures. The test material was presented by a frontal loudspeaker at a one-meter distance to the subject according to ISO 8253- 3:2012 [45].

2.7 ECAP thresholds

The clinical Custom Sound (EP) software with its AutoNRT algorithm [46] was used to measure ECAP thresholds intra- and postoperatively. Stimulation and recording parameter settings were kept at default, i.e. monopolar, biphasic pulses, stimulus and masker pulse width of 25 μs, stimulus-masker gap of 400 μs.

2.8 Data analysis

Statistical analyses were performed using SPSS 22 version 22.0 (IBM, Armonk, N.Y., USA); figures were created with MATLAB^{TM} software (The MathWorks, Inc, Natick, Massachusetts). The Shapiro-Wilk test was applied for testing whether the data are normally distributed. Since the normal distribution does not apply to all variables, the Mann-Whitney U-test was used to test the equality of two samples and the Kruskal-Wallis test was used for comparing the equality of multiple samples. Furthermore, median values were calculated as well as 25th and 75th percentiles (P25, P75). Fisher’s exact test and Chi-squared test with Yates’s correction were used to evaluate the associations of two and more than two categorical variables, respectively. Statistical significance was defined as $p < 0.05$.

3 Results

3.1 Demographic and CI-related characteristics

This work investigated the incidence as well as the audiological and electrophysiological outcome for translocations and scala tympani insertions of two perimodiolar electrodes. In order to avoid selection bias, the influence of demographic subject and CI-related characteristics (preoperative speech recognition with hearing aid at 65 dB SPL and 4PTA, patient’s age at implantation and gender, etiology, surgical approach) on the outcome under investigation was examined. Within both electrode types, no significant differences were found for all tested covariables between the ST insertion and translocation group ($p > 0.05$). The surgical approach was distributed

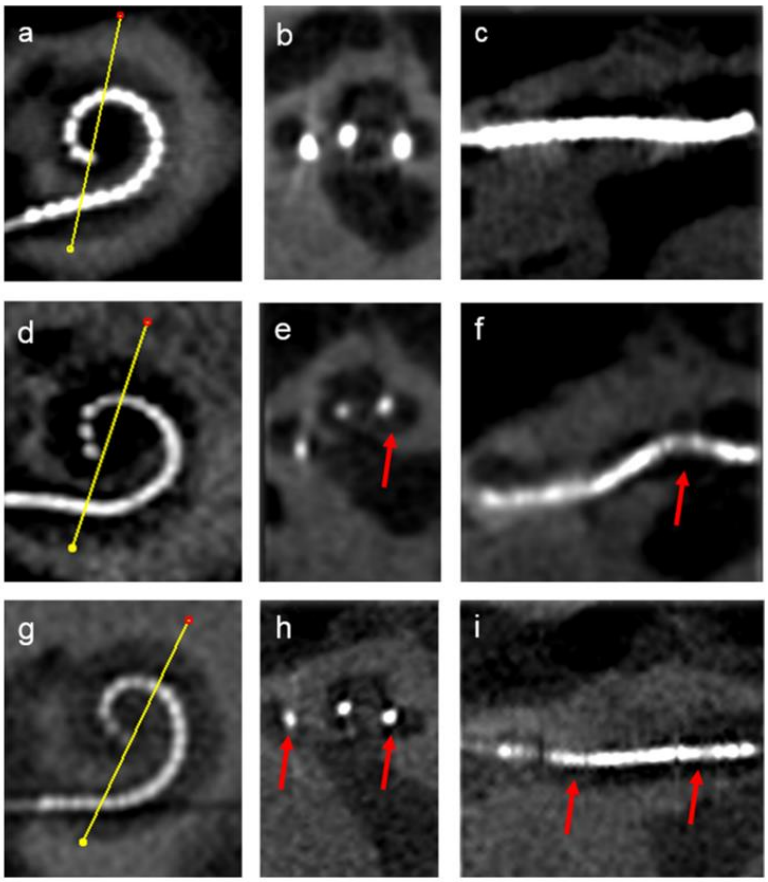

Figure 1. Exemplary scalar position comparison of a CI electrode evaluated by cross-sectional reconstructions of CT or DVT scans: "cochlear view" (a; d; g), transmodiolar according to the yellow line (b; e; h) and "cochlear unrolling" (c; f; i). Complete scala tympani insertion (a-c), complete scala vestibuli insertion (g-i) or translocation from scala tympani to scala vestibuli (d-f). Red arrows indicate the empty scala tympani.

significantly differently between CAE and SME ($p < 0.001$; see Table 1), according to electrode-specific manufactures Physician's Guides [28,31].

3.2 Electrode position and translocation rate

A complete ST position was achieved in 83.5% (n = 213) of all subjects. An electrode translocation occurred in 15.7% (n = 40) and in two subjects (0.8%) the electrode was completely inserted in the SV unintentionally. Because of the very small number of complete SV insertions (n = 2), further statistical analyses will focus primary on cases with ST insertions and translocations. As figure 2 illustrates, a translocation is significantly related to the electrode (Fisher's exact test, $p < 0.05$). The CAE translocated in 32/99 subjects (32.3%), the SME in 8/156 subjects (5.1%). This results in a ST rate of 65.7% (CAE) and 94.9% (SME). The position of a translocation, regarding the electrode contact number, is significantly ($p = 0.03$) higher with the CAE (median: E10; range: E2-E13) than with the SME (median: E7; range: E4-E12.5).

3.3 Speech recognition

With a ST placement the median speech recognition score was 75% (n = 65; range: 20-100%) in subjects with CAE and 72.5% (n = 148; range: 27.5-95%) with the SME (see figure 3).

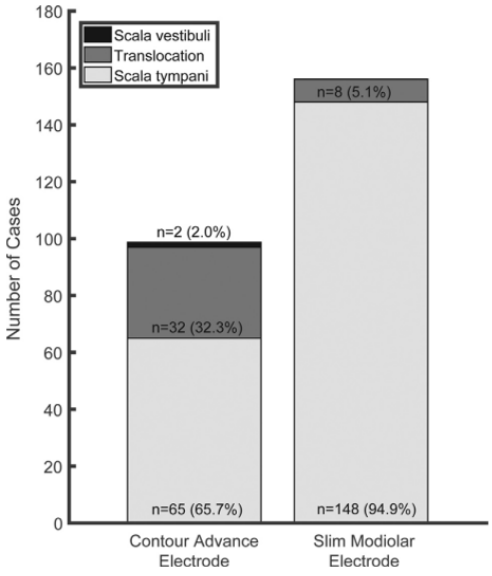

Figure 2. Absolute and relative incidence of complete ST, SV insertion and translocations from ST into SV in relation to electrode type: Contour Advance (n = 99) and Slim Modiolar (n = 156) electrode.

In cases with an electrode translocation, speech recognition scores show a median of 75% (n = 32; range: 45-100%) and 73.8% (n = 8; range: 40-80%), respectively.

The Kruskal-Wallis test was conducted to examine the differences on speech recognition scores according to electrode type and electrode position. No significant differences ($\chi^2 = 5.887$, $p = 0.117$, $df = 3$) were found among the four groups (scalar position: ST and translocation; electrode type: CAE and SME). Subjects S5 and S15 with complete SV insertion scored 70% and 65%, respectively.

3.4 ECAP thresholds

Intraoperative T-ECAP measurements were performed in all 255 subjects. At 225 electrode contacts, a valid T-ECAP was missing. In one subject no T-ECAPs could be registered at any electrode contact, giving an overall success rate of 95.6%. Postoperatively, the rate of available T-ECAPs was 90.7%. One subject did not perform the ECAP measurement within the defined time period.

Reasons for missing T-ECAPs, e.g., compliance problems or no reliable response at maximum current level [46], LAPL (loudest acceptable loudness level) or protocol deviation (no complete ECAP profile recorded).

Translocations show higher intraoperative ECAP thresholds in the medial and apical region of the electrode than ST insertions (see figure 4 and 5; left panel). Significant differences in intraoperative T-ECAPs between ST insertions and translocations were found at electrode contacts E7 to E22 ($p < 0.05$). At electrode contacts E12-E14, the P10-90 intraoperative T-ECAP range of the ST and translocation group minimal overlap. With both electrode types, the translocation 10% percentile is above the 90% percentile of the ST insertions. Postoperative ECAP thresholds have significantly decreased compared to the intraoperative measurements ($p < 0.05$), but translocations also showed higher T-ECAPs in the medial and apical electrode region than ST insertions (see figure 4 and 5; right panel). These differences are significant at the contact range E6 to E22 and E9 to E22 (CAE and SME; $p < 0.05$). For both intraoperative and postoperative. ECAP thresholds, no significant differences between ST insertions and translocations were found at the remaining basal electrode contacts ($p > 0.05$).

4 Discussion

4.1 Rate of electrode translocation

Primary aims of this study were to examine the scalar position with the CAE and the SME as well as the incidence of an electrode translocation. Our results indicate a complete ST insertion in 65.7% and 94.9% (CAE versus SME); translocations rates were 32.3% and 5.1%, respectively.

Previous studies presented similar incidence rates with the CAE for complete ST insertions (47.2 to 78.4%) [9,11,12,47,48] and slightly lower translocation rates (18 to 26%) [7,12,47,48] compared to this work. Unfortunately, some study groups solely present the rate of complete ST insertions, making a comparison with the translocation rate of this study difficult. O'Connell et al. [11] defined any electrode contact to be in the SV as SV insertion, resulting in a 52.8% rate of "SV insertions". Also Wanna et al. [9] presented 42% of electrodes not being completely inserted in ST. Since both studies only reported the rate of electrode placement outside the ST, a translocation rate up to 52.8% is possible. Regarding the electrode design (straight versus perimodiolar) all study groups observe that straight electrodes are associated with higher rates of complete ST placement. However, there is a huge variability for the ST insertion rate with the CAE. This can be explained by the well-known relation, that scalar positioning is mostly influenced by the surgical experience and surgery procedure [14], insertion approach [13] and cochlear morphology [48].

So far, there are only a few publications that analyzed the scalar positioning of the SME. Aschendorff et al. (2017) [15] presented the data of a multicentric study, showing no electrode translocation in 45 subjects. With a smaller number of subjects (n = 18 and n = 17), in neither Shaul et al. (2016) [47] nor Iso-Mustajärvi et al. (2019) [17] did a translocation occur. However, the study of McJunkin et al. (2018) [49] reported 3 translocations out of 23 subjects (13%); Nassiri et al. (2020) [50] recounted 1 case in 16 (6.3%) subjects.

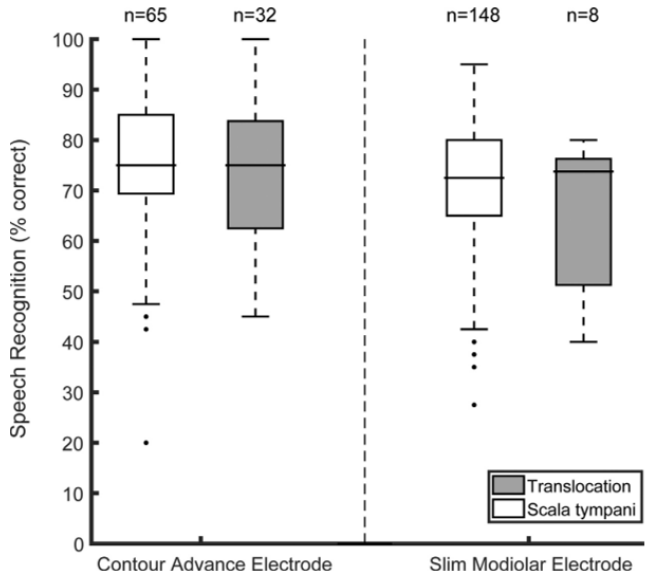

Figure 3. Speech recognition outcomes (Freiburg monosyllables in quiet @ 65 dB SPL) one year post CI activation for subjects implanted with a Contour Advance or Slim Modiolar electrode with either complete scala tympani insertion or electrode translocation. The Kruskal-Wallis test showed no significant differences. Median with 1st and 3rd quartile as well whiskers extend to 1.5 times the inter-quartile range are shown.

In our subgroup of 156 subjects with SME a complete ST insertion was achieved in 94.9%. Overall, this confirms that this perimodiolar electrode seems to provide a very high rate of complete ST insertion, which is comparable to straight electrodes (89-97%) [9,11,12]. Because of the similar electrode characteristics with regard to thickness and flexibility, the SME reduces the risk of an electrode translocation, additional trauma and therefore increases the chance of preserving residual hearing [16–18]. However, in eight cases (5.1%) an electrode translocation with the SME occurred. In order to investigate ECAP thresholds with an electrode translocation in a clinical manner, the position of a translocation was determined counting the electrode number. Nevertheless, it has to be mentioned, that the electrode contact number only approximates a position along the electrode due to the individual cochlear morphology and size, as well as different electrode dimensions. Typically, a ST to SV translocation with perimodiolar electrodes occurs in the basal cochlear turn opposite to the cochleostomy, corresponding to approximately 180-degree electrode insertion depth [7,12,29,51]. According to Landsberger et al. (2015) the average electrode contact number at the 180-degree angle with the CAE is E12 [52], which is broadly in line with the median electrode contact number E10 evaluated in this study. With the SME, 6 out of 8 translocations occurred at a lower electrode contact (median: E7) than the CAE median, indicating a more basal translocation. We assume that this can be caused by an inadequate orientation of the external sheath during the initial electrode insertion. In single cases we observed, that the sheath – for example if over inserted due to a large round window opening – can be potentially traumatic and even break through the basilar membrane, passing the electrode into the SV. Even though there are only a very small number of electrode translocations, it demonstrates once more, that the insertion procedure should be performed according to the manufactures Physician's Guide in order to minimize this kind of electrode misplacement.

4.2 Audiological outcome and scalar positioning of the electrode

Speech recognition in quiet was analyzed regarding the scalar positioning of the electrode, showing no significant differences between ST insertions and translocations. Scalar position influencing audiological performance has been discussed in only a few studies so far. One of the first reports from Aschendorff et al. (2007) [7] demonstrated significantly poorer monosyllabic and sentence scores in subjects with complete SV insertion (n = 12) versus complete ST insertion (n = 15). However, no differences were found in case of translocation (n = 9) versus ST insertion, which is consistent with our findings. Wanna et al. (2014) [9] investigating over 116 CI-ears also presented poorer hearing results (12.8% in

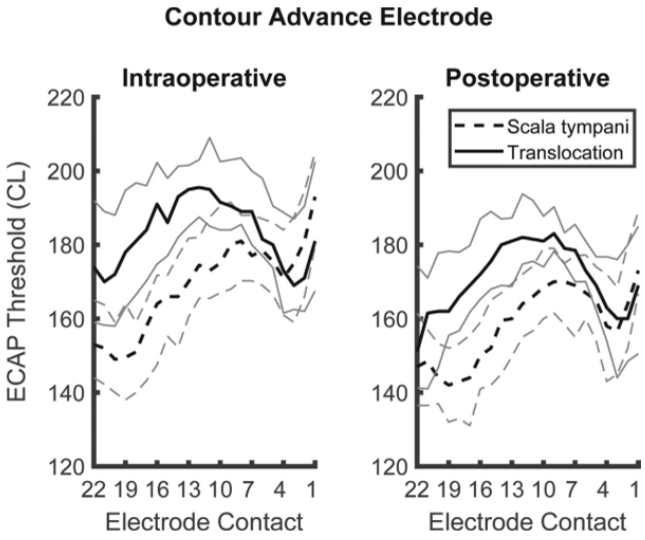

Figure 4. Intraoperative (left) and one year post CI activation (right) measured ECAP thresholds for subjects implanted with a Contour Advance electrode (n = 99). High contact numbers correspond to the apical portion of the electrode; low numbers correspond to the basal portion. Dashed lines show complete scala tympani insertions; solid lines, translocations from scala tympani into scala vestibuli. Median values are indicated by thick lines, thin lines illustrate the 25th and 75th percentiles.

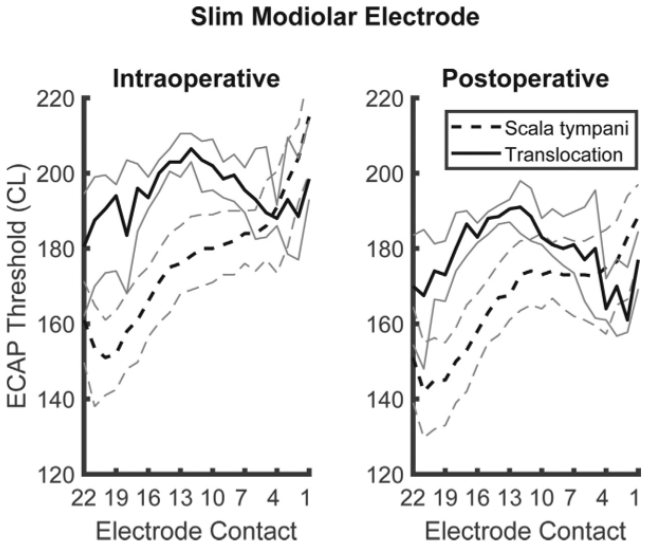

Figure 5. Intraoperative (left) and one year post CI activation (right) measured ECAP thresholds for subjects implanted with a Slim Modiolar electrode (n = 156). High contact numbers correspond to the apical portion of the electrode; low numbers correspond to the basal portion. Dashed lines show complete scala tympani insertions; solid lines, translocations from scala tympani into scala vestibuli. Median values are indicated by thick lines, thin lines illustrate the 25th and 75th percentiles.

CNC word scores; p = 0.045) in subjects with SV insertion; but their cohort also included subjects with only partial SV insertion (translocation). They did not find correlation for hearing in noise (HINT) or in sentence test (AzBio) regarding scalar positioning. In addition, Holden et al. (2013) [10] and O'Connell et al. (2016) [11] associate poorer audiological performance in CNC words to partial or complete SV insertion in overall 114 and 137 subjects, respectively. In a subgroup (n = 107), O'Connell additionally found better AzBio scores with ST insertions than SV insertions (60.5% versus 49.6%). Finally, the generalized linear models from Chakravorti et al. (2019) [19] revealed scalar position and modiolar proximity to be significantly correlated with CNC words and sentences in noise (BKB-SIN) scores in 120 subjects with a perimodiolar electrode. Some of these prior findings are contrary to our results and can be partially explained by differences with regard to the methods and inclusion criteria that were used. Even though these study groups [9–11,53] each investigated in a fairly huge cohort (n = 116-220), several different electrode types from various CI manufactures were included, which results in an increasing number of subgroups, reducing the sample size in homogeneous pools. Other factors, e.g. the inclusion of prelingual deafened subjects [53], a larger range of duration of CI experience (0.2 to 16.5 yrs.) [53] and a different audiological test setup (e.g., output level 60 dB) [10,11] will probably contribute to the diverse outcomes and is a further indication that postoperative audiological outcomes in CI users are likely determined by multiple factors. In order to minimize the effect of numerous covariates, by defining clear inclusion criteria, we tried to obtain homogeneous subgroups. Regardless of this, there might be other covariates that influence outcomes that we could not account for in this study, e.g. duration of auditory deprivation and fitting of the patient-related speech processor adjustments.

Finally, our results suggest that additional trauma caused by an electrode translocation does not affect audiological outcomes or does get compensated at the peripheral or more central stages of the nervous system. So far, we only tested speech recognition via monosyllabic words in quiet. In order to clarify the outcome, more complex listening situations need to be addressed via audiological testing (e.g., sentence test in noise) in further investigation. Additionally, speech recognition was analyzed only one year after CI activation. Therefore, future studies should address if there are long-term effects of the translocation-related intracochlear trauma.

4.3 ECAP thresholds

This work further investigated the effect of an electrode translocation on its auditory nerve interaction using ECAP thresholds. Other studies have shown a dependence of T-ECAPs on the electrode-to-modiolus distance, i.e. higher thresholds at larger distances [20–24]. As stated above, only translocations from ST to SV were analyzed, showing higher ECAP thresholds in the apical and medial electrode region than ST insertions. Since an electrode placement into the SV is accompanied with larger distances to the modiolus [54], higher T-ECAPs with translocations can be explained by this larger spacing. Similar results with perimodiolar electrodes were found by Mittmann et al. (2015) [26,27]. Also comparing translocations and ST insertions with the CAE and SME, Mewes et al. (2019) reported significant larger electrode-to-modiolus distances in translocations for insertion depths above 200 degrees [24]. As indicate above, a translocation with the SME occurred at a smaller electrode number than with the CAE (median: E7 versus E10). In comparison to that, both electrodes showed significantly higher intraoperative T-ECAPs for translocations at contacts above E7. This may be due to the different relationship between T-ECAP and electrode-to-modiolus distance, which is greater with the CAE than with the SME ($R^2 = 0.48$ versus $R^2 = 0.23$) [24]. However, with both perimodiolar electrodes, intraoperative T-ECAP measurements have the potential to detect translocations from ST to SV. Further investigations should focus on the development of a simple T-ECAP criterion to detect electrode translocations, based on the minimal overlap of the P10-90 intraoperative T-ECAP range between ST insertions and translocations at electrode contacts E12-E14.

5 Conclusions

This study examined the incidence as well as the audiological and electrophysiological outcome for ST insertions and translocations of perimodiolar electrodes (Nucleus CAE, SME). The incidence of a translocation was significantly lower with the SME than with the CAE (5.1% versus 32.3%). In the apical and medial electrode region, electrophysiological thresholds are higher with translocations than with complete scala tympani insertions. This provides additional information for detecting translocations compared to radiological imaging. However, the postoperative speech recognition in quiet was not affected by the scalar position in both electrodes.

References

[1] Rubinstein JT, Parkison WS, Tyler RS, Gantz BJ. Residual Speech Recognition and Cochlear Implant Performance: Effects of Implantation Criteria. Am. J. Otol 1999;20:445–52.

[2] Müller-Deile J. Verfahren zur Anpassung und Evaluation von Cochlear Implant Sprachprozessoren, Median-Verlag von Killisch-Horn GmbH. Heidelberg 2000.

[3] Hassanzadeh S, Farhadi M, Daneshi A, Emamdjomeh H. The Effects of Age on Auditory Speech Perception Development in Cochlear-Implanted Prelingually Deaf Children. Otolaryngol. - Head Neck Surg 2002;126:524–7, http://dx.doi.org/10.1067/mhn.2002.125110.

[4] Friedland DR, Venick HS, Niparko JK. Choice of Ear for Cochlear Implantation: The Effect of History and Residual Hearing on Predicted Postoperative Performance. Otol. Neurotol 2003;24:582–9, http://dx.doi.org/10.1097/00129492-200307000-00009.

[5] Blamey P, Artieres F, Başkent D, Bergeron F, Beynon A, Burke E, Dillier N, Dowell R, Fraysse B, Gallégo S, Govaerts PJ, Green K, Huber AM, Kleine-Punte A, Maat B, Marx M, Mawman D, Mosnier I, O'Connor AF, O'Leary S, Rousset A, Schauwers K, Skarzynski

H, Skarzynski PH, Sterkers O, Terranti A, Truy E, Van De Heyning P, Venail F, Vincent C, Lazard DS. Factors Affecting Auditory Performance of Postlinguistically Deaf Adults Using Cochlear Implants: An Update With 2251 Patients. Audiol. Neurotol 2012;18:36–47, http://dx.doi.org/10.1159/000343189.

[6] Hoppe U, Hast A, Hocke T. Audiometry-Based Screening Procedure for Cochlear Implant Candidacy. Otol. Neurotol 2015;36:1001–5, http://dx.doi.org/10.1097/MAO. 0000000000000730.

[7] Aschendorff A, Kromeier J, Klenzner T, Laszig R. Quality Control After Insertion of the Nucleus Contour and Contour Advance Electrode in Adults. Ear Hear 2007;28:75–9, http://dx.doi.org/10.1097/AUD.0b013e318031542e.

[8] O'Connell BP, Hunter JB, Wanna GB. The Importance of Electrode Location in Cochlear Implantation. Laryngoscope Investig. Otolaryngol 2016;1:169–74, https://doi.org/10.1002/lio2.42.

[9] Wanna GB, Noble JH, Carlson ML, Gifford RH, Dietrich MS, Haynes DS, Dawant BM, Labadie RF. Impact of Electrode Design and Surgical Approach on Scalar Location and Cochlear Implant Outcomes. Laryngoscope 2014;124:S1–7, https://doi.org/10.1002/lary.24728.

[10] Holden LK, Finley CC, Firszt JB, Holden TA, Brenner C, Potts LG, Gotter BD, Vanderhoof SS, Mispagel K, Heydebrand G, Skinner MW. Factors Affecting Open-Set Word Recognition in Adults with Cochlear Implants. Ear Hear 2013;34:342–60, http://dx.doi.org/10.1097/AUD.0b013e3182741a7.

[11] O'Connell BP, Cakir A, Hunter JB, Francis DO, Noble JH, Labadie RF, Zuniga G, Dawant BM, Rivas A, Wanna GB. Electrode Location and Angular Insertion Depth Are Predictors of Audiologic Outcomes in Cochlear Implantation. Otol. Neurotol 2016;37:1016–23, http://dx.doi.org/10.1097/MAO. 0000000000001125.

[12] Boyer E, Karkas A, Attye A, Lefournier V, Escude B, Schmerber S. Scalar Localization by Cone-Beam Computed Tomography of Cochlear Implant Carriers. Otol Neurotol 2015;36:422–9, http://dx.doi.org/10.1097/mao.0000000000000705.

[13] Jeyakumar A, Peña SF, Brickman TM. Round Window Insertion of Precurved Electrodes is Traumatic. Otol. Neurotol 2014;35:52–7, http://dx.doi.org/10.1097/MAO. 0000000000000194.

[14] Aschendorff A, Arndt S, Beck R, Schild C, Klenzner T. Insertion Results for ContourTM and Contour AdvanceTM Electrodes. Are There Individual Learning Curves? HNO 2011;59:448–52, http://dx.doi.org/10.1007/s00106-011-2319-7.

[15] Aschendorff A, Briggs R, Brademann G, Helbig S, Hornung J, Lenarz T, Marx M, Ramos A, Stöver T, Escudé B, James CJ. Clinical Investigation of the Nucleus Slim Modiolar Electrode. Audiol. Neurotol 2017;22:169–79, http://dx.doi.org/10.1159/000480345.

[16] Ramos-Macías A, Borkoski-Barreiro SA, Falcón-González JC, Ramos-De Miguel A. Hearing Preservation with the Slim Modiolar Electrode Nucleus CI532® Cochlear Implant: A Preliminary Experience. Audiol. Neurotol 2018;22:317–25, http://dx.doi.org/10.1159/000486409.

[17] Iso-Mustajärvi M, Sipari S, Löppönen H, Dietz A. Preservation of Residual Hearing After Cochlear Implant Surgery with Slim Modiolar Electrode. Eur. Arch. Oto-Rhino-Laryngology 2019;277:367–75, http://dx.doi.org/10.1007/s00405-019-05708-x.

[18] Holder JT, Yawn RJ, Nassiri AM, Dwyer RT, Rivas A, Labadie RF, Gifford RH. Matched Cohort Comparison Indicates Superiority of Precurved Electrode Arrays. Otol. Neurotol 2019;40:1160–6, http://dx.doi.org/10.1097/MAO. 0000000000002366.

[19] Garaycochea O, Manrique-Huarte R, Lazaro C, Huarte A, Prieto C, Alvarez de Linera-Alperi M, Manrique M. Comparative Study of Two Different Perimodiolar and a Straight Cochlear Implant Electrode Array: Surgical and Audiological Outcomes. Eur. Arch. Oto-Rhino-Laryngology 2019;277:69–76, http://dx.doi.org/10.1007/s00405-019-05680-6.

[20] Van Wermeskerken GKA, Van Olphen AF, Graamans K. Imaging of Electrode Position in Relation to Electrode Functioning After Cochlear Implantation. Eur. Arch. Oto-Rhino-Laryngology 2009;266:1527–31, http://dx.doi.org/10.1007/s00405-009-0939-2.

[21] Müller A, Hocke T, Mir-Salim P. Intraoperative Findings on ECAP-Measurement: Normal or Special Case? Int. J. Audiol 2015;54:257–64, http://dx.doi.org/10.3109/14992027.2014.969410.

[22] Poley M, Overmyer E, Craun P, Holcomb M, Reilly B, White D, Preciado D. Does Pediatric Cochlear Implant Insertion Technique Affect Intraoperative Neural Response Telemetry Thresholds? Int. J. Pediatr. Otorhinolaryngol 2015;79:1404–7, http://dx.doi.org/10.1016/j.ijporl.2015.05.038.

[23] Degen C, Büchner A, Lenarz T. Effect of Electrode Position on Electrophysiological and Psychoacoustic Parameters in Cochlear Implant Patients with Lateral and Perimodiolar Electrode Arrays. Laryngo-Rhino-Otol 2018;97:S166, http://dx.doi.org/10.1055/s-0038-1640286.

[24] Mewes A, Hey M, Brademann G, Ambrosch P. Electrophysiological and Imaging Diagnostics of the Scale Dislocation During Cochlear Implantation. Laryngo-Rhino-Otol 2019;98:S145, http://dx.doi.org/10.1055/s-00391686457.

[25] Perenyi A, Toth F, Dimak B, Nagy R, Schoerg P, Jori J, Kiss JG, Sprinzl G, Csanady M, Rovo L. Electrophysiological Measurements with Electrode Types of Different Perimodiolar Properties and the Same Cochlear Implant Electronics - A Retrospective Comparison Study. J. Otolaryngol. -Head Neck Surg 2019;48:1–7, http://dx.doi.org/10.1186/s40463-019-0361-8.

[26] Mittmann P, Ernst A, Todt I. Intraoperative Electrophysiologic Variations Caused by the Scalar Position of Cochlear Implant Electrodes. Otol. Neurotol 2015;36:1010–4, http://dx.doi.org/10.1097/MAO. 0000000000000736.

[27] Mittmann P, Todt I, Ernst A, Rademacher G, Mutze S, Göricke S, Schlamann M, Ramalingam R, Lang S, Christov F, Arweiler-Harbeck D. Electrophysiological Detection of Scalar Changing Perimodiolar Cochlear Electrode Arrays: A Long Term Follow-up Study. Eur. Arch. Oto-Rhino-Laryngology 2016;273:4251–6, http://dx.doi.org/10.1007/s00405-016-4175-2.

[28] Cochlear Ltd., Nucleus ® CI512 Cochlear Implant with Contour Advance ® Electrode: Surgeon's Guide., 2016. https://www.cochlear.com/ifu/documents/491694-en-ci512.(call date: 5th February 2020).

[29] Stöver T, Issing P, Graurock G, Erfurt P, ElBeltagy Y, Paasche G, Lenarz T. Evaluation of the Advance Off-Stylet Insertion Technique and the Cochlear Insertion Tool in Temporal Bones. Otol. Neurotol 2005;26:1161–70, http://dx.doi.org/10.1097/01.mao.0000179527.17285.85.

[30] Roland JT. A Model for Cochlear Implant Electrode Insertion and Force Evaluation: Results with a New Electrode Design and Insertion Technique. Laryngoscope 2005;115:1325–39, http://dx.doi.org/10.1097/01.mlg.0000167993.05007.35.

[31] Cochlear Ltd., Nucleus ® CI532 Cochlear Implant with Slim Modiolar Electrode: Physicians Guide., 2018. https://www.cochlear.com/ifu/documents/414154-en-ci532.(call date: 5th February 2020).

[32] Briggs RJS, Tykocinski M, Lazsig R, Aschendorff A, Lenarz T, Stöver T, Fraysse B, Marx M, Thomas Roland J, Roland PS, Wright CG, Gantz BJ, Patrick JF, Risi F. Development and Evaluation of the Modiolar Research Array - Multi-Centre Collaborative Study in Human Temporal Bones. Cochlear Implants Int 2011;12:129–39, http://dx.doi.org/10.1179/1754762811Y0000000007.

[33] Aschendorff A, Kubalek R, Turowski B, Zanella F, Hochmuth A, Schumacher M, Klenzner T, Laszig R. Quality Control After Cochlear Implant Surgery by Means of Rotational Tomography. Otol. Neurotol 2005;26:34–7, http://dx.doi.org/10.1097/00129492-200501000-00007.

[34] Güldner C, Weiß R, Eivazi B, Bien S, Werner JA, Diogo I. Intracochleäre Elektrodenlage: Beurteilung mittels "Cone Beam Computed Tomography" nach tiefer Insertion. HNO 2012;60:817–22, http://dx.doi.org/10.1007/s00106-012-2527-9.

[35] Husstedt HW, Aschendorff A, Richter B, Laszig R, Schumacher M. Nondestructive Three-dimensional Analysis of

Electrode to Modiolus Proximity. Otol. Neurotol 2002;23:49–52, http://dx.doi.org/10.1097/00129492-200201000-00012.
[36] Lecerf P, Bakhos D, Cottier JP, Lescanne E, Trijolet JP, Robier A. Midmodiolar Reconstruction as a Valuable Tool to Determine the Exact Position of the Cochlear Implant Electrode Array. Otol. Neurotol 2011;32:1075–81, http://dx.doi.org/10.1097/MAO.0b013e318229d4dd.
[37] Cohen LT, Xu J, Xu SA, Clark GM. Improved and Simplified Methods for Specifying Positions of the Electrode Bands of a Cochlear Implant Array. Am. J. Otol 1996;17:859–65.
[38] Verbist BM, Skinner MW, Cohen LT, Leake PA, James C, Boëx C, Holden TA, Finley CC, Roland PS, Roland JT, Haller M, Patrick JF, Jolly CN, Faltys MA, Briaire JJ, Frijns JHM. Consensus Panel on a Cochlear Coordinate System Applicable in Histologic, Physiologic, and Radiologic. Studies of the Human Cochlea, Otol. Neurotol 2010;31:722–30, http://dx.doi.org/10.1097/MAO.0b013e3181d279e0.
[39] Xu J, Xu SA, Cohen LT, Clark GM. Cochlear View: Postoperative Radiography for Cochlear Implantation. Am. J. Otol 2000;21:49–56, http://dx.doi.org/10.1016/s0196-0709(00)80112-x.
[40] Eisenhut F, Lang S, Taha L, Doerfler A, Iro H, Hornung J. Merged Volume Rendered Flat-panel Computed Tomography for Postoperative Cochlear Implant Assessment. Clin Neuroradiol 2019:1–8, http://dx.doi.org/10.1007/s00062-019-00832-x.
[41] Struffert T, Hertel V, Kyriakou Y, Krause J, Engelhorn T, Schick B, Iro H, Hornung J, Doerfler A. Imaging of Cochlear Implant Electrode Array with Flat-Detector CT and Conventional Multislice CT: Comparison of Image Quality and Radiation Dose. Acta Otolaryngol 2010;130:443–52, http://dx.doi.org/10.3109/00016480903292700.
[42] DIN 45621-1:1995-08, Word lists for Recognition Tests - Part 1: Monosyllabic and Polysyllabic Words, n.d. https://doi.org/https://doi.org/10.31030/27920.
[43] DIN 45626-1:1995-08, Sound Carrier with Speech for Recognition Tests - Part 1: Sound Carrier with Wordlists in Accordance with DIN 45621-1 (Recording 1969), n.d. https://doi.org/https://doi.org/10.31030/2791997.
[44] Hahlbrock K-H. Über Sprachaudiometrie und neue Wörterteste. Arch. Ihr- Usw. Heilk. u. Z. Hals- Usw. Heilk 1953;162:394–431.
[45] DIN EN ISO 8253-3:2012-08, Acoustics - Audiometric Test Methods - Part 3: Speech Audiometry (ISO 8253-3:2012); German Version EN ISO 8253-3:2012, n.d. https://doi.org/https://doi.org/10.31030/1861048.
[46] Van Dijk B, Botros AM, Battmer RD, Begall K, Dillier N, Hey M, Lai WK, Lenarz T, Laszig R, Morsnowski A, Müller-Deile J, Psarros C, Shallop J, Weber B, Wesarg T, Zarowski A, Offeciers E. Clinical Results of AutoNRT,TM a Completely Automatic ECAP Recording System for Cochlear Implants. Ear Hear 2007;28:558–70, http://dx.doi.org/10.1097/AUD.0b013e31806c1d1.
[47] Shaul C, Dragovic AS, Stringer AK, O'Leary SJ, Briggs RJ. Scalar Localisation of Peri-Modiolar Electrodes and Speech Perception Outcomes. J. Laryngol Otol 2018;132:1000–6, http://dx.doi.org/10.1017/S0022215118001871.
[48] Ketterer MC, Aschendorff A, Arndt S, Hassepass F, Wesarg T, Laszig R, Beck R. The Influence of Cochlear Morphology on the Final Electrode Array Position. Eur. Arch. Oto-Rhino-Laryngology 2018;275:385–94, http://dx.doi.org/10.1007/s00405-017-4842-y.
[49] McJunkin JL, Durakovic N, Herzog J, Buchman CA. Early Outcomes with a Slim, Modiolar Cochlear Implant Electrode Array. Otol. Neurotol 2018;39:e28–33, http://dx.doi.org/10.1097/MAO.0000000000001652.
[50] Nassiri AM, Yawn RJ, Holder JT, Dwyer RT, O'Malley MR, Bennett ML, Labadie RF, Rivas A. Hearing Preservation Outcomes Using a Precurved Electrode Array Inserted With an External Sheath. Otol. Neurotol 2020;41:33–8, http://dx.doi.org/10.1097/MAO.0000000000002426.
[51] Skinner MW, Holden TA, Whiting BR, Voie AH, Brunsden B, Neely JG, Saxon EA, Hullar TE, Finley CC. In Vivo Estimates of the Position of Advanced Bionics Electrode Arrays in the Human Cochlea. Ann. Otol. Rhinol. Laryngol 2007;116:2–24, http://dx.doi.org/10.1177/000348940711600401.
[52] Landsberger DM, Svrakic M, Roland JT, Svirsky M. The Relationship between Insertion Angles, Default Frequency Allocations, and Spiral Ganglion Place Pitch in Cochlear Implants, Ear Hear 2015;36:e207–13, http://dx.doi.org/10.1097/AUD.0000000000000163.
[53] Chakravorti S, Noble JH, Gifford RH, Dawant BM, O'Connell BP, Wang J, Labadie RF. Further Evidence of the Relationship Between Cochlear. Implant Electrode Positioning and Hearing Outcomes. Otol. Neurotol 2019;40:617–24, http://dx.doi.org/10.1097/MAO.0000000000002204.
[54] Roland JT, Fishman AJ, Alexiades G, Cohen NL. Electrode to Modiolus Proximity: A Fluoroscopic and Histologic Analysis. Am. J. Otol 2000;21:218–25, http://dx.doi.org/10.1016/s0196-0709(00)80012-5.

Erklärung des Eigenanteils an den erfolgten Publikationen

Alexander Mewes hatte folgenden Anteil an den folgenden Publikationen:

Publikation 1: Mewes, A., Burg, S., Brademann, G., Dambon, J.A. and Hey, M. (2022) Quality-assured training in the evaluation of cochlear implant electrode position: a prospective experimental study. BMC Med. Educ., 22(1), 386.

Beitrag zur Publikation im Einzelnen: Mein Eigenanteil an der Publikation erstreckte sich auf das Design der Studie (gemeinsam mit M. Hey), die Erhebung der Daten (gemeinsam mit S. Burg), die Auswertung der Daten sowie die Anfertigung des Manuskripts einschließlich der Erstellung aller Abbildungen und der Tabelle. Alle Ko-Autoren haben das Manuskript gegengelesen und genehmigt.

Publikation 2: Mewes, A., Bennett, C., Dambon, J., Brademann, G. and Hey, M. (2023) Evaluation of CI electrode position from imaging: comparison of an automated technique with the established manual method. BMC Med. Imaging, 23(1), 143.

Beitrag zur Publikation im Einzelnen: Mein Eigenanteil an der Publikation erstreckte sich auf das Design der Studie (gemeinsam mit M. Hey), die Erhebung und Auswertung der Daten (gemeinsam mit C. Bennett), die Interpretation der Daten sowie die Anfertigung des Manuskripts einschließlich der Erstellung der Abbildungen 1-4 und 6 (Abbildung 5 wurde von C. Bennett erstellt) sowie der Tabelle. Alle Ko-Autoren haben das Manuskript gegengelesen und genehmigt.

Publikation 3: Liebscher*, T., Mewes*, A., Hoppe, U., Hornung, J., Brademann, G. and Hey, M. (2021) Electrode translocations in perimodiolar cochlear implant electrodes: Audiological and electrophysiological outcome. Z. Med. Phys., 31(3), 265–275.

*geteilte Erstautorenschaft

Beitrag zur Publikation im Einzelnen: Mein Eigenanteil an der Publikation erstreckte sich auf das Design der Studie, die Erhebung, Auswertung und Interpretation der

Daten sowie die Anfertigung des Manuskripts (alles gemeinsam mit T. Liebscher) einschließlich der Erstellung der Abbildungen 1, 4 und 5 (Abbildung 2 und 3 wurden von T. Liebscher erstellt) sowie der Tabelle (gemeinsam mit T. Liebscher). Alle Ko-Autoren haben das Manuskript gegengelesen und genehmigt.

Die vorliegende Einschätzung über die erbrachte Eigenleistung wurde mit den an den Artikeln beteiligten Ko-Autoren/Ko-Autorinnen einvernehmlich abgestimmt.

_____	_____
Datum, Alexander Mewes	Datum, PD Dr. Matthias Hey

Danksagung

An dieser Stelle möchte ich allen beteiligten Personen meinen Dank aussprechen, die mich bei der Anfertigung meiner Dissertation unterstützt haben.

Meiner Frau Christina möchte ich herzlich danken für ihr Verständnis und die Geduld, mit der sie meine Arbeit bis zur Fertigstellung der Dissertation begleitet, und sich während dieser Zeit liebevoll um unsere beiden Kinder Ida und Mads gekümmert hat. Ohne die beständige Unterstützung meiner Familie wäre diese Arbeit nicht möglich gewesen.

Mein besonderer Dank gilt Matthias Hey für die ausgezeichnete Betreuung bei der Umsetzung der gesamten Arbeit. Matthias Hey hat meine bisherige wissenschaftliche Tätigkeit, ausgehend von der Bachelorarbeit, gefördert und geprägt. Ihm verdanke ich meinen beruflichen und wissenschaftlichen Werdegang.

Frau Prof. Petra Ambrosch danke ich für die Mitbetreuung dieser Arbeit, die Bereitstellung des Arbeitsplatzes und die freundliche Unterstützung meiner wissenschaftlichen Tätigkeit.

Des Weiteren möchte ich Tim Liebscher meinen Dank aussprechen, für die produktive und kooperative Zusammenarbeit an der gemeinsamen Publikation, die Ausgangspunkt für eine weitere Zusammenarbeit und hilfreichen Austausch war. Weiterer Dank gilt Tim für die kritische Durchsicht der Dissertation.

Bei Christopher Bennett und Sebastian Burg möchte ich mich für ihren Anteil an der jeweiligen Publikation bedanken. Allen Ko-Autoren der eingebrachten Publikationen sei gedankt für das Gegenlesen der Manuskripte und den hilfreichen geistigen Austausch.

Außerdem muss ich Goetz Brademann und Jan Dambon meinen Dank äußern, für die inhaltliche Einführung in den Bereich der Bildgebung bei Cochlea-Implantaten. Ohne diese Unterstützung wäre es nicht möglich gewesen, mir die Fähigkeit anzueignen, Aufnahmen der Bildgebung bei CI selbstständig zu analysieren und diese Fähigkeit im Laufe der Zeit zu vertiefen.

Herrn Müller-Deile möchte ich dafür danken, dass er, gemeinsam mit Matthias Hey, meinen wissenschaftlichen Werdegang initiiert und geprägt hat, und mir auch nach seinem Ausscheiden als Leiter der Audiologie jederzeit beratend zur Seite stand.

Für die finanzielle Unterstützung bei den gemeinsamen Forschungsvorhaben muss ich der Firma Cochlear Ltd. meinen Dank ausdrücken.

Abschließend ist es mir eine Verpflichtung, mich für die stets kollegiale Zusammenarbeit und den inhaltlichen Austausch in der Audiologie bei den Kolleg:innen zu bedanken: Annika Beyer, Britta Böhnke, Doris Dietrich, Andrea Gottschalk, Matthias Hey, Johannes Kolonko, Kevyn Kogel, Jean Patzig, Martin Olesch, Dirk Ose, Manuela Steinbömer, Sina Wahren, Sabrina Weiß und Sandra Zahn.

Eidesstattliche Versicherung

Ich versichere hiermit an Eides Statt, dass meine Dissertation, abgesehen von Ratschlägen meines Betreuers/meiner Betreuerin und meiner sonstigen akademischen Lehrer, nach Form und Inhalt meine eigene Arbeit ist, dass ich keine anderen als die in der Arbeit aufgeführten Quellen und Hilfsmittel benutzt habe, und dass meine Arbeit bisher keiner anderen akademischen Stelle als Dissertation vorgelegen hat, weder ganz noch in Teilen.

_____

Datum, Alexander Mewes